Norwegian University
of Life Sciences

Master`s Thesis 2018 60 ECTS
Faculty of Chemistry, Biotechnology and Food Science
Knut Rudi

Characterization of the Microbiota Composition Associated with the Hias Continuous Biofilm Process

Inger Andrea Nesbø Goa
Molecular Biology
Biotechnology

Acknowledgement

This master thesis was performed at the Norwegian University of Life Science, Department of Chemistry, Biotechnology and Food Science, with Professor Knut Rudi as main supervisor and the Developer/Researcher at Hias IKS, Sondre Eikås as secondary supervisor.

Firstly, I would like to thank Professor Knut Rudi for presenting me this exciting thesis, I have learned so much throughout this year. Thank you for always being available to answer my questions and giving me advice. Your positivity and knowledge has truly been motivating. I would also like to thank my secondary supervisor Sondre Eikås for taking the time to tour me around at Hias wastewater treatment plant in Hamar, and for teaching me about different treatment processes. A special thanks to Inga for always being so kind and patient when helping me with the laboratory work, you have taught me so much. I am so grateful for all my co-master students and the rest of the Microbial Diversity group, you have made my year.

Also, I would like to thank Hias wastewater treatment plant in Hamar for providing me with the materials, and all the additional results from the Hias continuous biofilm process plants.

Finally, a special thanks to my friends, and the girls at Palasset. Thank you for all the laughs and tears, without you I would not have managed this. Thanks to my family, for always encouraging me. I am so grateful for all the support you have given me.

Ås, May 2018
Inger Andrea Nesbø Goa

Sammendrag

Fosforrensing av avløpsvann er essensielt for å unngå eutrofiering som forstyrrer økosystem i overflatevann. Den vanligste behandlingsprosessen har vært kjemisk utfelling. Ulemper med denne prosessen, derimot, er at fosfor får en lav biotilgjengelighet. Siden fosfor begynner å bli globalt begrenset er nye behandlingsmetoder som gjenvinner fosforen høyst nødvendig. Visse fosfor-akkumulerende organismer (PAO) kan akkumulere fosfor aerobt og frigi anaerobt. Hias renseanlegg (Hias RA) i Hamar har utviklet en biologisk renseprosess, Hias kontinuerlige biofilmprosess (Hias prosessen), til å flytte PAO-biofilmer mellom aerobe og anaerobe soner for effektiv fosforrensing. Systemets effektivitet er avhengig av mikrobiota-sammensettingen. Selv om Hias-prosessen er effektiv, er derimot kunnskapen om mikrobiota-komposisjonen og funksjonen begrenset. Derfor undersøker dette studiet mikrobiota-komposisjonen på etablerende biofilmer under oppstarten av et fullskala Hias prosessanlegg for å kunne korreleres med fosfor-renseeffektiviteten. I tillegg undersøkes stabiliteten av ferdig etablerte biofilmer. Ved hjelp av PCR og Illumina 16S/18S rRNA metagenom sekvensering ble det observert at fosforrensingen nådde utstrømmingsgrensen (95%) på et overraskende tidlig stadium av biofilm-etableringen. I tillegg ble det målt en uforventet høy fosfor-renseeffektivitet under perioder med lav PAO mengde (>1.5%). Disse observasjonene indikerer muligens at de intracellulære poly-P lagrene til individuelle PAOer gjerne har en enorm kapasitet. Det ble også observert at mikrobiota-komposisjonen på etablerte biofilmer var mer stabil enn fosforrensingen. En mulig forklaring på dette kan være variasjoner i avløpsvannets substratinnhold, som primært bestemmer mikrobiota-funksjonen i biologiske RA. Videre ble det funnet ulike PAO komposisjoner i det etablerte pilot- og i det etablerende fullskala Hias prosessanlegget, som antageligvis skyldes forskjeller mellom anleggene. Kunnskapen om funksjonen til biologiske fosforrensesystemer og PAOenes poly-P lagringskapasiteten er derimot fremdeles begrenset, og det kreves derfor videre studier.

Abstract

Phosphorus removal from wastewater is essential to avoid eutrophication, causing disturbances of ecosystems in surface water. Chemical precipitation has been the common treatment process. However, this process results in low phosphorus bioavailability. Since phosphorus is becoming globally limited, new treatment methods recovering phosphorus are urgently needed. Certain phosphorus accumulating organisms (PAO) can accumulate phosphorus aerobically and release anaerobically. Hias wastewater treatment plant (WWTP) in Hamar has developed a biological treatment process, Hias continuous biofilm process (Hias process), for moving PAO-biofilms between aerobic and anaerobic zones for efficient phosphorus removal. The system`s efficiency is dependent on the microbiota composition. However, although the Hias process is efficient, the knowledge about the microbiota composition and function is still limited. Therefore, this study investigates the microbiota composition on establishing biofilms in the start-up of a full-scale Hias process plant, in order to correlate the microbiota composition with the phosphorus removal efficiency. In addition, the stability of already established biofilms is investigated. Through quantitative PCR and Illumina 16S/18S rRNA metagenome sequencing it was observed that the phosphorus removal reached the efflux limit (95%) at a surprisingly early stage of biofilm establishment. In addition, it was detected an unexpectedly high phosphorus removal during periods of low PAO abundance (>1.5%). These observations may indicate that the intracellular poly-P storage of individual PAOs possibly have a huge capacity. It was also discovered that the microbiota composition on established biofilms was more stable than the phosphorus removal. A possible cause of phosphorus removal instability can be due to variations in the wastewater substrate content, which primarily determine the function of the microbiota in biological WWTP. Further it was observed different PAO compositions in the established pilot- and the establishing full-scale Hias process plants, which is possibly due to differences between the plants. However, the knowledge of the function of the biological wastewater phosphorus removal systems and the PAO`s poly-P storage capacity are still limited, thus further studies are required.

Abbreviations and Definitions

AS	Activated sludge
AOB	Ammonium oxidizing bacteria
Biofilm	Microcolonies attached to a surface, embedded in self-produced extracellular polymeric substances
BSA	Bovine Serum Albumin
ddPCR	Digital droplet polymerase chain reaction
dNTPs	Deoxynucleotides triphosphates
dsDNA	Double stranded DNA
EBPR	Enhanced biological phosphorus removal
EPS	Extracellular polymeric substance
Eutrophication	Excessive nutrients in a water body which induces growth of plants and algae and in turn results in oxygen depletion
GAO	Glucose accumulating organisms
Hias process	Hias continuous biofilm process
KF plate	KingFisher 96 well plate
MBBR	Moving bed biofilm reactor
NGS	Next generation sequencing
NOB	Nitrite oxidizing bacteria
OTU	Operational taxonomic unit
PAO	Phosphor accumulating organisms
PCR	Polymerase chain reaction
Poly-P	Poly-phosphate
qPCR	Quantitative polymerase chain reaction
RFU	Relative fluorescence units
SBR	Sequencing batch reactors
SCOD	Soluble chemical oxygen demand
TAE	Tris-acetat EDTA
VFA	Short chain fatty acid
WWTP	Wastewater treatment plant

Table of contents

1 Introduction

Phosphorus removal from wastewater is essential to avoid the issue of eutrophication (i.e. enrichment of nutrients resulting in excessive growth of algae in water bodies) and pollution in surface water (Sharpley et al., 2003). Today several technologies, both established and under development, are used to remove phosphorus from wastewater. However not all the technologies are suitable for phosphorus recovery. Chemical precipitation for example, which is the traditional used method results in a low bioavailability for phosphorus (Rybicki, 1998. Since phosphorus is becoming globally limited, new approaches to recover phosphorus is urgently needed. Biological phosphorus removal from wastewater has become one of the most economical and sustainable treatment methods and has the potential to replace today`s main non-renewable phosphorus source derived from phosphate rocks (Morse et al., 1998).

Biological wastewater phosphorus removal is based on certain organisms which can accumulate phosphorus aerobically and release anaerobically (Nielsen et al., 2010). By exposing phosphorus accumulation organisms (PAOs) for alternating anaerobic and aerobic conditions these organisms can remove phosphorus. This method has been utilized and evolved much since it was discovered for more than 50 years ago (Morse et al., 1998). Hias wastewater treatment plant in Hamar have developed a continuous biofilm (i.e. microcolonies attached to a surface-material) process (Hias process) where they move PAO-biofilms between an aerobic and an anaerobic zone for efficient phosphorus removal (Saltnes et al. 2017). The efficiency of the system is dependent on the microbiota composition of the biofilm (Nielsen et al., 2010). However, despite the evolution of biological wastewater phosphorus removal, the knowledge about the microbial ecology in these plants are still limited. Without understanding the microbial ecology, it is likely that the biological method will never reach its full potential (Seviour et al., 2003). Studying the microbiota composition during biofilm establishment in the startup of a full-scale continuous biofilm process can possibly reveal information about how the efficiency of biological wastewater phosphorus removal can increase. This may be an important addition to solving the global issue of phosphorus scarcity.

1.1 The Biological Role of Phosphorus

Phosphorus is the building block of DNA, RNA, and ATP, and is essential for all life. The element phosphorus exists in several forms, including red, white, and black phosphorus (Kofstad & Pederson, 2018). However, these forms are highly reactive and is never found as a free element (Desmidt et al., 2015). Instead phosphorus is found in many minerals and mainly as phosphate rock (Cordell & White, 2011). In aqueous solutions phosphorus exists in two main forms, dissolved and particulate. where orthophosphates (PO_4^{3-}) are the primary dissolved form (lenntech.com, 2018).

Phosphorus cannot be substituted in plant growth, thus not in food production (Cordell. et. Al 2009). The agricultural soil does not contain a high enough amount of phosphor ions, and the growth of plants and crops is therefore dependent on phosphor fertilizers. Currently applied phosphor fertilizers come from the non-renewable source, finite phosphate rock, which is estimated to be limited in the next 30-300 years (Cordell & White, 2011). Consequently, new renewable phosphor sources are urgently needed.

Although phosphorus is essential for plant growth and cell formation it can disturb aquatic life (Sharpley et al. 2003). After the green revolution in the 1950s, the phosphorus fertilizer use increased drastically in line with the industrial agriculture growth (Patel, 2013). This resulted in alternation of the phosphorus cycle (Cordell & White, 2011), and runoff of excessive nutrients from agriculture to surface waters cause the issue of eutrophication and dead zones (Withers & Hayharth, 2007; Correll, 1998). However, although there is no substitute for phosphorus in plant growth, there is a substitute for the fertilizer source, phosphate rock (Cordell. et. Al 2011). Wastewater for example is a major phosphorus source.

Municipal wastewater may contain 2-20 mg/L phosphorus where the major part is inorganic. Households and especially industry such as agriculture, release large amount of phosphorus into wastewater every day. The average individual phosphorous contribution is around 2.18 g/day and the number seem to increase because phosphorus is a large constituent of synthetic detergents (lenntech.com, 2018). Since phosphorus are responsible for eutrophication, the phosphorus discharge limit for wastewater treatment plants has been set to ~0.4 mg/L or 95% (Comber et al., 2015; Saltnes et al. 2017). In general, when phosphorus is removed from

wastewater, the wastewater must first go through a mechanical treatment step, where larger particles is filtered out. In the next step the soluble phosphorus must be converted into non-soluble compounds, either as precipitated chemical compound or accumulated in bacterial cells. The final treatment step involves separation of bound phosphorus (precipitated or accumulated) from the treated wastewater (Rybicki, 1998).

From the beginning of phosphorus wastewater removal in the 1950s until today, chemical precipitation has been the mainly used process (Rybicki, 1998). The process involves addition of metal salts to wastewater, resulting in precipitation of an insoluble metal phosphate which in turn is removed by sedimentation (Wang et al., 2005). Although chemical precipitation has the advantage of being reliable, and the level of phosphorus in effluent is low, there are several disadvantages about this process, including high costs. But most importantly, chemical precipitation product is typical phosphorus bound as metal salts (Minnesota pollution control agency, 2005). These phosphorus compounds have a low bioavailability and cannot be reused as fertilizer in the agriculture. Since phosphorus is becoming a scarce resource, biological wastewater treatment systems has been given more attention. Biological phosphorus removal from wastewater is an efficient treatment method which gives phosphorus a high bioavailability (Morse et al., 1998; De-Bashan & Bashan, 2004).

1.2 Microorganisms Associated with Biological Wastewater Phosphorus Removal

The function and efficiency of a biological wastewater treatment system is highly determined by the function of the microbiota communities (Saunders et al., 2016). Since the knowledge of the microbiota compositions in biological phosphorus removal systems is still limited, the stability and reliability of the treatment can be problematic. Only the last decades new biotechnology tools have made it possible to study and identify the core microorganisms responsible for treatment processes such as phosphorus removal. The majority of studies on biological phosphorus wastewater treatment plants (WWTP) have focused on PAOs and their major competitor's glycogen accumulating organisms (GAO). However, there are also other important bacteria groups which interact in the ecosystem and affect the overall process in

the plants. A Danish study performed on 25 full-scale Enhanced biological phosphorus removal (EBPR) plants (section 1.3.1) showed that these bacteria includes filamentous bacteria, hydrolysers, fermenters, nitrifies, and denitrifies. Figure 1.1 shows the average abundances of the functional groups found in all the 25 Danish EBPR plants, where the results were given by quantitative fish (Nielsen et al., 2010).

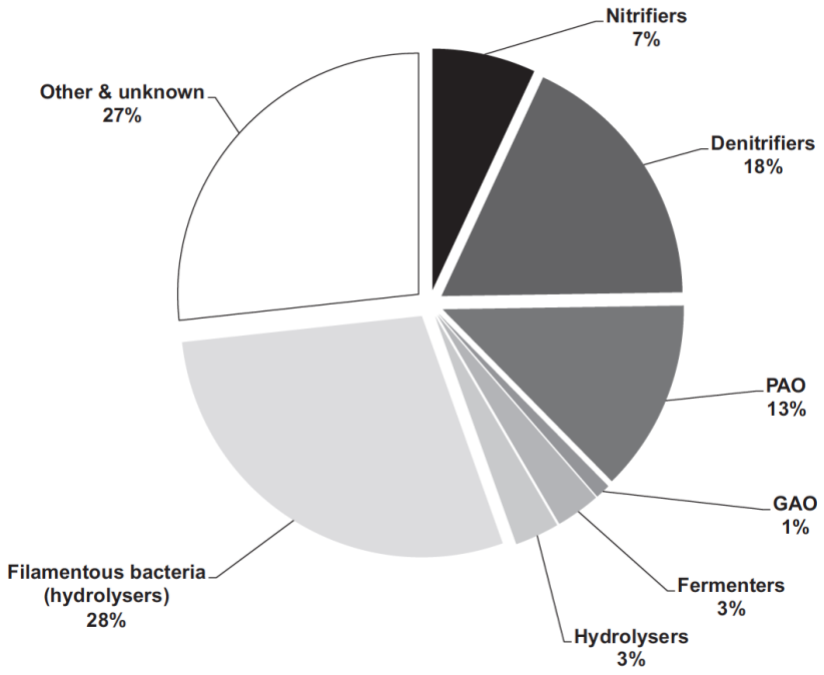

Figure 1.1 Average abundance of the functional groups found in Danish EBPR plants (Nielsen et al. 2010).

1.2.1 Phosphorus Accumulating Organisms (PAOs)

The mechanism of PAOs are found in bacteria, microalgae and fungi, but the main focus for biological phosphorus removal in treatment plants has been on bacteria (Tarayre et al., 2016).

The genus *Accumulibacter* and *Tetrasphaera* is the most abundant PAO bacteria in EBPR plants (section 1.3.1). The metabolism of these bacteria is quite different, and the physiology of especially *Tetrasphaera* are still limited. The majority of *Tetrasphaera* can hydrolyse starch, ferment glucose, consume amino acids, and grow anaerobically (Nielsen et al., 2010). In contrast, the genus *Accumulibacter* are found with several distinct species with and

without the ability of denitrification. In addition, the main *Accumulibacter* carbon sources are acetate, propionate and some amino acids (Shen & Zhou, 2016).

Aerobically, both *Accumulibacter* and *Tetrasphaera* accumulate phosphate mainly as poly-Phosphate (poly-P) (Lanham et al., 2014). Poly-P has important function in regulating enzymatic activity, gene expression, among others (Tarayre et al., 2016). The P-accumulation are affected by physicochemical properties such as the anaerobic/aerobic phase time, temperature, pH, volatile fatty acid composition, and the concentration of certain metal ions (Nielsen et al.2010). During the anaerobic phase, *Accumulibacter* accumulate volatile fatty acids (VFA) formed by chemoorganotrophic fermentative bacteria. The carbon source is stored in the form of poly-β-hydroxyalkanoates (PHA). The chemical composition of PHA is determined by the carbon source, where acetate assimilation synthesize poly-β-hydrobutyrate (PHB) and propionate produces poly-β-hydroxyvalerate (Seviour et al., 2003).

If the carbon sources in a wastewater plant is acetate, it converts to Acetyl-CoA intracellularly in the anaerobic zone (figure 1.2.a). The reaction uses energy generated by hydrolysis of ATP to ADP, releasing P from the cell into the wastewater. The Acetyl-CoA is in turn metabolized into PHA. During the aerobic phase the PAOs accumulate phosphate in the form of poly-P by oxidizing PHA to gain energy (figure 1.2.b). This process is the opposite of the anaerobic phase, and PHA is now used for cell growth and the regeneration of the poly-P reserves. PHA degradation leads to Acetyl-CoA synthesis through the TCA cycle. The TCA cycle generates energy from oxidation and carbon for new cell growth. Some of the generated energy is used for soluble P uptake from the environment and to incorporate it into poly-P. While, another part of the energy and carbon is used to regenerate glycogen (Tarayre et al. 2016).

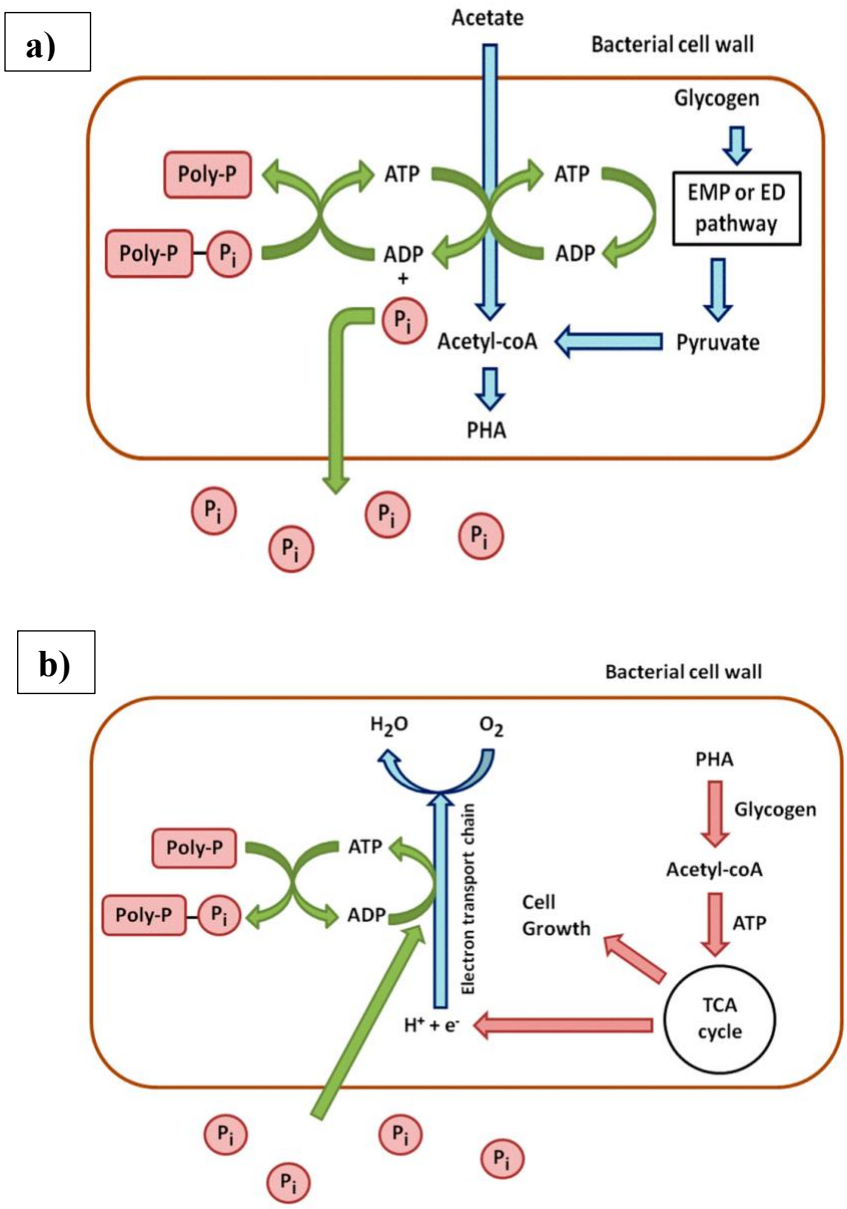

Figure 1.2. The metabolism of *Accumulibacter*-PAO. a) Anaerobic metabolism of *Accumulibacter*-PAO with Acetate as carbon source. PHA is stored and phosphor released. b) Aerobic metabolism of PAO. Poly-p is stored and PHA is oxidised (Tarayre et al. 2016)

1.2.2 Other Functional Bacteria in Traditional Biological Wastewater Phosphorus Removal Systems

The functional bacteria species composition in a biological phosphorus removal system is primary determined by the available substrate. The incoming wastewater in the anaerobic zone contain different carbon compounds (figure 1.3). These might be macromolecules such as proteins, polysaccharides, lipids and nucleic acids, or soluble substrates including amino

acids, VFAs, glucose, long-chain fatty acids (LCFA), glycerol, short polypeptides and oligosaccharides. Before PAOs can take up these carbon sources, the macromolecules require hydrolysis, which is primarily performed by filamentous bacteria consisting of exoenzymes. Hydrolysis of lipids are mostly performed by *Microthrix,* proteins mostly by a diversity of *Choloroflexi*, whereas starch is hydrolysed by *Tetrasphaera*. In addition, most likely other unknown hydrolysing species are present (Nielsen et al. 2010).

After hydrolysis, fermentation of the soluble components is needed. In biological phosphorus removal systems, fermentation is often performed by bacteria including *Clostridia*, *Tetrasphaera, Streptococcus, Lactococcus* and *Rhodoferax*. These can synthesize carbon compounds such as acetate and propionate, which is the main *Accumulibacter*-PAO and GAO carbon sources in addition to some denitrifies. GAOs such as, *Competibacter* and *Propionvibrio*, are the main PAO competitors which has a similar metabolism (Nielsen et al., 2010). They compete for the same carbon sources and store it intracellularly as PHA. However, they do not accumulate phosphate aerobically, and can thus defect the phosphorus treatment if they win the carbon competition (Zhu et al., 2015; Carvalheira et al., 2014). Filamentous and fermenting bacteria typically do not compete for acetate or other readily biodegradable substances, and instead filamentous bacteria primarily consume glucose (Nielsen et al., 2010).

A typical biological phosphorus removal system contain AOB-nitrifies such as *Nitrosomonas* and *Nitrospira*, and NOB-nitrifiers such as *Nitrospira* and *nitrotoga*. In addition to denitrifies, such as *Acidovorax*, and *Simplicispira*. These bacteria are able to remove another important nutrient, nitrogen, from wastewater by working together in the highly important nitrogen cycle process. Aerobically, the nitrifies first oxidize ammonium to nitrite (AOBs) and then oxidize nitrite to nitrate (NOBs). Then anaerobically, the denitrifies reduces nitrate to nitrogen by oxidizing an electron acceptor, which might be oxygen and/or nitrate and nitrite. Therefore, the denitrifies can inhibit the phosphorus removal. When nitrate is present in the anaerobic zone, the denitrifies will consume the carbon before the PAOs. This results in a lower PAO carbon accumulation, and thereby lower phosphorus accumulation in the aerobic zone (Akin & Ugurlu, 2004). However, some EBPR systems (section 1.3.1) has incorporated an additional anoxic zone (no O_2 but presence of nitrate) for simultaneous phosphorus and nitrogen removal (Meyer et al. 2005). Studies have shown that instead of using oxygen as an electron acceptor some PAOs can use nitrate, and it was demonstrated

that the genera of PAO was able to grow and accumulate phosphorus in the anoxic zone. In addition to using nitrogen as an electron acceptor, these denitrifying PAOs (DPAOs) does not use organic substances in the anoxic zone. The primary difference between PAOs and DPAOs is the electron acceptor, where PAO uses oxygen aerobically, and DPAO uses nitrate under anoxic conditions but both accumulate carbon anaerobically (Lee & Yun, 2014).

If the wastewater substrate content is stable, other factors may influence the functional bacteria composition. This includes the residence time in the different zones. By for example increasing the time in the anaerobic zone, the hydrolysis and fermenting process time increase and more fermenting products such as acetate will be produced. I addition, different physicochemical properties influence the bacteria composition: 1) respiratory capability, if the bacteria are obligate/facultative aerobes, fermentative, or denitrifying, 2) the cellular substrate uptake rate and substrate affinities, 3) the capability of storing substrates intracellular (PHA, poly-P, glycogen) as energy reserves, 4) capability of excreting surface-associated exoenzyme for macromolecule degradation, 5) a cell surface with ability of attaching to the biofilm/floc surface. For example, the hydrophobicity of the cell surface can determine how easy some bacteria can attach to a biofilm/floc (section 1.4), 6) the ability to survive starvation. The bacteria growth rate and yield can affect the ability of surviving during starvation, 7) sensitivity to oxygen level and different chemicals can affect different bacteria genus differently. Also, the pH, temperature, and the ion content can affect the microbiota composition in an EBPR system (section 1.3.1) (Nielsen et al., 2010).

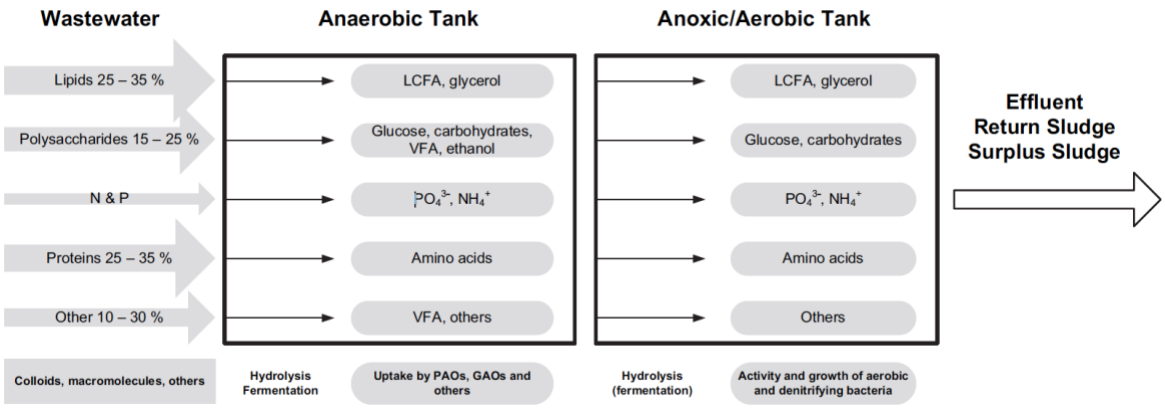

Figure. 1.3. The overall flow of organic matter and active functional microbial groups in a typical EBPR plant (Nielsen et al., 2010).

1.3 Biological Phosphorus Removal from Wastewater

The most general method used for biological wastewater treatment is the activated sludge process. In the Activated sludge (AS) process a microbial biomass suspension (activated sludge) is capable of removing nutrients. The design of the treatment plant decides what an activated sludge WWTP can remove, which could be nitrogen and phosphorus, in addition to organic carbon substances (Gernaey et al., 2004). In principle there are three main components of an AS system (Figure 1.4): an aeration tank, that function as a bio reactor, a final clarifier for separation of AS solids and treated wastewater, and a return sludge (RAS). The RAS transfer the settled AS from the clarifier to the influent of the aeration tank to re-seed the new wastewater. The mixture of wastewater and biological mass is often referred to as Mixed Liquor (MLSS). The dry solid concentration of MLSS typically range from 3 to 6 g/L. Due to biological growth, the sludge eventually excesses the desired MLSS concentration of the aeration tank. The excess solids are called waste activated sludge (WAS) and is removed from the treatment process (Gouveia & Pinto, 2000).

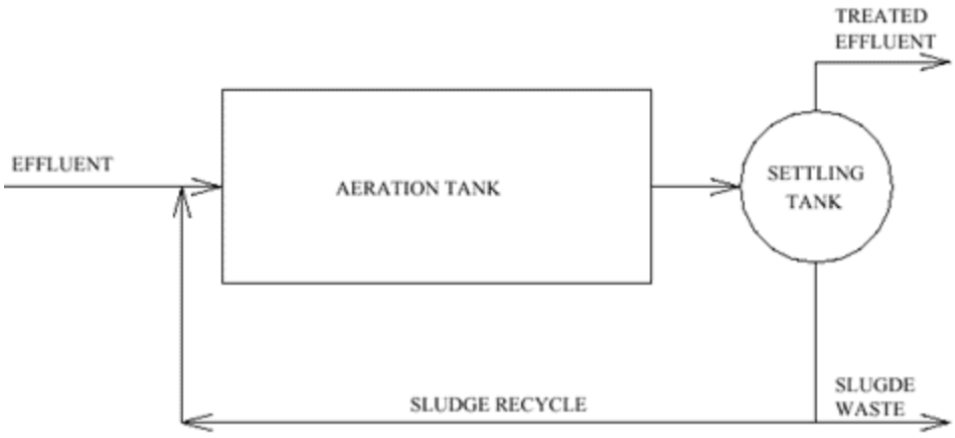

Figure 1.4 General activated sludge treatment plant (Gouveia & Pinto, 2000).

1.3.1 Enhanced Biological Phosphorus Removal (EBPR) from Wastewater

The most common method for phosphorus removal is based on an AS process which is commonly referred to as enhanced biological phosphorus removal (EBPR). This process uses the ability of PAOs to store poly-p by exposing PAOs for alternating anaerobic -and aerobic conditions (figure 1.5a). EBPR was accidently discovered for more than 50 years ago, and since then the method has evolved and many different full-scale plants, with a varying efficiency, has been developed.

In South Africa, Barnard along with a group of co-workers carried out the pre-work of what Barnard published as a guideline for successful EBPR in 1974. Barnard suggested that an anaerobic reactor was needed to receive the initial influent wastewater containing the easily degradable carbon and energy source. In addition, an anoxic zone was necessary to limit the concentration of nitrate entering the anaerobic zone (figure 1.5b). The present of nitrate in the anaerobic zone would fail the EBPR process since denitrifying bacteria is able to anaerobically respire and block the supply of organic substrate, making them no longer available for the PAOs. Maintaining anaerobic condition in the anaerobic zone was also strictly because in the present of oxygen, the PAO metabolism would shift. He also suggested that the biomass would be recycled through alternating anaerobic and aerobic conditions (Seviour et al., 2003). Mostly, EBPR systems are activated sludge process with continuous flow reactors containing several tanks to accommodate the different zones. Another mode of operation is to use a single tank, periodic fed, fill and draw system, also known as sequencing batch reactors (SBR). In the SBR the system`s different zones are separated in the one reactor by time (Seviour & Blackall, 2012).

AS processes have some challenges including return of oxygen and nitrate, and a large volume requirement. In addition, to reach the phosphorus discharge limit of ~95 %, an additional chemical precipitation treatment step is used, although it results in a low phosphorus bioavailability and should be avoided.

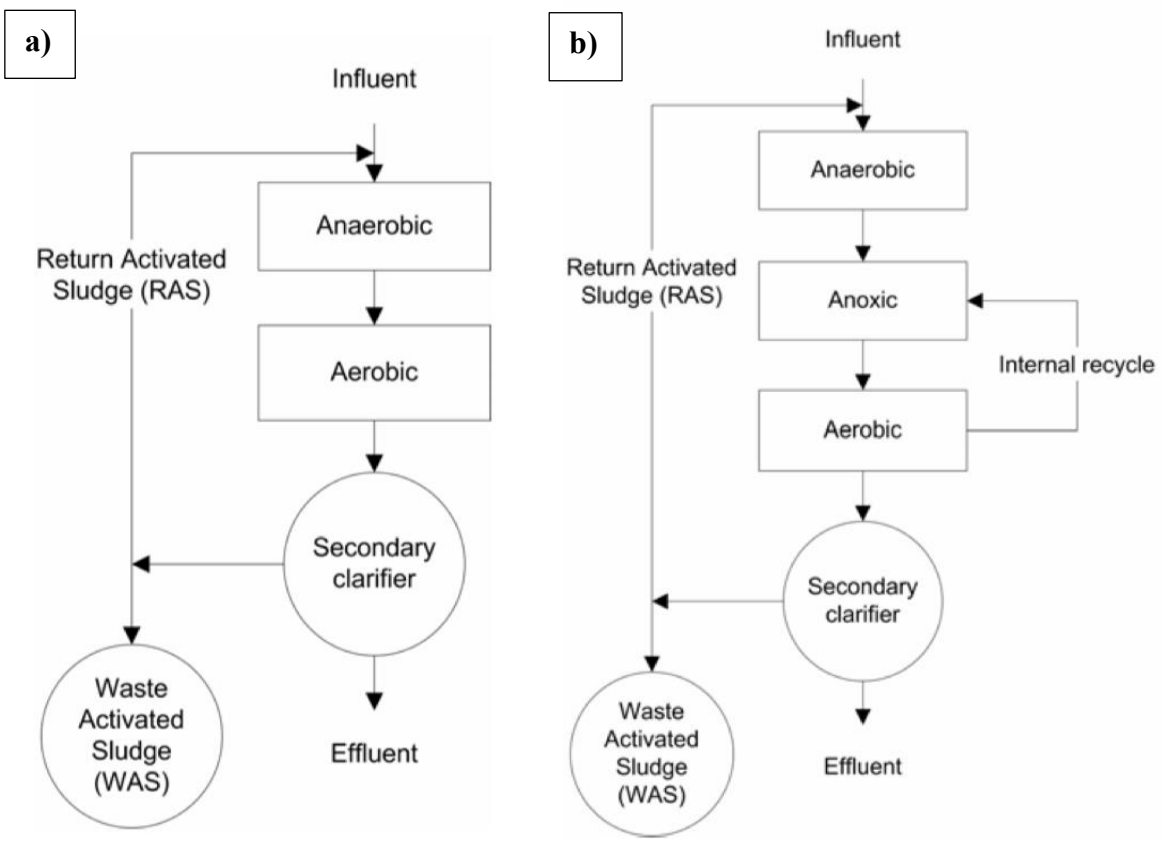

Figure 1.5 Schematic overview of an EBPR system a) Anaerobic/aerobic EBPR process. b) Anaerobic/anoxic/aerobic EBPR process (Minnesota pollution control agency, 2005).

1.3.2 Moving Bed Biofilm Reactor

Hias WWTP in Hamar, the study site of the current study, have developed a moving bed biofilm reactor (MBBR) system called Hias continuous biofilm process (Hias process). The Hias process is based on the traditional EBPR process. It started with a pilot plant with a volume of 7 m^3 and a biofilm-carrier filling level of approximately 60% (Saltnes et al., 2017). The process was efficient, and in Mai 2016 they expanded to a full-scale plant with a volume of 730 m^3, which today treat municipally wastewater. The system utilizes the properties of a biofilm process (section 1.4) which gives a high efficiency per unit volume, and compared to standard EBPR, a less volume is required. Moreover, there is no sludge return so the process is less dependent on sludge separation. The first part of the plant is an anaerobic zone with mechanical stirring, whereas the second part is an aerobic zone were oxygen is added through the bottom of the plant (Figure 1.6). The time ratio in the anaerobic and aerobic zone is commonly around 30/70. Firstly, the inlet wastewater flows into the anaerobic zone, before the biofilm-carriers flows with the water-flow to the aerobic zone. At the end of the aerobic

zone the treated water flow out of the plant for further separation. The biofilm-carriers is mechanically lifted out of the water and transported back to the start of the anaerobic zone (figure 1.6). The sludge that falls of the biofilms at the end of the aerobic zone, is further processed through phosphorus recovery.

The phosphorus recovery process at Hias WWTP consists of several steps. The sludge is first mixed with a polymer, before it goes through a disc-filter, resulting in ~1.5-2% dry matter. The dry matter is then added to an anaerobic tank with mechanically stirring for ~10 hours. In this tank the PAOs release ~40% phosphorus from intracellular poly-P. The de-watering process is repeated, leading to another ~10% dry matter that is pumped to the anaerobic tank where more phosphorus is solubilised. Eventually, ~40-60% phosphorus is precipitated by struvite ($Mg + PO_4 + NH_4$), which is a product with high bioavailability. In addition, the remaining phosphorus in the sludge is also biological accessible (Sondre Eikås, personal communication, 12 April, 2018).

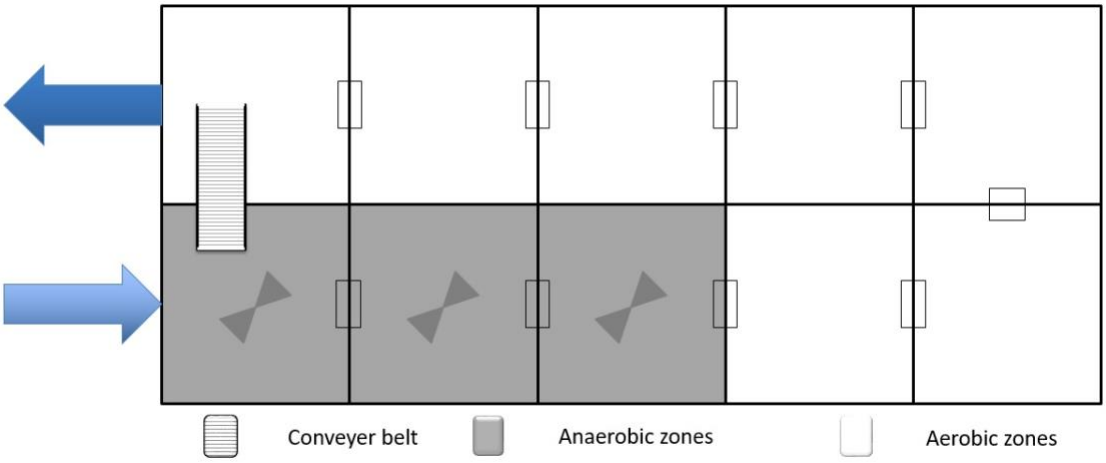

Figure 1.6 Schematic presentation of the Hias process. First the water flows into the anaerobic (grey) zone with 60% biofilm content. Secondly the biofilms flow with the water flow into the aerobic (white) zone. At last the treated water flows out of the plant and the biofilms is transported mechanically out of the water and back into the anaerobic zone (Saltnes et al. 2017).

1.4 Biofilm

A biofilm is microcolonies attached to a surface, embedded in self-produced extracellular polymeric substances (EPS) (Zhu et al., 2015). EPS consists mainly of polysaccharides but also substances such as proteins, phospholipids, and nucleic acids. The EPS provides mechanical stability and protects the microbial community against the outer environment (Chmielewski et al., 2003). In nature, biofilm formation is favoured for survival and approximately 99% of earth living bacteria stays attached to surfaces. The biofilm microbiota population can both consist of single species or of diverse microbiota compositions living together in a society. Biofilm formation can occur on a variety of surfaces, and depending on the location, it can be an advantage or disadvantage (Mahami & Adu-Gyamfi, 2011). For example, biofilm contributing to pollution in the food industry can both cause health problems and economic loss (Chmielewski & Frank, 2003). In contrast, the WWTP industry has developed methods based on for example PAO biofilm-carriers, for phosphorus removal. A biofilm can start to develop after only 5-30 s and the development is affected by physicochemical properties of the material surface, liquid medium, and bacterial cell-surface (Donlan, 2002; Chmielewski & Frank, 2003).

Properties of the material surface influence the attachment of free-living bacterial cells. Studies shows that an increase in surface roughness increases the microbial colonization. This is due to shear force reduction and that rougher surfaces have higher surface areas. The surface material hydrophobicity also influences the attachment. Studies has found that microorganisms attach faster to hydrophobic, non-polar surfaces such as plastic than to hydrophilic surfaces such as glass (Donlan, 2002). In addition, when a material is exposed to a liquid medium, the surface quickly become coated by organic polymers from the medium, this conditioning film can induce the microbial attachment rate and extension (Mahami & Adu-Gyamfi, 2011. Another factor influencing the attachment is the properties of the aqueous medium.

Aqueous characteristics such as temperature, pH, and nutrient level may influence the microbiota attachment to a material surface. Studies have shown that attachment in different aqueous systems has seasonal affection (Donlan, 2002). The temperature and pH may also influence the metabolism of bacteria differently and affect their growth rate. In addition,

some studies show that the microbial attachment increases when the medium nutrient content increases (Mahami & Adu-Gyamfi, 2011). Another factor which may influence the attachment is the flow velocity. In a liquid, cells act as particles and a relative high velocity will associate the bacterial cell with the surface material faster. However, if the velocity reaches a certain point it can result in detachment of the bacteria (Donlan, 2002). The biofilm formation is also affected by cell properties.

Bacteria cell-surface properties such as hydrophobicity, the presence of filaments (fimbriae and flagella), and EPS content, all influence the microbial attachment rate and extension of the material surface. For example, hydrophobic interaction can be formed between a hydrophobic cell-surface and hydrophobic material surface. Fimbria which consists of hydrophobic amino acid residues contributes to the hydrophobicity and the attachment (Donlan, 2002). Studies has shown that flagella have an important function in early stages of attachment by overcoming the repulsive forces associated with the material surface and it also showed that surface protein induces attachment. However, hydrophobicity generally decreases as growth rate increases (Chmielewski & Frank, 2003). Another cell surface property influencing biofilm formation is EPS, which primarily consist of polysaccharides which may be neutral or anionic. This property can cause association with divalent cations such as calcium and magnesium, which in turn can cross-link with the polymer strand and give a stronger binding force in a developed biofilm. EPS can be hydrophobic, but in most cases, ESP are both hydrophobic and hydrophilic. The production of EPS are influences by nutrient level of the growth medium. Excess access to carbon, and limited access to nitrogen, potassium, or phosphorus can promote the EPS production (Donlan, 2002). In addition, studies have shown that the formation and development of biofilms is regulated by gene expression and exchange between cells, and a special cell-to-cell communication called quorum sensing (Chmielewski & Frank, 2003).

The establishment of a biofilm from free-living organisms is generally divided into five stages (figure 1.7) The first step involves a reversible attachment of the first cells to a conditioned surface. Followed by an irreversible attachment as the cells forms stronger interactions with the material surface. Moreover, the attached cells produce EPS which also promote the irreversible attachment. The second stage is recognized by micro-colonization as the attached cells grows and divides. At the third stage, secondary colonizers and nutrients are attach onto the growing biofilm and a complex multi-layered structure is formed which

leads to the fourth stage, biofilm maturation. During the fifth stage, biofilms detaches and disperse where micro-colonies, colonize surfaces in new areas and form new biofilms (Mahami & Adu-Gyamfi, 2011).

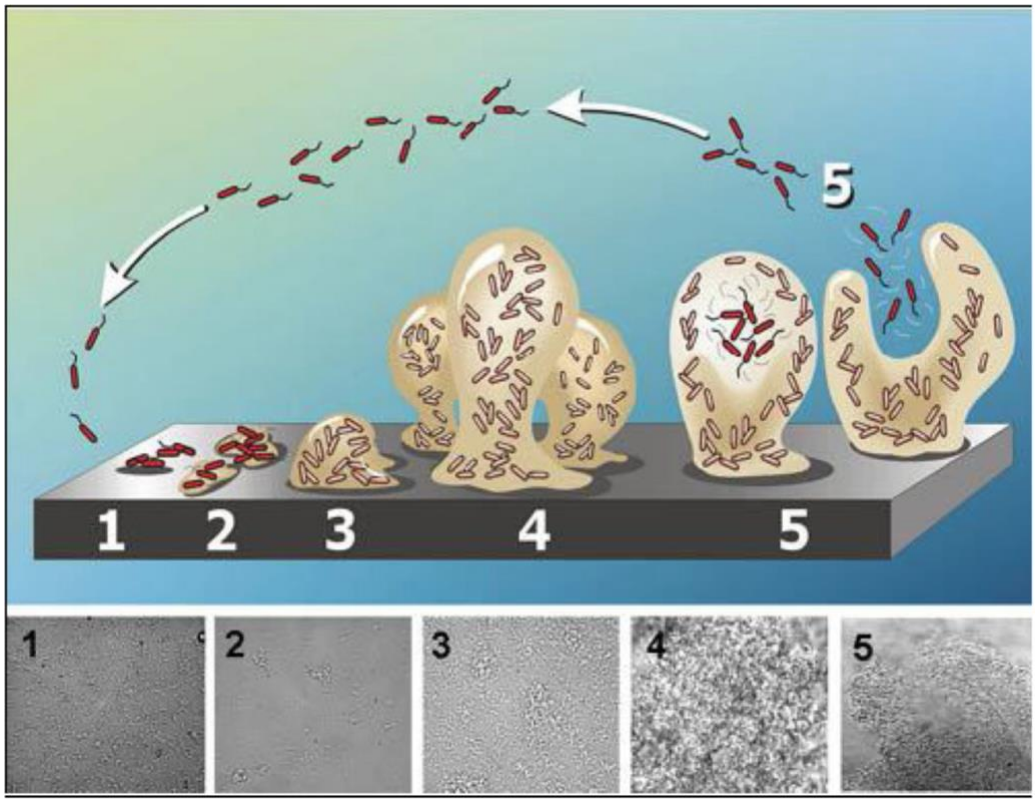

Figure 1.7. Schematic representation of biofilm formation. Biofilm formation and development are generally divided into five stages including 1) Attachment 2) colonization 3) secondary colonization 4) biofilm maturation 5) Dispersion (Mahami & Adu-Gyamfi, 2011).

Typical established biofilm microbial communities are heterogeneous and live together in an environment where they can exchange genes and nutrients, and communicate by quorum sensing (Mahami & Adu-Gyamfi, 2011). A diverse microbiota community can have symbiotic relationships, but it can also be competitive. When the biofilm matures, it adapts to oxygen and nutrients, and the population alters. Discrete microcolonies within the EPS are separated by water channels which allow diffusion of nutrients, metabolites and oxygen, and export waste products. The bacteria with the highest metabolic activity usually occurs at the outer biofilm matrix layer near the water channels. Moreover, at the biofilm-liquid phase there are most often aerobic bacteria. Whereas at the inner biofilm core there is a niche for bacteria which can survive at low oxygen and nutrients levels and has various metabolic rates (Chmielewski & Frank, 2003).

During a biofilm life cycle, layers of the biofilm can be detached and dispersed. This can occur by shedding of daughter cells from actively growing cell or by shearing and sloughing (Mahami & Adu-Gyamfi, 2011). The knowledge of the shedding of daughter cells process is limited, but it might be explained by studies suggesting that the surface hydrophobicity of the divided daughter cells vary from chemostat-interact biofilms or resuspended biofilm cells (Donlan, 2002). Expression of specific genes and quorum sensing has also been associated with detachment of cells from the biofilm. Detachment can also be induced by three main physical detachment processes which includes 1) shearing (constant removal of small portion of the biofilm), 2) sloughing (rapid removal) and 3) abrasion (detachment caused by collision between particles from the bulk fluid and the biofilm) of the attached cells (Mahami & Adu-Gyamfi, 2011). Sloughing and shearing may be induced as the biofilm grows in size and some cells become far from the energy and nutrients from the external environment. In addition, waste and toxin accumulation may also trigger cell death and detachment. Sloughing can also be caused by an alternating nutrient concentration. For example, low carbon levels can cause higher EPS synthesis, which can induce detachment. However, high levels of carbon can also trigger sloughing (Chmielewski & Frank, 2003). In addition, studies have showed that sloughing might be induced by the presence of protozoa (Zhu et al., 2015).

1.5 Quantification and Sequencing Tools for Metagenome Studies

Before conventional microbiological technology was developed, determination of microbiota compositions and their function was a huge challenge. Today however, culture-independent, revolutionary technology with high throughput, high efficiency and quick computation is accessible for metagenome studies. These revolutionary tools include, polymerase chain reaction (PCR)- based DNA profiling technologies, quantitative PCR (qPCR), next-generation sequencing (NGS), and bioinformatics analysis (Gong et al., 2012). Methods based on these tools have enabled more complete studies on metagenomes and can be used to determine the microbiota composition in a biological wastewater treatment plants.

1.5.1 Polymerase Chain Reaction

PCR is used to amplify one or a few specific parts of interested in a genome, fragment varying from 100-10.000 base pairs. The method can provide enough amplicons of the target DNA region, which can be sequenced or visualized by gel electrophoresis (Reece et al., 2011).

In a typical PCR reaction, the following reagents should be included, DNA polymerase, dNTPs, $MgCl_2$, a forward and reverse primer, PCR buffer, nuclease-free water, and template DNA (more information in Appendix A). The PCR reaction commonly consists of 30-35 cycles of the following thermal conditions. Firstly, a denaturation step is run at ~95^{o}C. At this temperature the hydrogen bonds between the DNA strands breaks, and two single strands (ssDNA) is generated. Secondly, an annealing step is run at ~50-60^{o}C, depending on the primer sets. At the right temperature the primer set binds complementary to the ssDNA at the target region. Thirdly, an elongation step is run at ~72^{o}C. In this step DNA polymerase synthesize a new copy of the template DNA by adding complementary dNTPs in the 5`-3`direction (Sigmaaldrich.com, 2018).

Since the technique was first developed, many improvements have been made and many modified versions have evolved. These include qPCR and digital droplet PCR, among others.

1.5.2 Quantitative PCR

During conventional PCR, the PCR product or amplicon is detected and measured after the reaction has completed in an end-point analysis. In quantitative PCR or real-time PCR as the name says, the accumulation of amplification product is measured during the reaction, and the product is quantified after each cycle. This gives the advantage of determining the initial number of copies of template DNA with high accuracy. In microbiota studies, qPCR is often used to measure the total amount of a specific bacterial group in a community or an environmental sample (Sigmaaldrich.com, 2018).

As conventional PCR, qPCR includes the same reagents and typically 40 cycles of denaturation, annealing, and elongation with the same thermal conditions. In addition, qPCR

includes a fluorescent reporter dye which is used as an indirect measure of the amount of nucleic acid present during each amplification cycle (Appendix A, table A3). The florescent signal is proportional to the quantity of PCR amplicons produced during the repeating phases of the reaction where a high number of PCR products gives a stronger fluorescent signal. There are two types of reporter molecules, these includes a sequence specific probes such as, TaqMan, which binds to the target region. In addition to a double stranded binding dyes which is conjugated to primers, such as SYBR Green or EvaGreen. When dsDNA-binding dyes is free in a solution or only bond to ssDNA, the signal emitted is too weak to be detected. As the amount of dsDNA increases during a PCR reaction, more dye binds to the amplicons and the fluorescents signal intensity increases (Brankatschk et al., 2012).

To be detected by qPCR machines the fluorescence signal must reach a certain cycle threshold (Ct) value to overcome background noise. The Ct value is the cycle number where enough PCR product is amplified, and the fluorescence signal reach the detectable level. qPCR analysis is performed by using amplification plots where the number of PCR cycles is plotted on the x-axis and the fluorescence which is proportional to the amplified product amount in the samples is plotted on the y-axis. The Ct-value of a reaction is determined by the original template amount at the start of the amplification reaction. Samples containing high amounts of original templates, requires less amplification cycles to generate enough PCR amplicons to reach detectable level of fluorescence signal. Oppositely, low amounts of original templates, requires more amplification cycles to generate enough PCR amplicons to reach a detectable fluorescence signal level (biorad.com, 2018).

Absolut qPCR analysis can be achieved by comparing Ct-values of test samples to a standard curve. A standard curve is generated by different known amount of a template which is analyzed by qPCR. The Ct-values from the analysis are plotted on the x-axis and the log of starting quantity of the sample on the y-axis. The quantity of the test samples is calculated by an equation generated from a linear regression data analysis. The Ct-values for the sample must be in the range of the standard curve for this approach to be affective (Pabinger et al., 2014).

1.5.3 Digital Droplet PCR

As qPCR, digital droplet PCR (ddPCR) is used to estimate the amount of nucleic acid in a test sample. However, in contrast to qPCR, ddPCR does not depend on a standard curve for absolute quantification. ddPCR is a valuable technique which can for example be used for detection of rare alleles, identifying mutant genes against wild-type, and quantification for next-generation sequencing approaches (Yang et al. 2014). During ddPCR, target nucleic acid sequences (template) is quantified by randomly partitioning sample DNA into individual water-in-oil droplets, such that each droplet contains zero, one, or more copies of the target template (Pinheiro et al., 2011). Fluorescence probe-based PCR amplification of the template will then occur within each droplet in a sequence-specific manner. The fluorescence of each droplets is individually measured after the PCR amplification (Attali et al., 2016). The droplets with presence of PCR product is defined as positive, whereas the droplets without PCR products as negative. By calculating the ratio of positives to the total partitions, the absolute amount of target nucleic acid in the original samples before partitioning can be found (Yang et al. 2014).

1.5.4 Next Generation Sequencing

Genomic analysis of complex environmental samples is highly important for understanding evolutionary history, and functional and ecological biodiversity in for example a biological WWTP (Shokralla et al., 2012). The request of revolutionary technologies for delivery of rapid, low cost and accurate genome information has never been greater. The conventional Sanger DNA-sequencing technology which was developed by Frederick Sanger and his colleagues in 1977, dominated the sequencing industry for more than two decades. However, after the introduction to next-generation sequencing for more than a decade ago, there has been an exchange from the application of the Sanger sequencing method (Metzker, 2010). Next-generation sequencing is a high-throughput, relatively cheap technology, which is both efficient and accurate, and the platforms can reveal information about the genome, transcriptome, or epigenome of any organism. There are several various NGS platforms with different sequencing technologies and Illumina sequencing technology is one of them. Illumina sequence is a sequence by synthesis technology which generates more than 90% of

the worlds sequencing data. The Illumina workflow can be divided into four basic steps, library preparation, Cluster generation, sequencing, and data analysis.

Library preparation is the first step of the workflow. During preparation, the DNA sample is fragmented, and the 5`and 3` ends is modified with specific oligonucleotide adaptors. The second step involves cluster generation. At this step the library fragments are added onto a flowcell containing surface bound oligonucleotides complementary to the fragment adaptors (Figure 1.8.a). The bounded DNA will then be copied before the end of the copied DNA strand bends over to a new oligonucleotide on the flowcell, forming a bridge (Figure 1.8.b). Clusters on the flowcell will then be generated through bridge amplification. The reverse strand generated through bridge amplification is then cleaved off, followed by attachment of a sequencing primer to the free end of the DNA. This leads to the next step, sequencing (Figure 1.8.c), where four fluorescent labelled bases compete to bind to the sequencing strand, base by base. Each base has a unique fluorochrome with a unique colour and a laser excites and read the unique colour of the base binding to the sequencing strand. In this way the colour signal reveals the DNA sequence (Figure 1.8.d). The fluorochrome blockes the 3`OH on the growing DNA strand, preventing a new base to bind before the flourochrome has detached, giving a high accuracy (Voelkerding et al., 2009; Illumina.com, 2017).

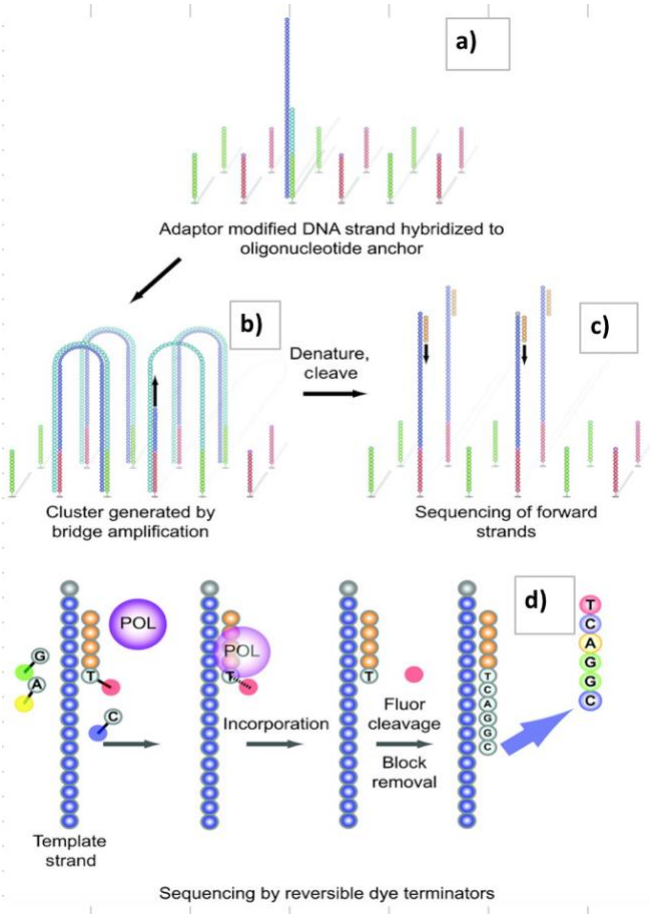

Figure 1.8. Schematic overview of Illumina sequence technology. a) Single-stranded, adaptor-modified DNA is hybridizing with complementary oligonucleotides on the flow cell. b) Clonally amplified clusters are generated through bridge amplification. Clusters are denaturated and cleaved. c) Addition of primers, polymerase and 4 reversible dye terminators, initiate sequencing. d) The incorporated fluorescence is recorded. Before the next synthesis cycle the fluor and block is removed (Voelkerding et al., 2009).

1.6 Bioinformatics Tools to Analyse Wastewater Microbiotas

1.6.1 Processing of 16S -and 18S rRNA Sequencing Data

QIIME - or Quantitative Insights Into Microbial Ecology, analyse raw 16S DNA sequence data, generated from platforms such as Illumina, through an open-source bioinformatics pipeline. The analysis involves demultiplexing and quality filtering, operational taxonomic unit (OTU) picking, taxonomic assignment, phylogenetic reconstruction and diversity

analyses (Kuczynski et al. 2012). QIIME can be used for studies of thousands of microbial samples and compare billions of sequences. The website is available at http://qiime.org/.

1.6.2 Databases to Analyze Taxonomy and Function

SILVA is an up to date, quality-controlled database of fully aligned ribosomal RNA (rRNA) gene sequences from *Eukaryota*, *Bacteria*, and *Archaea.* The first version of datasets in SILVA was made available, February 2007, by the Microbial Genomics and Bioinfomatics Researsh Group in Bremen, Germany in partnership with the RIBO GmbH company. Version 132 was released in December 2017, and the number of available small subunit rRNA gene sequences was 6.073.181 and large subunit rRNA gene sequences was 907.382. SILVA provides an ideal reference for high-throughput classification of data from next-generation sequencing (Quast et al. 2012). The website is available at https://www.arb-silva.de.

BLAST, or The Basic Local Alignment Tool is a search program for similar sequences. At BLAST, nucleotide or protein sequences is compared against a database of known sequences and calculate the statistical significance of matches. The program is used for both evolutionary and functional relationships between sequences in addition to help identify members of gene families (Johnson et al. 2008). The website is available at https://blast.ncbi.nlm.nih.gov/Blast.cgi

MiDAS provides a database with information of the microbes in activated sludge engineered ecosystems, and other similar biological wastewater treatment systems including systems with biofilm, granules and membrane-bioreators. The MiDAS project of characterising the microbial diversity in activated sludge plants was started at Aalborg University in Denmark in 2006. The taxonomy is based in the SILVA database (Mcllroy et al., 2015). The website is continuously updated at are available at http://www.midasfieldguide.org.

1.7 Aim of Thesis

Eutrophication and pollution of surface water caused by excessive contents of nutrients results in disturbances for aquatic life. However, the problem can be avoided by removing phosphorus from wastewater. Since phosphorus is becoming globally limited, biological wastewater phosphorus removal approaches which recovers the phosphorus has become highly spread and the process has a great potential to replace todays main phosphorus source derived from phosphate rock. The function, stability and efficiency of a biological wastewater treatment system is highly determined by the function of the microbiota communities. However, the knowledge of how different functional bacterial groups work together in an ecosystem and affect the overall process in biological phosphorus removal plants, is still limited.

Therefore, the main aim of this thesis was to **determine the microbiota composition on biofilm-carriers** in order to examine the potential **correlation with the phosphorus removal efficiency**.

To achieve this aim, we had the following sub-goals:

- To analyse biofilm establishment in the start-up of the establishing full-scale Hias process plant
- To analyse the biofilm stability in the established pilot Hias process plant
- To associate biofilm composition with phosphorus removal efficiency and other chemical parameters.

llumina 16S -and 18S rRNA metagenome sequencing will be used to determine the microbial taxonomic composition of both prokaryotes and eukaryotes. In addition, will qPCR be used for quantitative analysis.

2 Material and Methods

Hias WWTP in Hamar was the study site of this thesis. The material was collected from the laboratory-scale established pilot Hias process plant (i.e. established pilot plant). In this plant the biofilms were well established and previous phosphorus removal results has reached the efflux limit of 95% removal (Hias). In addition, material was collected from the full-scale Hias process plant (i.e. establishing full-scale plant) during its start-up. In this plant the biofilms were under establishment. In the results and discussion, the Hias process will often be referred to as a MBBR. The following experiments were carried out at Norwegian University of Life Science, 2017/2018.

2.1 Material Collection

The material for the experiments was the MBBR biofilm-carriers, K1 and K3 (Kaldnes, Norway) (Figure 2.1). The biofilm-carriers were collected in parallel from an established pilot (K1) -and an establishing full-scale (K3) plant by workers at Hias WTTP. The biofilms from the full-scale plant were collected approximately once every week from the start-up in May 2016, in a period from 03.06.16 to 06.09.17. The biofilms from the pilot plant were collected approximately once a week from 27.10.16 to 06.09.17. The material collection took place at the end of the aerobic zones (Figure 2.2) and mostly, three or more biofilms was taken. From each collection time, triplicates were selected when possible, to be analysed individually. After the last collection, the samples were transported on ice from Hamar to NMBU, Ås, and then stored in a – 20^{o}C freezer.

Figure 2.3 shows a schematic overview of the experiments. Material collection, sample preparation, DNA extraction, 16S/18S rRNA qPCR, and library preparation of 16S/18S rRNA amplicon for Illumina sequencing were performed in parallel on the pilot and full-scale samples.

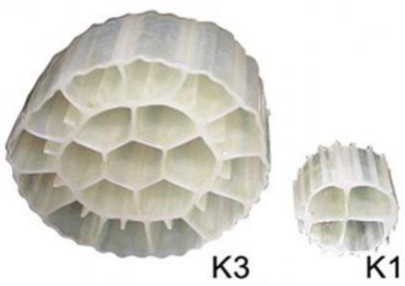

Figure. 2.1. The Kaldnes bio-carriers. The figure shows the K3 and K1 bio-carriers with surface area of 500m^2/m^3 (www.krugerkaldnes.no, 2018).

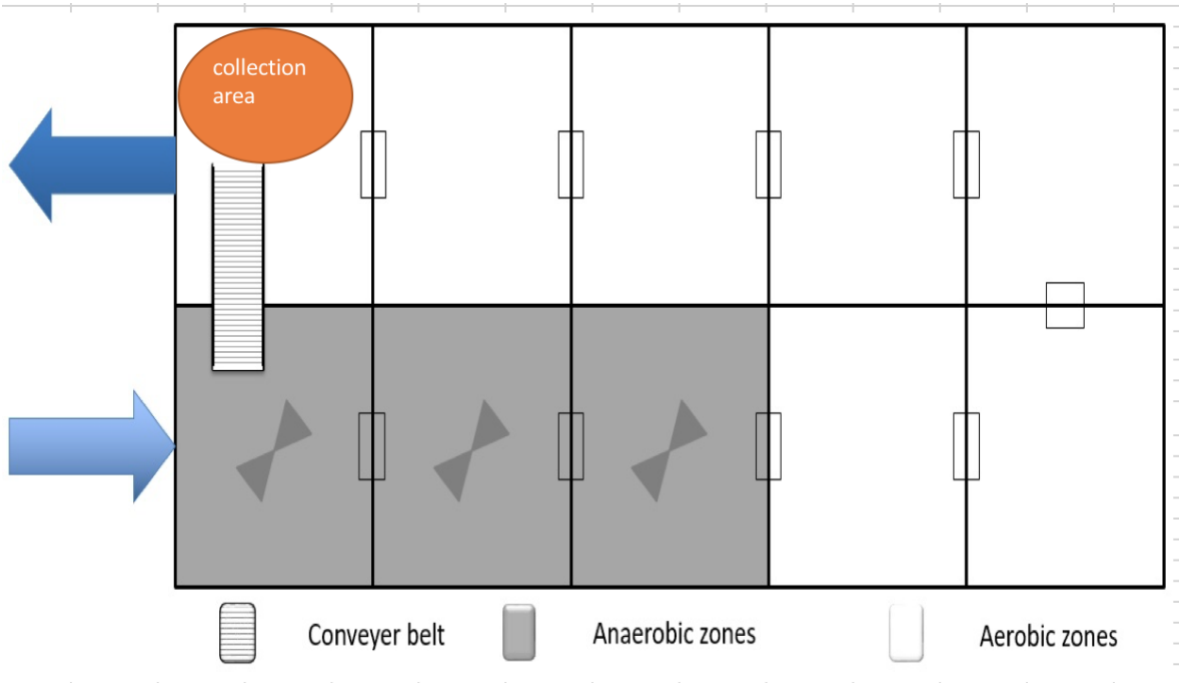

Figure 2.2 Schematic presentation of the Hias process, showing the collection area at the end of aerobic zone (orange circle) (Saltnes et al., 2017).

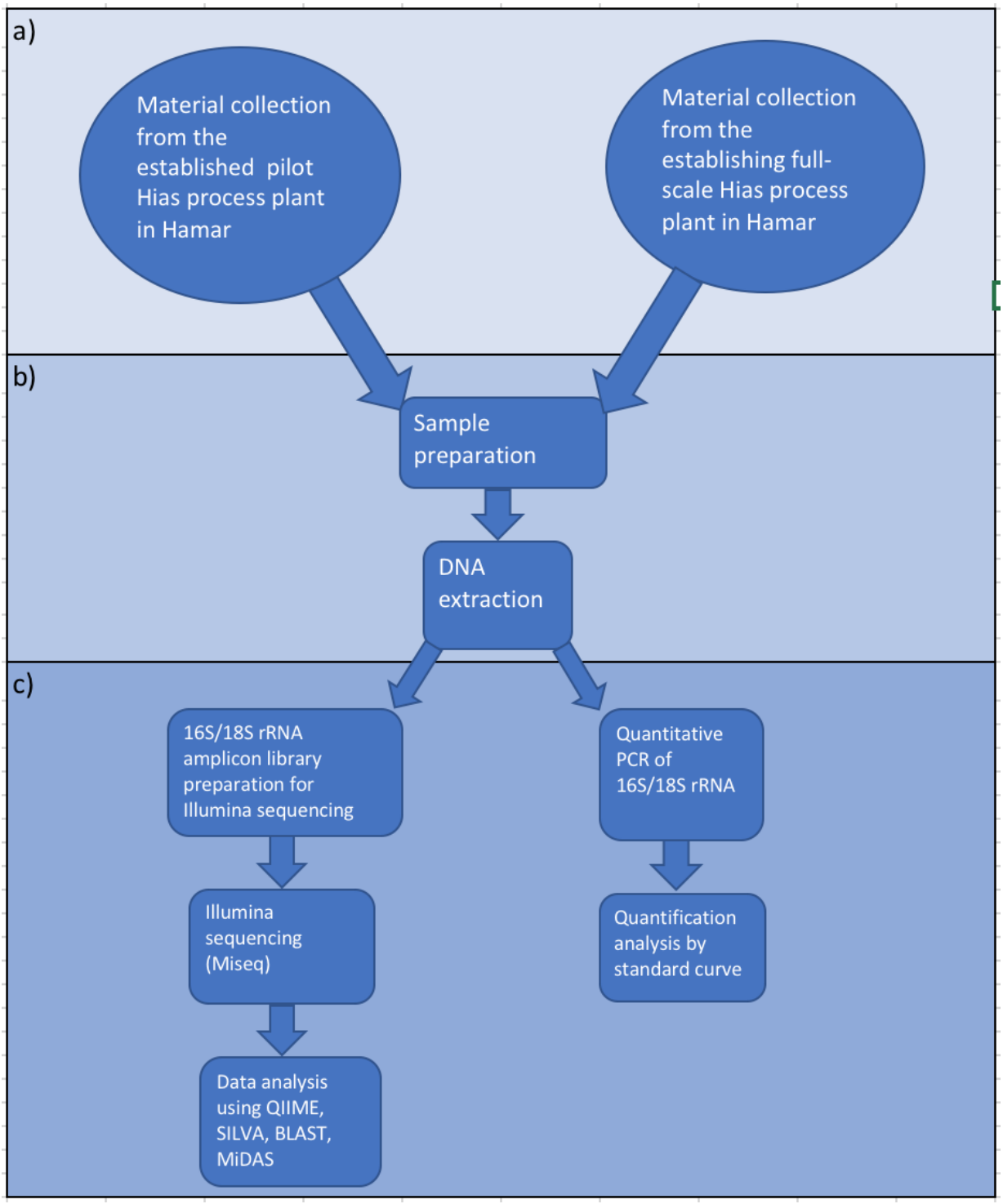

Figure 2.3. Flowchart of the experiments. a) The materials for the experiments were collected weekly in parallel from the established pilot -and the establishing full-scale Hias process plant in Hamar. b) The samples were prepared before DNA extraction. c) A two stage PCR reaction was performed in parallel on the weekly samples from the Pilot - and full-scale plant for library preparation of 16S/18S rRNA amplicon for Illumina sequencing. In addition, quantitative analysis was performed on the same samples.

2.2 DNA Lysis

Before DNA lysis, the biofilms were treated mechanically to access the DNA inside cell. First, the biofilms were cut with a scissor to fit 2 mL test tubes (Sarstedt, Germany). The whole K1 biofilms were used, while only ¼ of the K3 biofilm was used, due to large size. The cutting was performed in a fume hood to avoid contamination, and the biofilms were stored in Starstedt tubes containing glass beads (Sigma Aldrich, Norway, 0.25 g<106µM) and 500 ml STAR buffer (Roche, Germany). In addition, the scissors were washed with 96% ethanol and dried with tissue between each sample. The remaining ¾ of the K3 biofilms was further stored at – 20^{o}C.

The glass beads crush the cell membrane mechanically, whereas the STAR buffer keeps the DNA stable and prevent unwanted organism growth. The samples were in turn crushed 2 x 40 s in FastPrep96 (MP Biomedicals, USA) at 1800 rpm with 5 min break between the rounds. The breaks are important to avoid high temperatures which can degrade the DNA. At last the samples was centrifuged at 13000 rpm for 10 min to separate the supernatant which was further used for the extraction.

2.3 DNA Extraction and PCR Purification

2.3.1 Genomic DNA Extraction

DNA was isolated by the KingFisher flex robot (Thermo Scientific, USA) using the MagMidi LGC kit (LGC genomics, UK). First 50 µL of the supernatant from the previous section (2.2) was transferred to a KingFisher 96 well plate (Thermo Scientific, USA). Lysis buffer and proteinase was added to each well to cleave proteins and peptides, to get further access to the DNA. Next the KF plate incubated at 55^{o}C for 10 min, followed by the extraction. DNA extraction consisted of several steps, including a binding step where the samples was added Mag particles. The Mag particles are paramagnetic and forms salt bridges with negatively charged DNA. In addition, three washing steps was performed by the reagents BLM1 and BLM2. These reagents contain salts that keeps the DNA attached to the Mag particles, in addition to remove other unwanted compounds. At last an elution step was preformed

causing the DNA to release from the Mag particles, leading to a final product of isolated DNA. The DNA was stored at -20^{o}C for further use.

2.3.2 Ampure PCR Product Purification

Automatic purification by Biomek® 3000 Laboratory Automation Workstation (Beckman Coulter, USA) with AMPure® XP beads (Beckman Coulter, USA) was performed on PCR products after each of the two stage PCR processes. In addition, a manual purification was performed on the pooled library amplicon. Purifying PCR products before sequencing is important to remove contaminates such as primers, excessive nucleotides, or other components such as competing enzymes or buffer components. Purification involves four main steps including, binding, two times washing, and elution.

First, DNA is added into a 1:1 (08X manually) AMPure® XP beads soulution. The AMPure® XP beads are paramagnetic and forms salt bridges with the negatively charged DNA. Following, the supernatant becomes clear and in turn removed. The next two steps involve washing with 80% ethanol. Ethanol was made fresh to avoid absorption of water from the air, which can impact the results. Finally, an elution step with nuclease-free water breaks the salt bridges between the AMPure® XP beads and the DNA, leaving the pure product in the supernatant.

2.4 Polymerase Chain Reaction

Different PCR technologies was used during the experiments, including a two-step PCR process, ddPCR and qPCR. All experiments included a positive and a negative control. *Escherichia coli* (*E. coli*) served as positive control for 16S amplification, and salmon DNA was used for 18S amplification. Nuclease-free water served as negative control.

2.4.1 PCR for Illumina Sequencing Library Preparation

A two-step PCR process was performed during the Illumina sequencing library preparation of 16S -and 18S rRNA amplicon. The first step involved amplification of the desired fragments

with universal primers, and the second step involved amplification with index primers to attach Illumina adapters. The purpose of this was to make the reaction more solid and to get smoother amplifications. After each PCR process the product were purified (2.3.2).

2.4.1.1 First Stage PCR

All first stage PCR reactions consisted of "5 x HOT FIREPol® Blend Master Mix Ready to Load" (Solis Biodyne, Estonia), which is a ready-mixed solution containing all the essential reagents for a PCR reaction (Appendix A, Table A.1). Each reaction contained a concentration of 1x" 5x HOT FIREPol® Blend Master Mix Ready to Load", 0.2 µM of each primer (Invitrogen™, Thermo Fischer Scientific, USA), and 0.1-20 ng/µL of DNA (2-5 µl). Different primer sets were used for amplification of the 16S - and 18S rRNA gene. The universal prokaryote primers PRK341F and PRK806R were used for amplification of the variable regions, V3 and V4 of the 16S rRNA gene. In contrast, the eukaryote primers 3NDF and V4_Euk_R2 was used to amplify the variable region, V4 of the 18S rRNA gene. The 3`end of both primer sets were designed to bind to the specific regions of the genes. Details about the primers are listed in Table 2.1. Before amplification the solution was mixed by spinning.

All PCR reactions for Illumina sequencing library preparation were performed on a 2720 Thermal Cycler (Applied Biosystem, USA), and the following thermocycling program was used for amplification of the 16S/18S gene. First an initial denaturation step was set at 95°C for 15 min, followed by 30/35 cycles of denaturation step at 95°C for 30 s, annealing step at 55°C/59°C for 30 s, and elongation step at 72°C for 45 s. At last an elongation step was run at 72°C for 7 min before cooling at 4°C ∞.

2.4.1.2 Index PCR

The index PCR reaction contained the ready-to use mix "5 x FIREPol® Master Mix Ready to Load" (Solis Biodyne, Estonia) (Appendix 1, Table A2). Each reaction contained a final concentration of 1 x "5x FIREPol® Master Mix Ready to Load", 0.2 µM of each index primer (Invitrogen™, Thermal Fischer Scientific, USA), and 0.1-20 ng/µL of DNA (2-5 µL). During index PCR, the 5`end of the primers were modified with an adaptor sequence, in addition to an Illumina sequence region, and a unique primer tag sequence. The adaptor sequence is

complementary to oligonucleotide sequences on the flow cell surface of the Illumina sequence platform. 16 unique forward -and 36 unique revere primers were utilized, which gives 576 possible different primer combinations. By combining the primers differently, every sample had a unique primer combination to ensure separation of the samples during sequencing (Listed in Appendix B). The index primer was dispensed into the wells of PCR plates by the The Eppendorf epMotion 5070 robot. After mixing the solutions, the samples were amplified.

The 16S/18S rRNA gene was amplified with the following thermocycling program. An initial denaturation step was set at 95^{o}C for 5 min, before 10 cycles of denaturation step at 95^{o}C for 30 s, annealing step at 55^{o}C/59^{o}C for 1 min, and elongation step at 72^{o}C for 45 s. Finally, an elongation step was set at 72^{o}C for 7 min, followed by cooling at 4^{o}C ∞.

2.4.1.3 Digital Droplet PCR

Digital droplet PCR (Bio-Rad, USA) was used to measure the concentration of the pooled amplicon library. ddPCR measures absolute quantities by counting nucleic acid molecules encapsulated in water-in-oil droplet partitions.

The droplet generation was prepared by making four individual parallel dilution serials (10^{-6}-10^{-9}) of the amplicon library. In addition, a reaction master mix generated, which included 1 x "2 x Super mix for EvaGreen" (Bio-Rad, USA), 0.2 µM Illumina colony forward primer, 0.2 µM Illumina revers primer (Thermal Fischer Scientific, USA), and nuclease-free water. The master mix and the four amplicon library dilution serials were then transferred into two PCR strips and in turn mixed.

During the droplet generation, specific pipetting techniques was used according to BioRad to avoid bubbles. First, the solution from the preparation step and EvaGreen generation oil, was added into a sample well of cartridge. Next, a gasket was hooked on and then the droplet generation started. After the droplet generation, mixing was avoided due to vulnerability. The obtained droplets were transferred into a PCR plate (BioRad, USA) and sealed with Foil Heat Seals at 180^{o}C for 5 s in a Plate sealing instrument form BioRad. At last, the samples were quantified.

The following thermal conditions was used for the ddPCR reaction. An enzyme activation step was set at 95°C for 5 min, followed by 40 cycles of denaturation step at 95°C for 30 s, annealing step at 60°C for 30 s, and elongation step at 72°C for 45 s. Finally, a signal stabilization step was run at 4°C for 5 min, followed by an enzyme deactivation step at 90°C for 5 min, before cooling at 4°C ∞.

2.4.2 Quantitative PCR

Quantitative PCR was used to detect and quantify the original DNA copies of the prokaryotes and eukaryotes present on the biofilms from the pilot –and full-scale plants.

All qPCR reactions consisted of the ready-to use solution "5 x HOT FIREPol® EvaGreen® qPCR supermix" (Solis BioDyne, Estonia) (Appendix A, Table A3). Each reaction contained a final concentration of 1x "5 x HOT FIREPol® EvaGreen® qPCR supermix", 0.2 µM of the same primers as described in section 2.4.1.1, and 0.1-20 ng/µL of DNA (2 µL) The reagents were well mixed and then detected by LightCycler480 II (Roche, Germany).

The thermal conditions for the qPCR reaction of the 16S/18S rRNA gene were as following. An initial denaturation step was run at 95°C for 15 min, followed by 40 cycles of denaturation step at 95°C for 30 s, annealing step at 55/59°C for 30 s, and elongation step at 72°C for 45 s.

After amplification, absolute quantification analysis was preformed to find the total amount of bacteria and eukaryote in the samples from both the established pilot and establishing full-scale plant. This was achieved by comparing the samples Ct-values to a standard curve. An individual standard curve was generated for both the 16S and 18S rRNA gene analysis by different known amount of a template which was analyzed by qPCR. The Ct-values from the analysis was plotted on the x-axis and the log of starting quantity of the samples on the y-axis. An equation was generated from the linear regression data analysis and was used to calculate Log10 of 16S/18S rRNA gene copy number per sample.

Table 2.1. An overview of the different primers that were used for PCR and their properties.

Primer name	Primer sequence 5`-->3`	Target gene	Gene length	Annealing temp (˚C)	References
PRK341F	CCTACGGGRBGCASCAG	V3-V4 region of 16S rRNA	466	55	Yu et al. 2005
PRK806R	GGACTACYVGGGTATCTAAT	V3-V4 region of 16S rRNA	466	55	Yu et al. 2005
3NDF1	GGCAAGTCTGGTGCCAG	V4 region of 18S rRNA	450	59	Cavaller-Amith et al. 2009
V4_Euk_R2[2]	GACTACGACGGTATCT(AG)ATC(AG)TCTTCG	V4 region of 18S rRNA	450	59	Bråte et al. 2010

2.5 Next Generation Sequencing

2.5.1 16S -and 18S rRNA metagenome sequencing

The next generation sequencing technology, Illumina sequencing, was used for 16S -and 18S rRNA metagenome sequencing to identify the prokaryotes and eukaryotes present on the biofilm carriers. Prior to sequencing, the procedure included several preparation steps. Firstly, library quantification, normalization, and pooling of the index PCR product was performed. The index PCR product concentrations were quantified with Qubit reagents and measured by Cambrex – FLX 800 CSE (Thermo Fischer Scientific, USA). The index PCR products were then pooled into a library amplicon according to the concentration in a roughly way. Further, 5 µL index PCR products were transferred form samples with RFU (Relative fluorescence units) between 800-1200, 10 µL index PCR products were transferred form samples with RFU <800, whereas 2.5 µL index PCR products were transferred form samples with RFU >1200. Next, the pooled library amplicon was manually purified by Ampure purification. The pure library was then absolute quantified by ddPCR. The ddPCR results were in turn used to quantify the concentration (nM) of the pooled library amplicon in excel. At last the pooled library was diluted to 4 nM, in 10 mM Tris pH 8.5.

The second preparation step involved denaturation and dilution of the library and a PhiX control (Illumina, USA). PhiX serve as a control in serval areas, including cluster generation, sequencing, and alignment. First, 4 nM library was added into a 1:1 0.2 N sodium hydroxide (NaOH) solution. NaOH denature double stranded DNA into single stranded DNA. The denatured DNA was then diluted 1:100 in hybridization buffer, HT1. Followed by another dilution in HT1, leading to a final concentration of 6 pM. In parallel, the PhiX control was denatured in NaOH and diluted in HT1. In the final preparation step, the library amplicon

was combined with 15% of the PhiX library solution. The final library was at last loaded into the MiSeq reagent cartridge for template loading on the MiSeq flow cell.

2.5.2 Analysis of 16S -and 18S rRNA Sequencing Data

The 16S -and 18S rRNA sequences were processed and analysed individually through the QIIME pipeline in several steps. The sequences went through pre-processing which involved, demultiplexing, truncating primers and quality filtering. The following step involved OTU-processing, were the OTUs were first clustered at a 97% homology level creating an OTU-table, and then the OTUs were given a taxonomy by a reference-search in the SILVA database. The last pipeline step involved a core diversity analysis. In this step alfa and beta analyses were made, and taxonomic tables. In addition, different taxonomic plots were generated, rarefaction plots and Unifrac principal coordinates analyses. A few OTUs with poor classification went through a further reference-search in BLAST. The 16S rRNA OTU-tables were further used to analyse the functional bacteria composition, and to analyse the development of biofilms in the establishing full-scale plant.

The composition of functional bacteria was investigated in the samples from both the established pilot and the establishing full-scale plant. First, known functional bacteria common in EBPR systems were searched for in the 16S rRNA OTU-table. In addition, abundant OTUs were searched against the MiDAS database to find if they had any known function. Next, the average abundance of OTUs with the same functional bacteria family/genus/species was calculated. Then trendlines were made, where the average functional family/genus/species abundance was plotted against the material collection week number. In addition, trendlines representing only bacteria groups with same function were constructed, where the average abundance of functional bacteria group was plotted against the material collection week number.

Further OTU analyses were performed to investigate the biofilm development on bio-carriers during the establishment of the full-scale plant. The investigation was performed by first finding the most abundant bacteria (attaching bacteria) in the first weekly sample from the OTU-table. The OTU sequence limit was set to >90 sequences to be considered attaching bacteria. Trendlines were then made to present the development of the attaching bacteria

from the first to the last week of development, where the average abundance of attaching bacteria was plotted against the material collection time from the established full-scale plant.

The biofilm development was further investigated by analyzing the development of the bacteria which represented the highest abundance in the last weekly sample (most established bacteria). This was done in the opposite way as describe above, where the OTU-table was used to find the most abundant bacteria in the last weekly sample. The OTU sequence limit was again set to >90 sequence. Trendlines were then made to present the development of the most established bacteria from the first - to the last week of development, where the average abundance of the most established bacteria was plotted against the material collection time from the establishing full-scale plant.

2.6 DNA Quantity and Integrity

2.6.1 Gel Electrophoresis

Agarose gel electrophoresis was used to analyze PCR products. The method is efficient and can separate fragments of sizes between 100 bp-25 kb. After each round of the two stage PCR process, the following was performed on randomly selected samples.

Firstly, a 1% agarose gel was prepared by mixing agarose (Sigma Aldrich, Germany) in 1x tris-acetate ethylenediaminetetraacetic acid (TAE) buffer. The solution was dissolved by boiling, followed by cooling in water bath. TAE buffer was both used in the gel and as a running buffer. When agarose dissolves in TAE buffer, channels of pores forms where DNA can diffuse. 1% agarose is optimal for separation of the 16S/18S rRNA fragments with sizes of 450-500 bp. Before jellification, Peq (Saveen & Werner, Sweden) was added to the solution. Peq and DNA forms a fluorescent complex which is visible in UV light and makes it possible to track the fragments during and after the electrophoresis.

Secondly, the electrophoresis was prepared. 5 µL of PCR product, in addition to controls and 100 bp ladder (Solis BioDyne, Estonia) were loaded into individual wells at the gel in a gel electrophoresis camber. The PCR product either contained a ready-to load mix, or it was added a loading dye. At last, the electrophoresis was run at 80 V for 30 min and the results

where visualized in UV light using The Molecular Imager® Gel Doc™ XR Imaging system with Quantity one 1 – analysis software v.4.6.7 (BioRad, USA).

2.6.2 DNA Quantification with Qubit Reagents

Genomic DNA -and PCR product concentrations were measured by Qubit™ fluorometer (Thermo Fischer Scientific, USA) or Cambrex –FLX 800 CSE (Thermo Fischer Scientific, USA). A 1:200 Quant-iT™ Working Solution (Life Technologies, USA) was prepared from Quant-iT™ and Quant-iT™ buffer. The solution consists of fluorophores, which becomes fluorescent when bound to DNA. The intensity of the DNA-fluorophore complex is decided by the amount of the target molecule in the sample. Qubit™ fluorometer measurement was performed by adding 2 µL DNA template/PCR product into 198 µL working solution. In contrast, Cambrex – FLX 800 CSE measurement was performed by adding 2 µL PCR product into 70 µL working solution in the wells of a nunc plate. The calibration was set as recommended by the producer.

2.7 Wastewater Analyses

The wastewater in the established -and establishing Hias process plants were analysed in parallel with the material collection to get data to correlate with the microbiota composition. The wastewater was detected and analysed by workers at Hias WWTP in Hamar. They detected the percentage removal of PO_4 and soluble chemical oxygen demand (SCOD), the wastewater SCOD -and PO_4 load per day. All samples were grab samples, taken manually and filtered through 1 µm fiberglass filter and analysed for dissolved phosphorus and SCOD with a NOVA spectroquant 60 spectrometer (Sondre Eikås, personal communication, 17 April, 2018). In addition, the inlet volume and the temperature of the wastewater was measured. All data were used to make plots, with the wastewater data was plotted against the material collection week number.

3 Results

3.1 Quantitative DNA Analyses

After the DNA extraction of the samples from the established pilot -and establishing full-scale plant, qubit measurements were performed on a few selected samples to ensure presence of DNA. The measurement showed that all samples contained DNA with a concentration ranging between 13.1 and 44.7 ng/µL.

Quantification of the bacteria and eukaryotes in the samples were detected by qPCR. Figure 3.1 shows the total copy number of 16S (a, c) -and 18S rRNA gene (b, d) plotted against the weekly samples from the established pilot (a, b) -and establishing full-scale plant (c, d). Total copy number of 16S rRNA gene in the pilot plant samples ranged approximately between 10^6-10^9 (Figure 3.1.a), while 18S rRNA gene in the pilot samples ranged approximately between 10^4-10^8 (Figure 3.1.b). The total copy number of 16S rRNA gene in the full-scale plant samples ranged between 10^5-10^9 (Figure 3.1.c), while the 18S rRNA gene in the full-scale plant ranged approximately between 10^3-10^5 (Figure 3.1.d).

There were small shifts in the total 16S rRNA gene copy number the first 17 weeks in the pilot plant, before it increased and stabilized (Figure 3.1.a). The total 18S rRNA copy number in the pilot plant had variations through the whole timeline (Figure 3.1.b). The total copy number increased the first 14 weeks, before it droped, and increased in week 16-20, before the number droped again. Towards the end, the total copy number increased gradually. There was a gradual decrease in total 16S rRNA gene copy number from week 1-28 in the establishing full-scale plant (figure 3.1.c). From week 29-31 the number started to increase again and somewhat stabilized. The number of 18S rRNA copy number increased the first 6 weeks in the establishing full-scale plant (Figure 3.1.d), while from week 7-17 the number of copies dropped, and varied a slight towards the end of the experiment.

a)

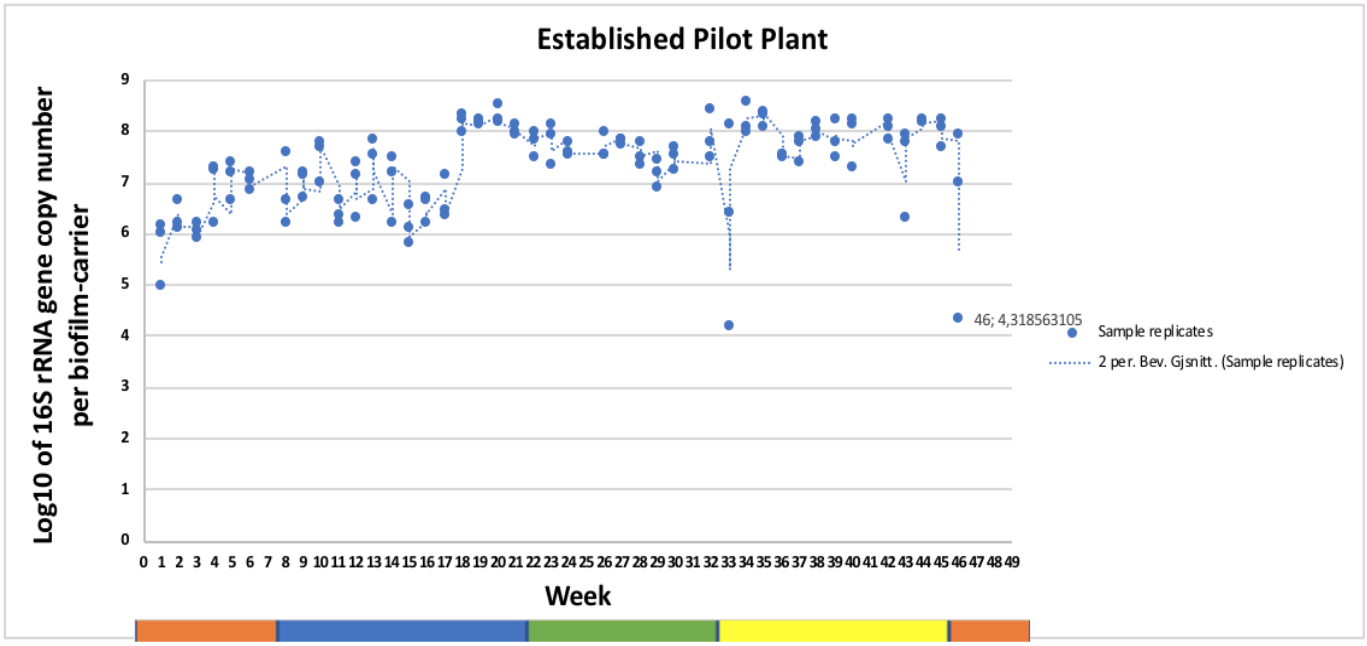
Established Pilot Plant
Log10 of 16S rRNA gene copy number per biofilm-carrier
Week
46; 4,318563105
Sample replicates
2 per. Bev. Gjsnitt. (Sample replicates)

b)

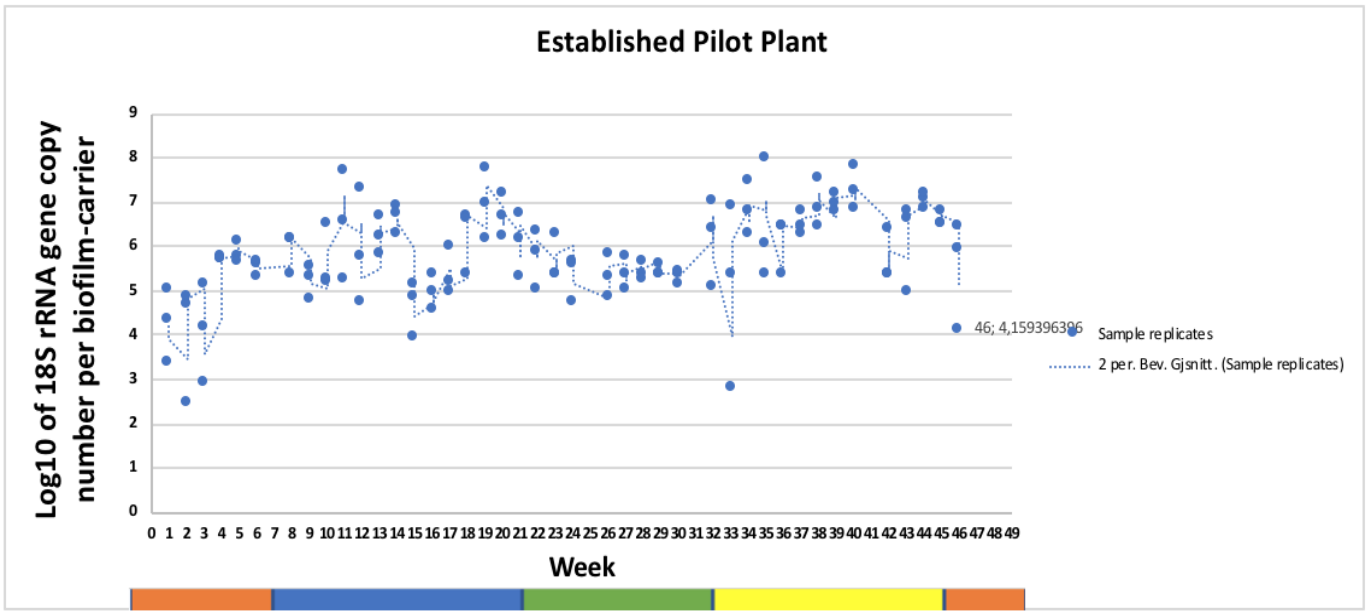
Established Pilot Plant
Log10 of 18S rRNA gene copy number per biofilm-carrier
Week
46; 4,159396396
Sample replicates
2 per. Bev. Gjsnitt. (Sample replicates)

c)

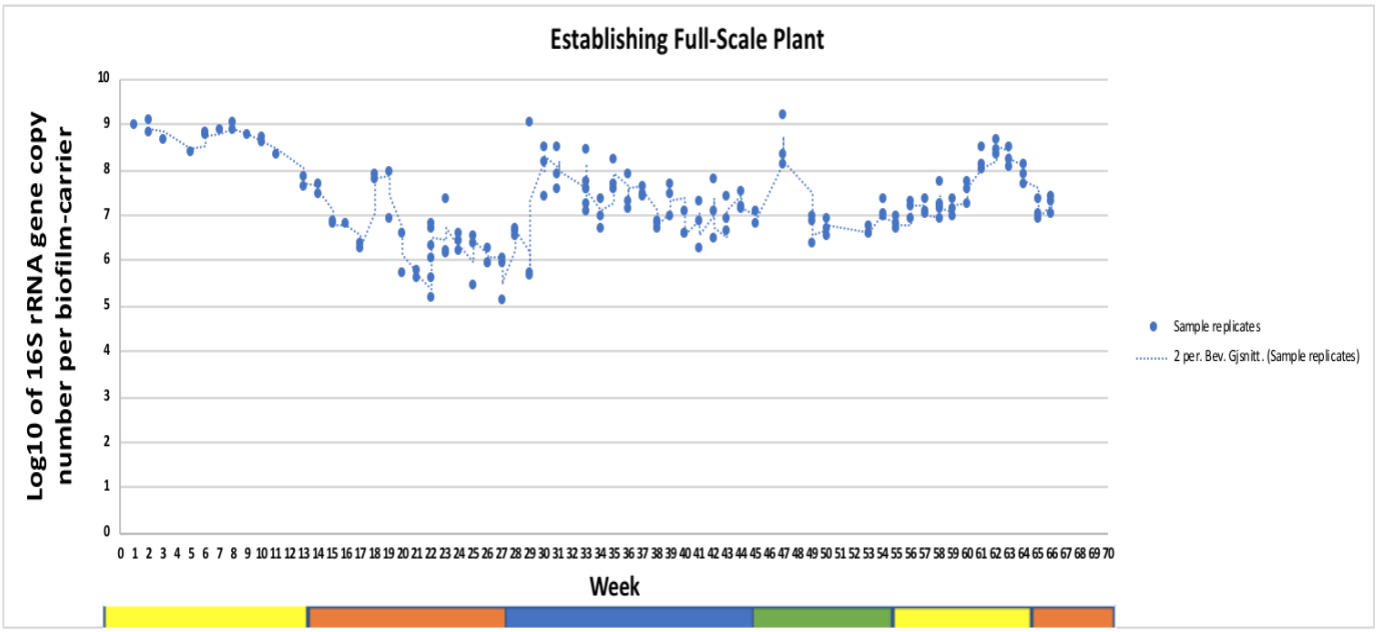

d)

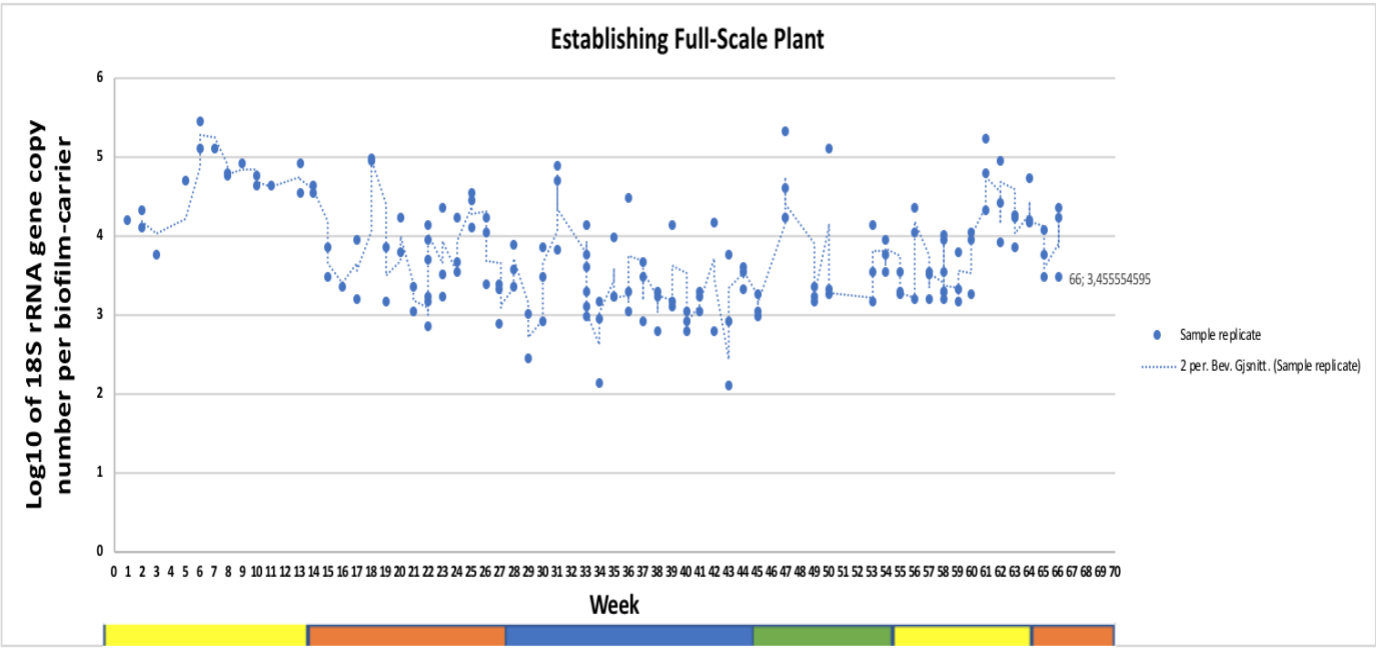

Figure 3.1. Log10 of the total copy number of 16S (a, c) -and 18S rRNA gene (b, d) plotted against the weekly samples from the established pilot (a, b) -and establishing full-scale plant (b, d). The season of the weekly samples are shown in color-codes. Yellow = summer, orange = autumn, blue = winter, and green = spring.

3.2 16S/18S rRNA Metagenome Analyses

The microbiota -and eukaryotic composition were determined by 16S -and 18S rRNA metagenome sequencing. The 16S rRNA metagenome sequencing was performed on samples from both the established pilot -and the establishing full-scale plant. In contrast the 18S rRNA metagenome sequencing were only preformed on the samples from the established plant, due to low amount of eukaryotic DNA in the samples from the full-scale plant. All sequences were analyzed in QIIME.

A total of 4406897 16S rRNA sequences and 2931910 18S rRNA sequences were detected in the samples from the established pilot plant after the quality filtering. The 16S rRNA sequences were clustered with 97% homology level using SILVA database to construct an OTU-table. The OTU-table was then process again, where 9000 sequences were randomly chosen to ensure an even sequence information, leaving out 17 samples. The final OTU-table contained 113 samples with 1678 OTUs. The same processing was done for the 18S rRNA sequences, however the OTU-table was processed with 2000 randomly chosen sequences instead of 9000 for an even sequence information. 39 samples were left out and the final OTU-table contained 99 samples with 835 OTUs.

In the samples from the establishing full-scale plant a total of 4790874 16S rRNA sequences were detected after the quality filtering. The same processing as described above was performed on the 16S rRNA sequences from the establishing full-scale plant. 9000 sequences were randomly chosen to ensure an even sequence information for the OTU-table construction, leaving out 15 samples. The left-out samples included the last nine weekly samples. The final full-scale samples contained 116 sample with 2021 OTUs.

3.2.1 α-diversity

α-diversity was performed for bacteria -and eukaryote species diversity investigation in samples from the established pilot plant and for bacteria species diversity investigation the establishing full-scale plant. Rarefraction curves were made by diversity calculations in QIIME, where the average number of observed species was plotted against the amount of

sequences per samples. Calculations where preformed on samples from the established plant to compare the bacteria and the eukaryote species diversity in the samples between the weeks (Figure 3.2.a). The samples had a similar bacteria diversity between the weeks, but differences were detected with the lowest bacteria diversity difference in the samples from the first week. In contrast, the eukaryote diversity was lower and more different between the weeks (Appendix C, Figure C.1). The calculations were also done on samples from the establishing full-scale plant to compare the bacteria species diversity in the samples between the weeks (Figure 3.2.b). Compared to the bacteria species diversity in the established plant, these samples were more different in diversity between the weeks and the lowest diversity was detected in the samples from the first -, second -and third week.

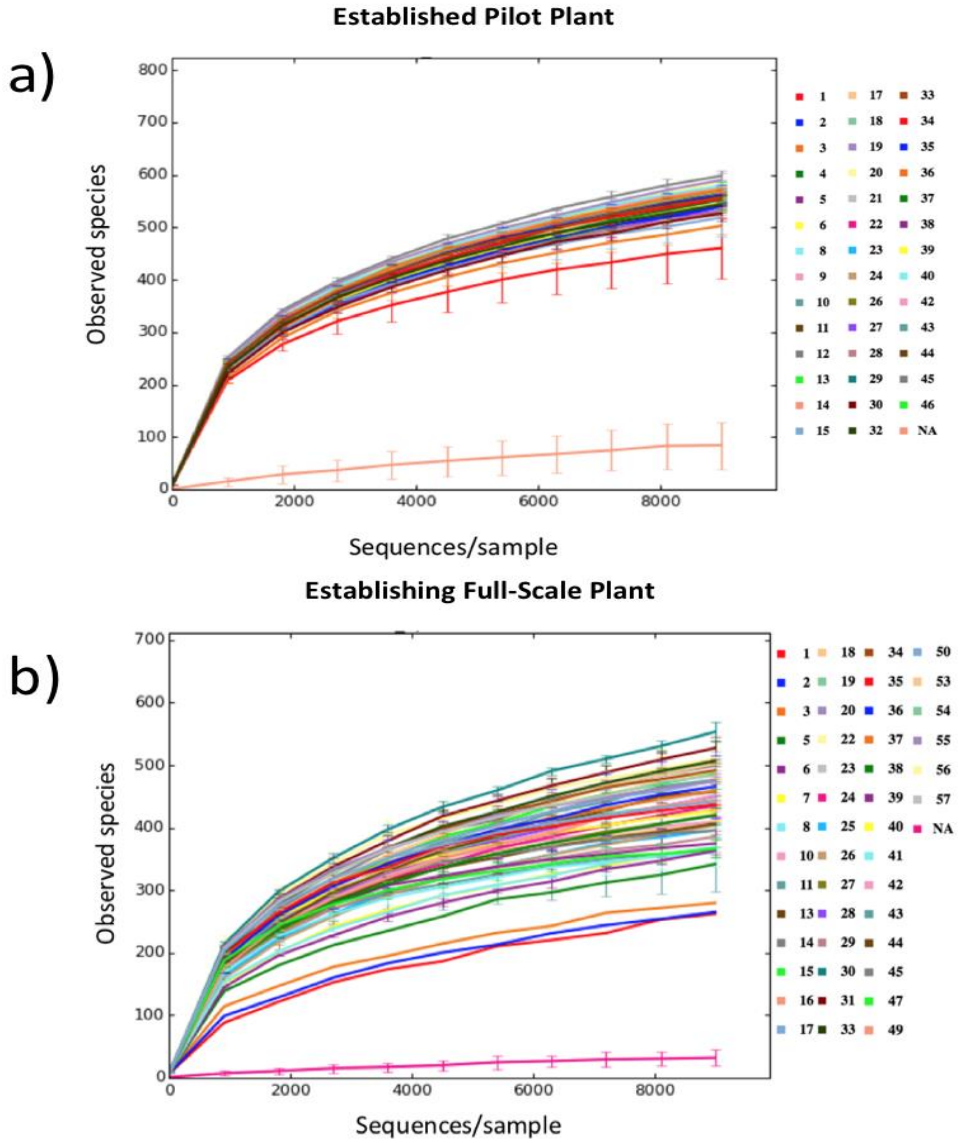

Figure 3.2 Rarefaction curves of observed bacteria species in the number of sequences per sample. The Colours represent the weekly samples. a) Observed bacteria species in weekly samples from the established pilot plant. b) Observed bacteria species in weekly samples from the establishing full-scale plant. The deviant represents the positive control (NA).

3.2.2 β-diversity

UniFrac principal coordinate`s analysis (PCoA) plot was used to analyze the variation between the bacteria -and the eukaryote samples from the established plant, and the variation between the bacteria the establishing plant. The Unweighted Unifrac PCoA plot of the established plant samples show two close groupings of the bacteria samples (red and green circle) (Figure 3.3.a). In contrast the eukaryotic samples were highly spread (Appendix C, Figure C.2). The Unweighted Unifrac PCoA of the establishing plant samples shows the

differences in the bacteria samples was higher compared to the established plant (Figure 3.3.b). The variation decreased with time, where the first weekly samples were more different (green circle) than the last weekly samples which is more grouped (red circle).

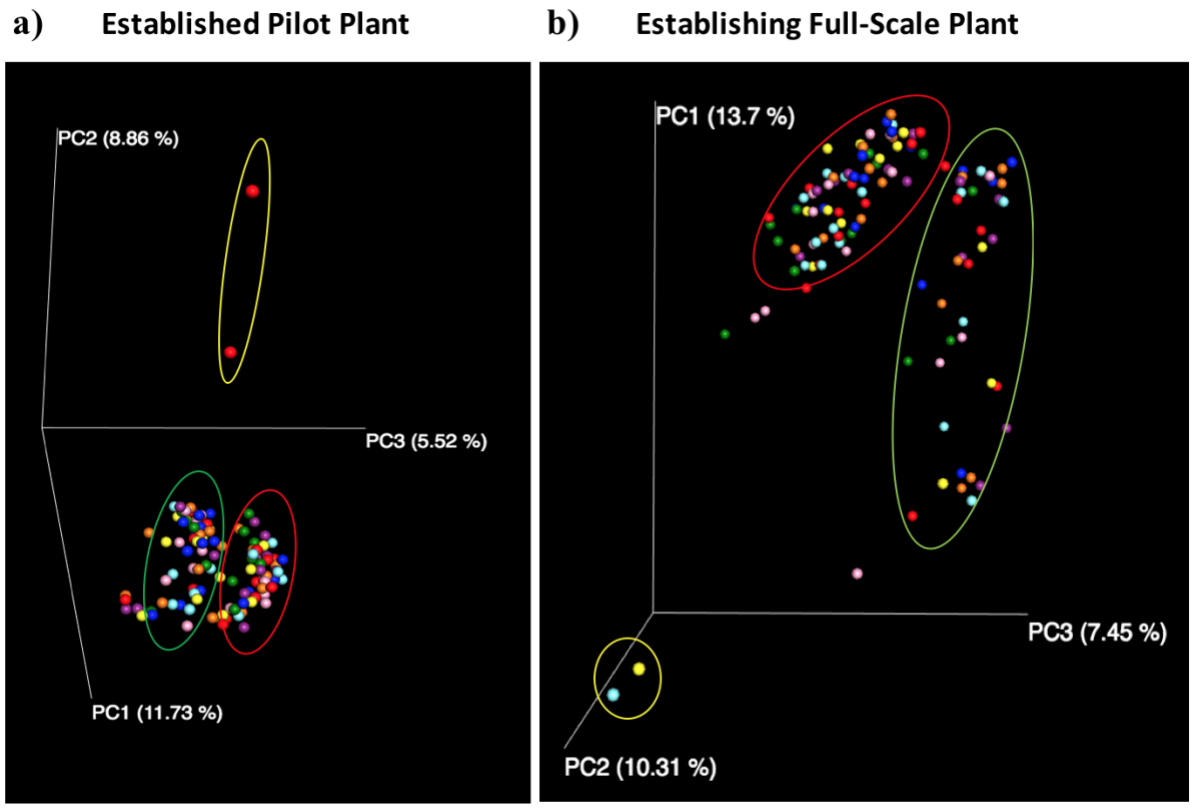

Figure 3.3 Unweighted Unifrac PCoA plots. a) Variation between the weekly samples from the established Pilot plant. The green and red circle shows two close groupings. b) Variations between the weekly samples in the establishing full-scale plant. The green circle represents the first weekly samples, whereas the red circle represents the latest weekly samples. The positive controls are shown in the yellow circle.

3.2.3 Taxonomic Analysis

Bar-charts were generated to investigate the bacteria and eukaryotic taxonomic composition in the samples from the established pilot -and the establishing full-scale plant at genus level (Figure 3.4). The taxonomic composition of bacteria at genus level were highly diverse throughout the experiment in the pilot plant (Figure 3.4.a). The composition was somewhat stable but had clear shifts in week 18 and 39. The first three weekly samples from the full-scale plant had a lower diversity (Figure 3.4.b). However, the rest of the samples had a more diverse bacteria taxonomy compared to the pilot plant. In addition, the full-scale taxonomy had clear shifts from week to week, except for the last two weeks.

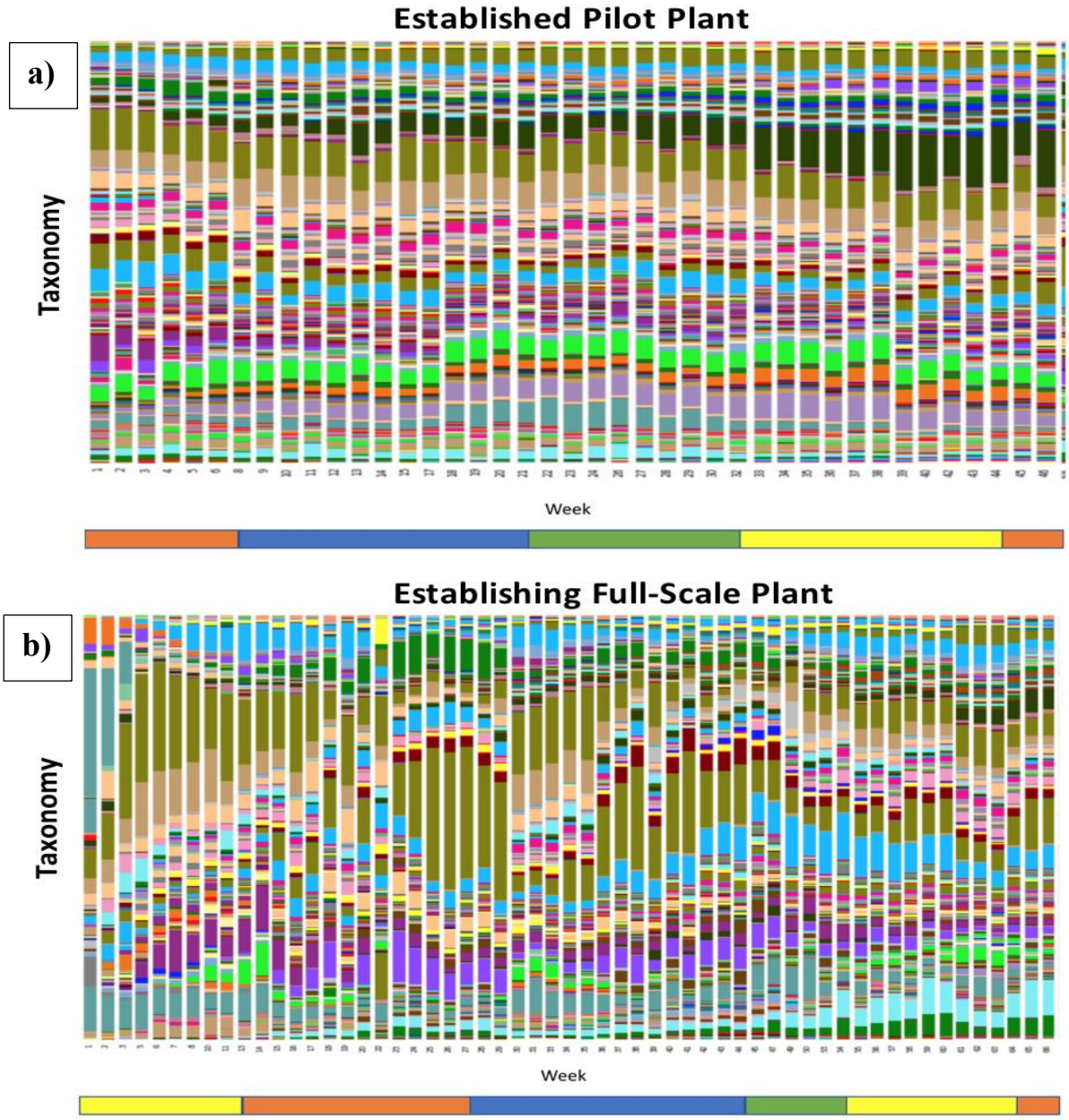

Figure 3.4 Bar chart showing the taxonomy at genus level of the bacteria found in the weekly samples form the established pilot (a) -and the establishing full-scale plant (b). The season of the weekly samples are shown in color-codes. Yellow = summer, orange = autumn, blue = winter, and green = spring.

The eukaryote taxonomic composition was only determined in the pilot samples, and showed a less diverse taxonomy, compared to the analyses of bacteria (Figure 3.5). In addition, compared to the stable bacteria taxonomy in the pilot samples the eukaryote taxonomy had clear shifts from week to week. The dominating eukaryote belonged to the genus, *Telotrochidium, Cryptomycota, Salpingoecidae, Vorticella, and Rhogostoma.*

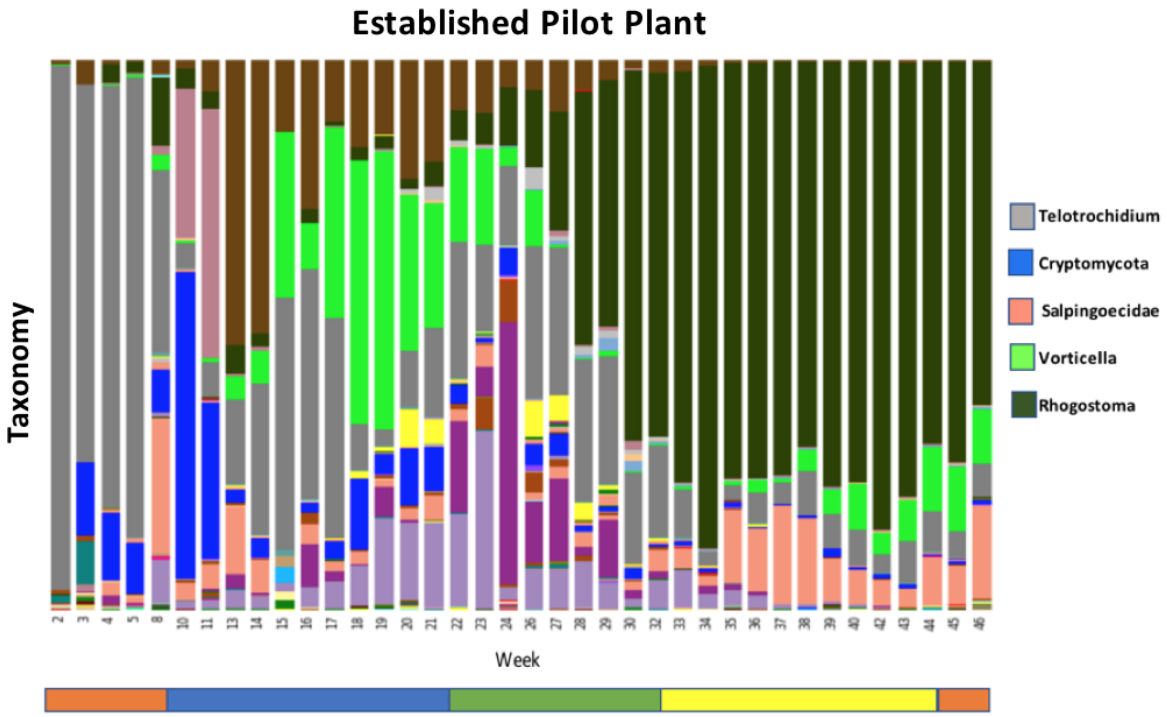

Figure 3.5 Bar chart representing the taxonomy at genus level of eukaryotes found in the weekly samples form the established pilot plant. The season of the weekly samples are shown in color-codes. Yellow = summer, orange = autumn, blue = winter, and green = spring.

3.3 Functional Bacteria Analyses

Trendlines were made to investigate the composition of functional bacteria in the samples from the established pilot -and the establishing full-scale plant. Figure D.1 in Appendix D, show the average abundance of functional bacteria family/genus/species plotted against the material collection week. *Accumulibacter*-PAO was the most abundant functional bacteria with an average abundance of 7.16% in the established pilot plant (Appendix D, Figure D.1.a). In contrast the average abundance of *Tetrasphaera*-PAO was only 1.57%. The filamentous bacteria, *Saprospiraeceae*, was the second most abundant functional bacteria with an average of 4.46%, whereas the third most abundant functional bacteria were the denitrifying, *Hydrogenophaga,* with an average of 4.21%.

Figure D.1.b in Appendix D, show the development of the functional bacteria family/genus/species in the establishing plant. The figure shows major shifts through the whole time-line. The most abundant bacteria in the first weekly samples was the

denitrifying/fermenting bacteria, *Flavobacterium*, with an average abundance of 7.68%. The average abundance of *Accumulibacter*-PAO in the first weekly sample were 1.53%, while in the last weekly sample it was 1.77%. The average abundance of *Tetrasphaera*-PAO were 0.02% in the first weekly sample, whereas as high as 6.60% In the last weekly sample..

Figure 3.6 shows the average abundance of bacteria groups with same function (a, c), and the phosphorus -and SCOD removal (b, d) plotted against the material collection week from the established (a, b) -and the establishing plant (b, d). The average abundance of all functional bacteria found in the samples from the establishing plant was 40.61%, and the abundance was stable from start to end of the sampling time (Figure 3.6.a). The average abundance of PAO was 8.73%, and ranged between 2.98-15.91%. The average abundance of GAO was 0.28%, and ranged between 0.06-0.49%. The average abundance of nitrifies was 0.05%, and ranged between 0.01-0.15%, while the average abundance of denitrifies was 16.38%, and ranged between 12.33-22.09%. The average abundance of fermenting bacteria was 10.28%, and ranged between 5.30-16.25%, whereas the average abundance of filamentous bacteria was 4.89%, and ranged between 3.12-6.37%. The average PO_4 removal was 94.45% in the established plant and ranged between 78.68-98.69% (Figure 3.6.b). The average SCOD removal was 65.97%, and ranged between 47.29-78.00% (Sondre Eikås, personal communication, 11 April, 2018).

Figure 3.6.c shows the development of the functional bacteria in the weekly samples from the establishing full-scale plant. The average abundance of functional bacteria varied a lot through the time-line. The average PAO abundance ranged between 0.7-8.38%, while the GAOs ranged between 0.01-1.45%. The average abundance of denitrifies ranged between 3.16-40.39%, while the nitrifies was completely absent. The average abundance of fermenting bacteria ranged between 7.91-24.61%, and the filamentous bacteria ranged between 0.72-8.17%. Figure 3.6.d shows, the development of the PO_4 -and SCOD removal from week 1 to week 57 during the establishment of the full-scale MBBR plant. The PO_4 removal range between 29.77-99.02%, where the PO_4 removal after week 1 was 31.70%, while 98.47% after week 57. The SCOD removal range between 18.33- 82.96%, where the SCOD removal after week 1 was 78.75% and 65.71% after week 57 (Sondre Eikås, personal communication, 11 April, 2018).

a)

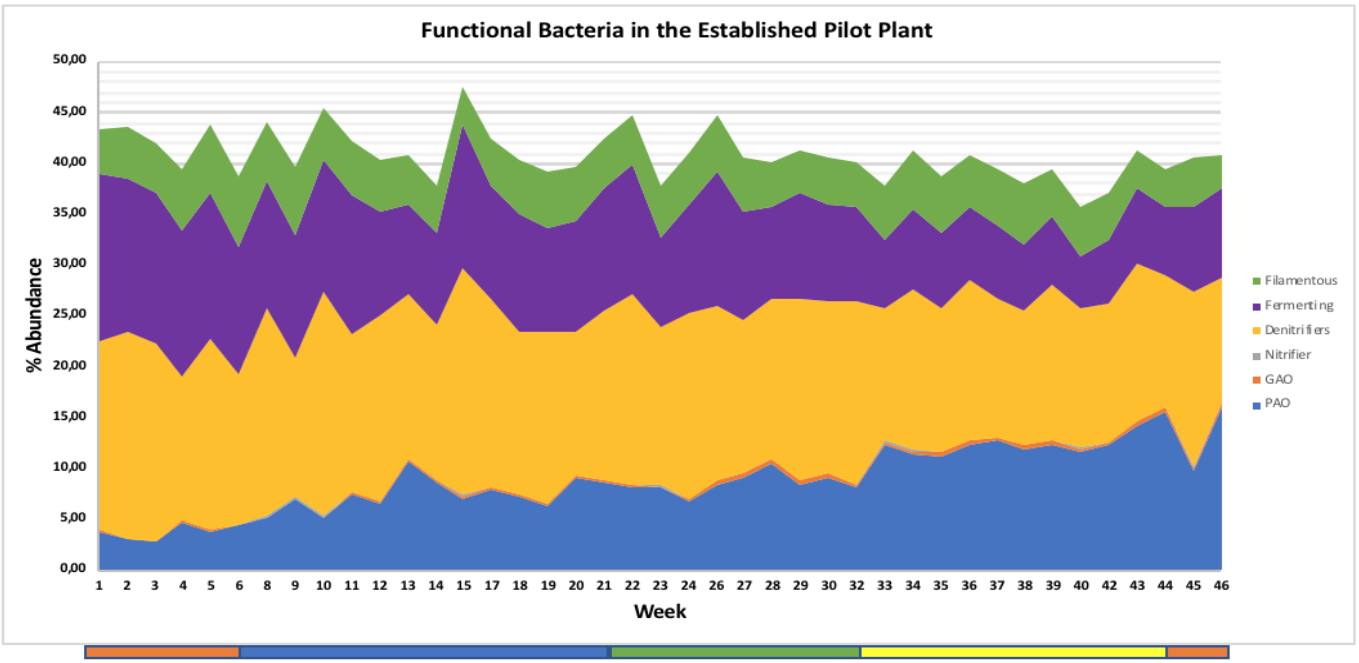
Functional Bacteria in the Established Pilot Plant
% Abundance
50,00
45,00
40,00
35,00
30,00
25,00
20,00
15,00
10,00
5,00
0,00
1 2 3 4 5 6 8 9 10 11 12 13 14 15 17 18 19 20 21 22 23 24 26 27 28 29 30 32 33 34 35 36 37 38 39 40 42 43 44 45 46
Week
Filamentous
Fermenting
Denitrifiers
Nitrifier
GAO
PAO

b)

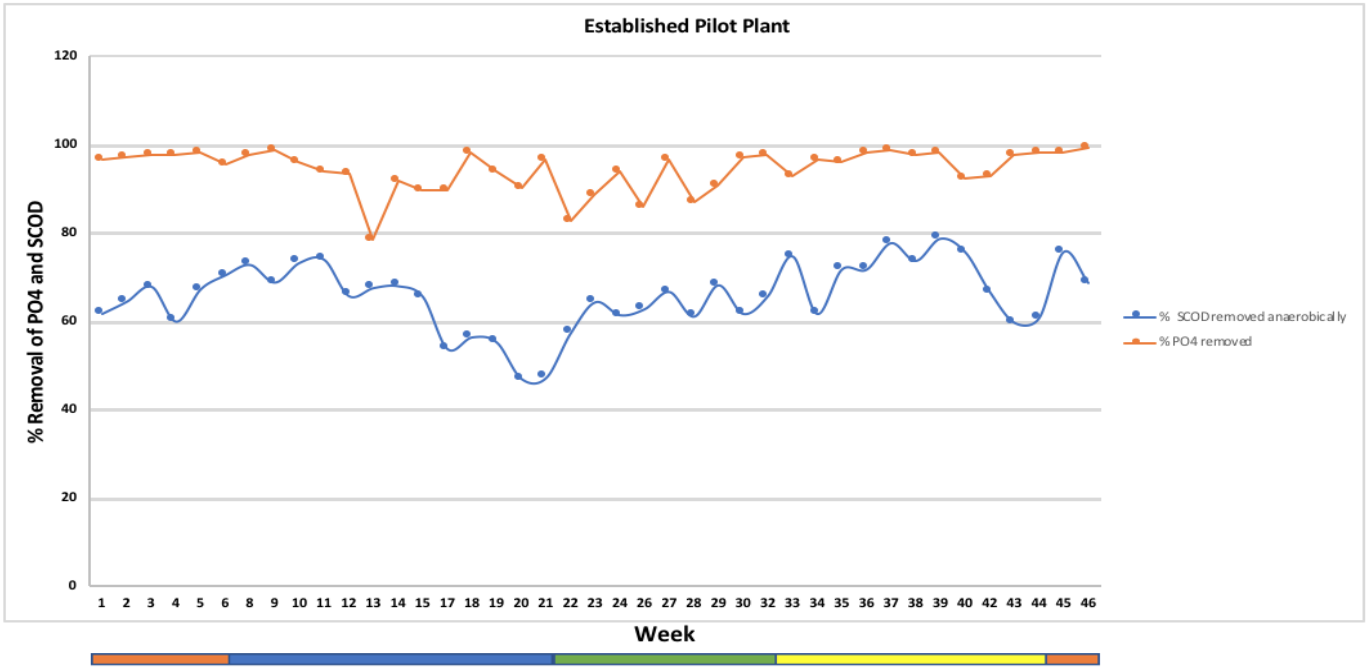
Established Pilot Plant
% Removal of PO4 and SCOD
120
100
80
60
40
20
0
1 2 3 4 5 6 8 9 10 11 12 13 14 15 17 18 19 20 21 22 23 24 26 27 28 29 30 32 33 34 35 36 37 38 39 40 42 43 44 45 46
Week
% SCOD removed anaerobically
% PO4 removed

c)

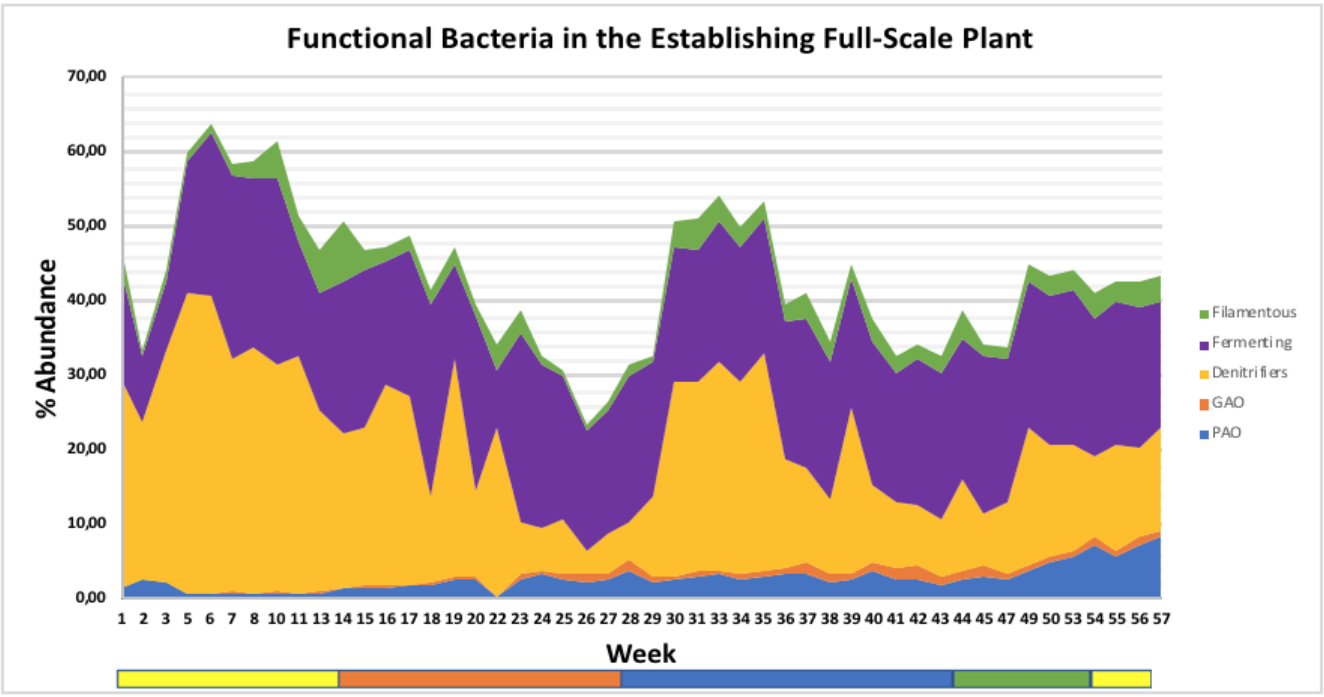

d)

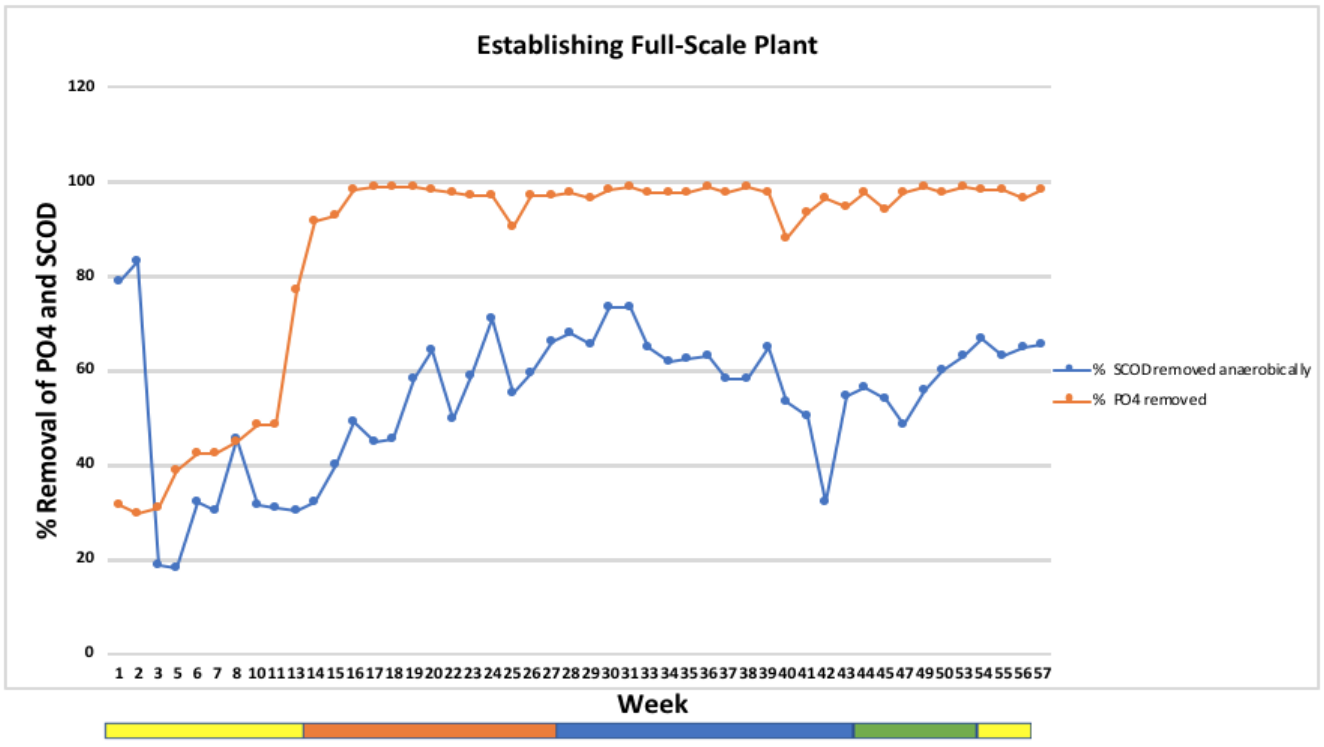

Figure 3.6. Average abundance of the functional bacterial groups (a, c), -and phosphorus -and SCOD removal (Sondre Eikås, personal communication, 11 April, 2018) (b, d) plotted against the sample collection week number in the established (a, b) -and the establishing plant (c, d). The season of the weekly samples are shown in color-codes. Yellow = summer, orange = autumn, blue = winter, and green = spring.

3.4 Analyses of Developing Biofilms During the Establishing of a Full-Scale MBBR Plant

Figure 3.7.a shows the development of attaching bacteria from the first to the last week of development, with the average bacteria abundance plotted against the material collection time. The number of attaching bacteria decreases with time. The most abundant attaching bacteria belonged to *Arcobacter* which made up 30.28 % of the biofilm after one week. However, after three weeks, the abundance of *Arcobacter* decreased to 0.39%. The second most abundant attaching bacteria belonged to *Chryseobacterium* which made up 10.60 % of the biofilm after one week, but further in the time-line they was found with an average abundance of 3.26%. The third most abundant attaching bacteria belonged to *Zoogloe*, with an average abundance of 8.24 % after the first week. However, after the following week, the average abundance of this bacteria was less than 0.02 %.

Figure 3.7.b shows the development of the most abundant bacteria groups on the most established biofilm the from the first to the last week of development, with the average bacteria abundance plotted against the material collection week. Many of the bacteria found on the most established biofilms (week 57) was not found in the beginning of the developing biofilms. The average abundance of the bacteria in the first weekly sample was less than 0.03%. Only three of the established bacteria was found with a relative high abundance at that time, including *Chryseobacterium* (7.44%), *Albirhodobacter* (1.56%), and *Accumulibacter* (1.53%). The abundance increased gradually with many shifts through the time-line. However, around week 44 the abundance somewhat stabilized. The figure shows that the most abundant bacteria on the most established biofilm belonged to *Albirhodobacter*, with an average abundance of 8.51% after 57 weeks (1.56%, week 1). The second most abundant bacteria belonged to *Tetrasphaera* with an average abundance of 6.60 % after 57 weeks (0.02 %, week 1). The third most abundant bacteria belonged to *Thermomona,* with an average abundance of 4.24 % after 57 weeks (0.02 % week 1).

a)

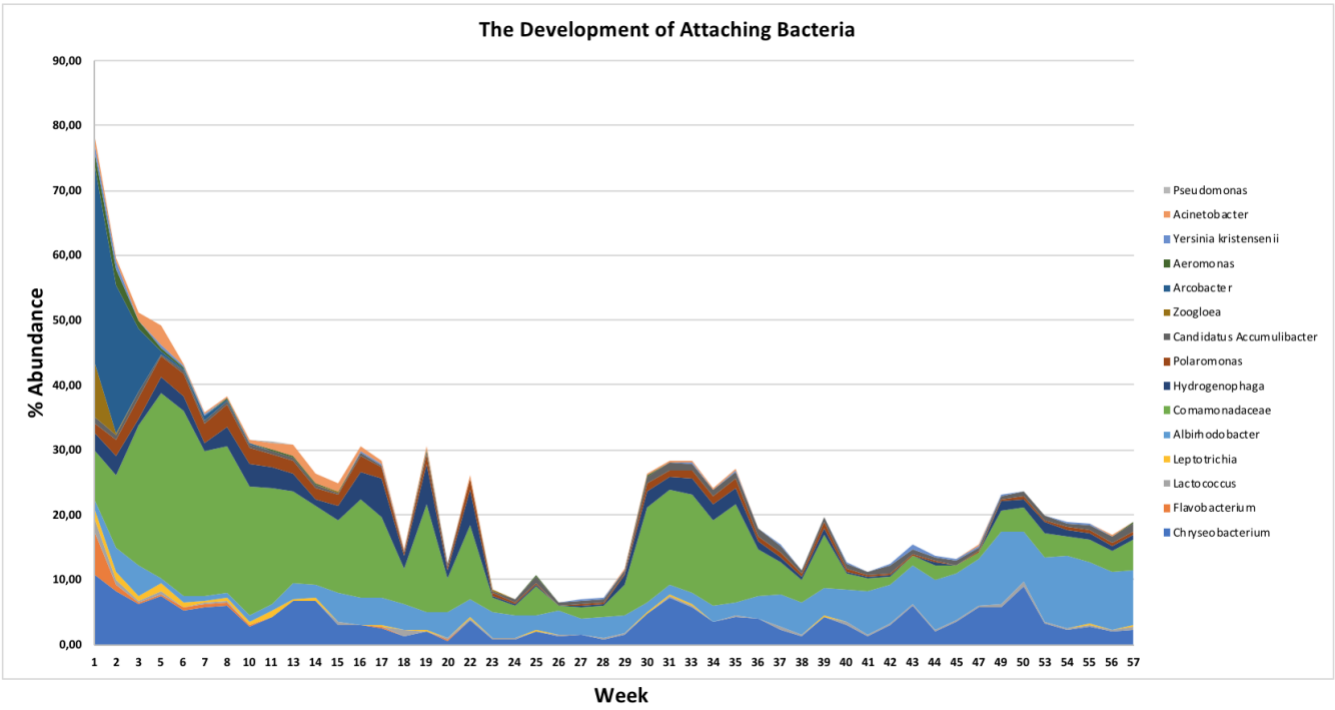

b)

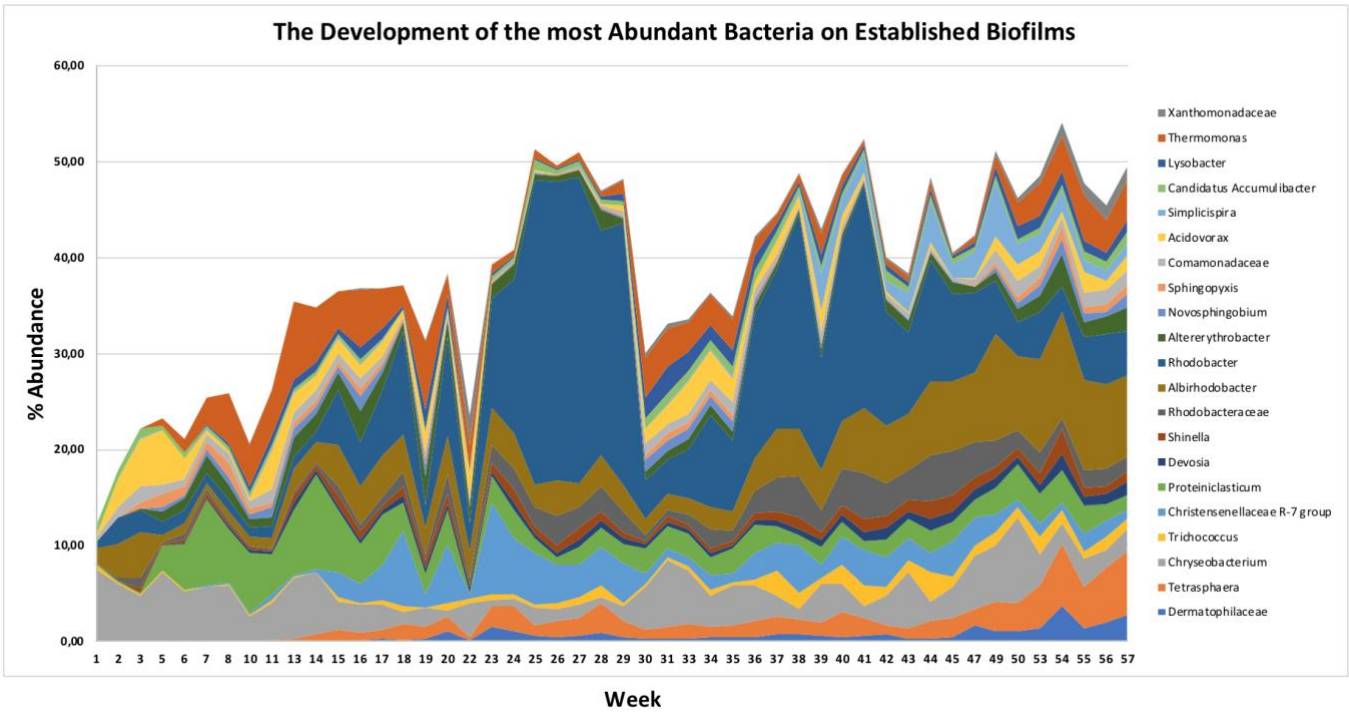

Figure 3.7 Biofilm development. a) % abundance of the first biofilm-carrier attaching bacteria. The figure shows the development of the bacteria that were first attached to the biofilm-carrier from week 1 to week 57. The OTU sequence limit for attaching bacteria was set to >90 sequences. b) The most abundant bacteria (%) on an established biofilm. The figure shows the development of the most abundant bacteria found in the samples collected in week 57, from the first week after full-scale up-start. OTU sequence limit for the most abundant bacteria on an established biofilm-carrier was set to >90 sequences.

4 Discussion

Both the phosphorus removal results from the established -and the establishing plant showed that the Hias process is an efficient alternative to the traditional EBPR system. The phosphorus removal in the establishing full-scale plant reached the efflux phosphorus limit (95%) already after 16 weeks, with an average removal of 97% (Figure 3.6.d) (Saltnes et al., 2017). In contrast, the average removal in the establishing plant was 94.45% (Figure 3.6.b).

4.1 Biofilm Establishment

The highest bacteria amounts were detected in the first weekly samples from the establishing plant (Figure 3.1.c). In addition, both the taxonomic results (Figure 3.4.b), and the α -and β-diversity results (Figure 3.2.b, 3.3.b), showed that the bacteria diversity was relative low and similar the first three weeks. In the first weekly samples, there was 15 bacteria groups which constituted ~80% of the biofilm. Among these was the genus *Zoogloea*, which is considered a bacterium responsible for activated sludge floc formation, and the genus *Accumulibacter* (PAO) (figure 3.7.a) (Rosselló-Mora et al., 1995). Since a biofilm formation can start within 5-30 s and because the first analyses were detected one week after the full-scale MBBR start-up, these results most likely show the late attachment/-colonization phase which also is causing the high bacteria amount (Chmielewski & Frank, 2003). The explanation behind the relative low diversity in the first weekly samples are most likely due to the ability of some bacteria to attach faster to a surface than others (i.e. attaching bacteria). Biofilm development is affected by different physicochemical properties of the wastewater, biofilm-carrier surface, and bacterial cell-surface (Dolan, 2002), and since the properties of the wastewater and the carrier surface was the same for all the bacteria in the establishing MBBR plant, the properties of the bacteria cell-surface most likely was the determining biofilm formation factor.

From week 3, the taxonomic results show that the bacteria diversity increased and altered clearly from week to week (Figure 3.4.b). Also, clear diversity differences were found between weeks for the α -and β-diversity (Figure 3.2.b, 3.3.b). Around week 12, the bacteria amount decreased gradually and reached the bottom around week 20 (Figure 3.1.c). In

addition, the attaching bacteria decreased already from week 2 (Figure 3.7.a). The increasing diversity is most likely showing the secondary colonization phase, where the attaching bacteria facilitate attachment for other non-attaching bacteria. During a biofilm development, a diversity of bacteria group can attach, and the biofilm multiply rapidly. The bacteria who wins the substrate competition and/or tolerate the inner biofilm-core with less oxygen, will survive, while the others will not and thus detach again (Chmielewski & Frank, 2003). Therefore, the rapid decrease in attaching bacteria is most likely caused by the secondary colonizers that outcompeted the bacteria. In addition, a previous study, investigating the microbial community evolution of biofilms during the start-up in a pilot MBBR, found that the rapid biofilm growth caused a sloughing phase as the bacteria amount reaches a certain upper point, which is probably the cause of the bacteria amount decrease in the present study (Zhu et al., 2015).

The quantitative results showed that after the sloughing, the bacteria amount increased again and stabilized around week 30 (Figure 3.1.c), whereas the taxonomic results show clear shifts all the way to week 50. The most stable bacteria diversity was detected the last three weeks (week 64-66), suggesting the biofilm establishment took more than a year (Figure 3.4.b). The α -and β-diversity also show that the bacteria diversity still differed between the weeks, but the differences decreased with time (Figure 3.2.b, 3.3.b). In addition, the taxonomic results show that the diversity stayed high in the most established biofilm, but the highest abundance was constituted by 21 bacteria groups (~50%) (Figure 3.7.b). The remaining abundance of attaching bacteria in the most established biofilm was only 20% (Figure 3.7.a). The increase in bacteria amount was expected because following a sloughing phase, before the biofilm matures, it is common that the bacteria amount increases again and then stabilize (Zhu et al., 2015). Simultaneously an exchange -and decrease in diversity is common, where the most competitive bacteria, including functional bacteria groups, would constitute the largest part of the biofilm. Although the taxonomic diversity in the present study was higher than expected, the 21 bacteria groups constituted the highest abundance, including functional bacteria. Most of the other remaining bacteria are likely to be bacteria groups that constantly attaches and detaches again as they do not survive the competition.

The biofilm establishment in the present study took more than a year, which is surprisingly since the phosphorus removal reached the efflux limit in week 16. In addition, the study

investigating the microbial community evolution of biofilms during the start-up in a pilot MBBR, found that the biofilms reached maturation after only 45 days, which is considerably shorter than what was found in the presence study (Zhu et al., 2015). The study was performed in laboratory-scale with synthetic wastewater and no alternating anaerobic and aerobic zones, giving contrasting condition to the present study. In the presence study the alternating anaerobic -and aerobic conditions may have affected the establishing time of the biofilms, as well as the time ratio in the different zones can vary (Nielsen et al., 2010). Physicochemical properties of the bacteria, such as respiratory capabilities can affect the biofilm competition among the different spices. Hence, depending on whether the bacteria are obligate aerobe or facilitative anaerobe, the competition among the species will be different in the different zones, and possibly increasing the time before the biofilm reach maturation. Other factors which could affect the establishing time is instability of the wastewater pH, salinity, and substrate content. In addition, a possible cause of the long biofilm establishing time could be due to the presence of protozoa, as they might induce bacteria detachment from the biofilm (Zhu et al., 2015). However, since the amount of eukaryotic DNA was low, the eukaryotes composition was not determined on the establishing biofilms. Thus, most likely they were not the cause of the high establishing time.

Although the phosphorus removal reached the efflux limit (week 16) before the biofilm were established (after week 50), the functional bacteria groups, including the PAOs, were present on the establishing biofilms from the start (Figure 3.6.c). In week 16 the PAO abundance were 1.55% and the removal were over 97%. In comparison, during the first 1-3 weeks, the established pilot plant PAO abundance was at its lowest (< 3 %), whereas the phosphorus removal was at its highest (~97%). Thus, the present study found no indication of a correlation between phosphorus removal and PAO abundance, suggesting that the poly-P storage of individual PAOs has major capacity. A previous study notes that the maximal efficiency of PAOs is far from being reached in common EBPR plant (Tarayre et al., 2016). Hence, a PAO abundance of 1.55% may be enough to remove the daily wastewater phosphorus income (~0,053 g/m^2 per day)) (Appendix E, Figure E.1 b). Yet, no previous studies have documented the maximum poly-P storage capacity of a PAO cell. It is likely the correlation between the establishing biofilm and the phosphorus removal can be better explained at gene level (Oyserman et al., 2016). A possible explanation could be that the gene expression found in the carbon and polyphosphate metabolic pathway of individual

PAOs partly varies with the overall PAO abundance in the plant, where low PAO abundance means high expression, whereas a high PAO abundance means a lower expression distributed among the PAOs. Another possibility could be that there are additional PAOs present which is not yet known.

4.2 Established Biofilms

The phosphorus removal results from the established pilot plant was somewhat stable, with small shifts during the cold period from week 13 to 34, where the lowest removal was detected during the winter (week 13, 22, 23, 26) (Figure 3.6.d). In contrast, previous results from the established pilot Hias process plant in Hamar, showed a relative stable and efficient phosphorus removal with a slight increase during the cold months (Sondre Eikås, personal communication, 13 April, 2018). They also observed that the phosphorus removal can vary greatly from day to day. Based on these results and since different temperatures can have various effects on bacteria groups, it was expected seasonal variations in the established pilot plant in both relation to the microbiota composition and thus the phosphorus removal (Nielsen et al., 2010). However, the bacteria taxonomic results (Figure 3.4.a) and the α -and β-diversity results (Figure 3.2.a, 3.3.a) show the whole microbiota composition was relative stable in all the weekly samples and there is no clear correlation with the phosphorus removal. Yet, since the average wastewater temperature was 8.1^{o}C in the winter and 12.5^{o}C in the summer (Appendix E, Figure E.3.a), these small seasonal temperature differences most likely does not affect the microbiota composition and thus not the phosphorus removal.

The SCOD (organic compounds) removal from the established pilot plant showed an average removal of 66%, raging between 47-79%. Compared to the phosphorus removal, the SCOD removal was less stable. At some points the phosphorus removal was high and the corresponding SCOD removal low, and conversely (Figure 3.6.b). Since the PAOs are dependent on anaerobic carbon accumulation (anaerobic carbon removal) in order to accumulate phosphorus aerobically (phosphorus removal) it was expected a correlation between phosphorus removal and the wastewater carbon content, where the later can vary greatly, depending on household -and industrial carbon release (Shen, N. & Zhou, Y., 2016). Although there was no clear correlation between the phosphorus -and SCOD removal, the SCOD results does not tell which organic compounds the wastewater consists of. Hence,

periods with high phosphorus -and low SCOD removal, the wastewater most likely consisted of high amounts of PAO carbon sources (VFA/some amino acids). Oppositely, low phosphorus -and high SCOD removal is most likely due to the removal of another organic compound consumed by a non-PAO. An unstable wastewater content can alter the microbiota composition which is probably causing the small weekly or monthly shifts (Nielsen et al., 2010). However, since the microbiota composition is somewhat stable it would be an idea to add easily degradable carbon (VFA) to the system during periods of lower phosphorus removal to increase the efficiency (Shen & Zhou, 2016). Or optionally increase the time in the anaerobic zone so the hydrolysers and fermenters have more time to produce VFA for the PAOs (Nielsen et al., 2010).

4.3 Functional Bacteria Groups

The functional bacteria abundance in the established pilot plant was somewhat stable, with an average of 40,61% (Figure 3.6.a), whereas in full-scale plant, as it began to stabilise from week 50, the average functional bacteria group abundance was 42% (Figure 3.6.c). In contrast, a Danish study performed on 25 traditional full-scale EBPR plants showed an average functional bacteria abundance of 73% (Figure 1.1) (Nielsen et al., 2010). Based on the Danish study, and previous results from the established Hias process plant which showed a high phosphorus removal efficiency, it was expected similar - or higher abundance than in the Danish EBPR plants. In addition, the Hias process uses the advantage of biofilm-carriers with a higher surface area which increases the area for the bacteria to attach and live (Saltnes et al., 2017). The unexpected low abundance can be due to different causes. For example, the functional bacteria groups might favour living in floc as in the Danish plants over living in biofilm on carriers. It may also be that other non-functional bacteria favour living in biofilm on carriers, which may lead to less space for the functional bacteria. Yet, most likely the differences are partly due to generally different wastewater content in the Hias process plants and the Danish plants.

4.3.1 Phosphorus Accumulation Organisms (PAOs)

The average PAO abundance in the established pilot MBBR plant, was 8.73 %, and ranged between 2.98-15.91%, where the abundance went from low to high (figure 3.6.a). The

findings of the present study were in range of the average PAO abundance of 13% in the Danish EBPR plants (Figure 1.1) (Nielsen et al., 2010). The high PAO abundance range in the present study correspond with the quantitative results where the bacteria amount was generally lower the first 18 weeks (~10^7), before it increased and somewhat stabilized (>10^7). A possible explanation for the ranges can be due to the presence of eukaryotes. However, the average eukaryote amount was less (<10^7) -but seemed to increase and decrease with the bacteria (Figure 3.1.b), and is hence likely not to explain the bacteria amount alone.

Another explanation behind the increase in bacteria amount including the PAOs could be due to growth after detachment and/or dispersion during the biofilm lifecycle. Detachment and dispersion can be caused by several factors, including shedding of daughter cells, specific gene expressions, and quorum sensing. In addition to physical detachment processes, for example when a biofilm grows in size, the cells in the biofilm core may not access energy and nutrients from the external environment fully. Also, a large biofilm can lead to accumulation of toxins which may induce detachment. Moreover, detachment can be caused by a high-water velocity or collision by particles from the fluid (Mahami & Adu-Gyamfi, 2011). Although the results do not show major decreases in the bacteria amount, detachment most likely occurred before the experiment started, causing lower bacteria amount the first 18 weeks. After detachment, a biofilm starts to grow again, which is probably causing the increase in week 19.

The average PAO abundance in the full-scale MBBR plant was 6.58% from week 50, where *Tetrasphaera* constituted ~77% of the PAOs (Figure 3.6.c). This was in contrary to the pilot plant where *Accumulibacter* constitute ~82% of the PAO. It is hard to explain the reason behind these differences due to lack of similar studies. It could possibly be due to the use of different Kaldnes carriers (K1 and K2), or the different volume-scales, where the average inlet wastewater was 80 m^3/t in the full-scale plant, while 0,72 m^3/t in the pilot plant (Appendix E, Figure E.4.a, E.4.b). Another possibility is that the differences are completely random since the biofilm formation in the pilot -and the full-scale plants are independent from each other. However, since the PAOs have different metabolism, the different contents of PAOs could possibly be the explanation behind the differences in phosphorus removal efficiency in the plants (Tarayre et al., 2016). In the full-scale plant, where *Tetrasphaera* constitute the highest part, the removal was more efficient (~97 %). Whereas in the pilot

plant, where the *Accumulibacter* constitute the largest part, the efficiency was generally lower (~94.45%). Although, the knowledge about *Tetrasphaera* metabolism is still limit it is known that in contrast to the *Accumulibacter,* they can consume certain amino acids. Therefore, the wastewater possibly contained substances favored by the *Tetrasphaera*, and thus leads to a more efficient removal in the full-scale plant.

4.3.2 Glucose Accumulating Organisms (GAOs)

The average GAO abundance was 0.28% in the established pilot plant, and ranged between 0.06-0.49% (Figure 3.6.a), whereas the full-scale plant had an average GAO abundance of 0.83% (from week 50) (Figure 3.6.c). The low abundance was expected in both plants due to the high average phosphorus removal efficiency and since the Danish EBPR plant had an average GAO abundance of 1% (Figure 1.1) (Nielsen et al., 2010). A high GAO abundance would defect the phosphorus removal since they compete against the PAOs for the same carbon sources anaerobically, but does not accumulated phosphorus aerobically (Zhu et al., 2015; Carvalheira et al., 2014). The periods with the lowest phosphorus removal efficiency could on the other hand be associated with a higher GAO abundance. Yet, no higher GAO abundance was detected in the periods of lower phosphorus removal, and most likely the GAOs had no negative effect on the overall system.

4.3.3 Fermenters

The average abundance of fermenting bacteria in the pilot plant was 10.28%, and ranged between 5.30-16.25% (Figure 3.6.a), whereas in the full-scale plant the average abundance was 19.10% (from week 50) (Figure 3.6.c). In contrast the average abundance of fermenters in the Danish plant was 3%. (Figure 1.1) (Nielsen et al., 2010). Based on the Danish study and since fermenters positively affect the overall phosphorus removal efficiency by producing VFA anaerobically, it was expected a relatively high fermenters abundance (Seviour et al., 2003). In contrast to the PAO range, the fermenters range went from high to lower, suggesting there may be a correlation between the two. It is likely that the wastewater contained much soluble carbon compounds favored by fermenters in the beginning of the timeline causing a higher growth (Nielsen et al., 2010). As the fermenters produces VFA/amino acids, the PAOs starts to grow and will hence constitute a larger space of the

biofilm-carries which in turn reduces the fermenters abundance. Moreover, as the fermenters decreases, the VFA/amino acid production decreases. Following the PAOs will decrease and the fermenters will increase again, and so the biofilm lifecycle goes.

4.3.4 Filamentous Bacteria

The average filamentous bacteria abundance in the pilot plant was 4.89%, ranging between 3.12-6.37% (Figure 3.6.a), whereas in the full-scale plant the average abundance was 3.10% (Figure 3.6.c). Compared to the Danish study, where the filamentous bacteria constituted the largest part with an average abundance of 28%, the results in the present study was surprisingly low (Nielsen et al., 2010). The filamentous bacteria have an important function in the attaching phase during a biofilm formation and many filamentous bacteria are also hydrolyser (Dolan, 2002). Since the incoming wastewater consist of macromolecules such as proteins, polysaccharides, and lipids, hydrolysers are highly necessary for the overall function of the Hias process plants (Nielsen et al., 2010). Without hydrolysers, the PAOs will not have access to enough of their carbon sources for PHA storage and in turn poly-P accumulation. However, since the phosphorus removal in Hias process plants was highly efficient it suggest that there are more filamentous bacteria and hydrolysers in the plants than what was found in the present study.

4.3.5 Nitrifies and Denitrifies

The average abundance of nitrifies was low, with an average abundance of 0.05% in the pilot plant, ranging between 0.01-0.15% (Figure 3.6.a), whereas in the full-scale plant the nitrifies where completely absent. In contrast, the Danish study showed an average of 7% nitrifies (Figure 1.1) (Nielsen et al., 2010). Although it could be possible to obtain simultaneous phosphorus and nitrogen removal, a low nitrifies abundance will not have a negative effect on the phosphorus removal, on the contrary (Meyer et al. 2005). Low amounts of nitrifies means low production of nitrate aerobically, which in turn lower the chance of nitrate transportation to the anaerobic zone. If nitrate becomes present in the anaerobic zone, denitrifies can use the nitrate as an electron acceptor and be able to consume the carbon before the PAOs, defecting the phosphorus removal (Akin & Ugurlu, 2004). In addition, the average denitrifies abundance in the pilot plant was as high as 16.38%, ranging between 12.33-22.09% (Figure

3.6.a), whereas in the full-scale plant the average abundance was 13.32%. This high abundance could be a risk for the phosphorus removal efficiency if nitrate becomes present in the anaerobic zone. However, the Hias process system has removed the chance of extensive oxygen and nitrate in the anaerobic zone by lifting the biofilm-carries out of the water during the transport (Saltnes et al., 2017). An idea to achieve simultaneously phosphorus -and nitrogen removal for Hias WTTP would be to incorporate an anoxic zone in the Hias process plant (Meyer et al., 2005).

4.4 Technical Challenges

No major deviants were found within the sample with triplicates from either the establishing -or the established plant. However, not all results from the establishing full-scale plant are from triplicate samples. Since the formation -and lifecycle of biofilms are individual between each biofilm-carrier, the formation stages and the biofilm lifecycle between the biofilms were likely not synchronic. Therefore, the overall system may have contained more or less bacteria than what was found on the biofilm-carrier in the present study. For example, if other biofilms in the establishing plant were further established than the samples analysed in this study, or the biofilms in the established plant may have had different detachment/growth phases during the biofilm lifecycle. Therefore, more accurate results would possibly be obtained by increasing the sample replicates.

Different methods with different advantages and disadvantages were used in the Danish study (quantitative FISH) and the present study (Illumina sequencing Miseq system), which may have given different results. In addition, a microbiota analysis preformed simultaneously on material collected from the same established pilot plant in another laboratory showed an average functional bacteria abundance of ~60-65 % (Sondre Eikås, personal communication, 11 April, 2018). This indicates that the differences in functional bacteria abundance in the established pilot -and full-scale Hias process plants, and the Danish EBPR plants are most likely partly due to the use of different methods.

4.5 Further Work

Research on the microbiota composition in biological WWTP is important to improve the efficiency and achieve a stable phosphorus removal to complete remove an additional chemical precipitation treatment step in the future. In the present study it was observed an efficient phosphorus removal at an unexpectedly early stage of the biofilm establishment. Since it also was detected a surprisingly high phosphorus removal efficiency during periods with low PAO abundance (>1,5%), it is likely that poly-P storages in individual PAOs have a huge capacity. However, in the present study the PAO poly-P storage capacity, was not examined. Thus, it would be interesting to further investigate individual PAO cells to find the maximal storage capacity. It would be favorable to study the PAOs at gene level in order to examine specific genes that might be up-regulated during times with a lower PAO abundance, or conversely.

It was also observed different PAO compositions in the established -and the establishing Hias process plants. Since the phosphorus removal efficiency in the two plants also differed slightly, it suggests that the metabolic rates of the PAOs differs. However, in the present study the PAO metabolism was not investigated. Hence, in the future it would be interesting to examine the PAOs metabolic pathways to see if one PAO can remove phosphorus more efficiently than the other.

5 Conclusion

The present study observed that phosphorus removal reaches the efflux limit (95%) at a surprisingly early stage of biofilm establishment in the start-up of a full-scale Hias continuous biofilm process plant. No clear correlation was found between the abundance of PAOs -nor any other functional bacteria groups, and the phosphorus removal. Yet, it was observed that the phosphorus removal efflux limit was reached with a PAO abundance >1.5%, suggesting that the intracellular poly-P storage of individual PAOs may have a huge capacity. In addition, it was observed that the microbiota composition on already established biofilms are more stable than the phosphorus removal, suggesting that instability of phosphorus removal is affected by the daily variations in the wastewater substrate content. Further it was found different PAO compositions in the established pilot -and the establishing full-scale plant, which also had a slightly different average phosphorus removal efficiency, suggesting that the metabolic rates of the PAOs may differs. However, the knowledge of the poly-P storage -and PAO metabolism is still limited and needs to be further investigated to better understand the function of biological phosphorus removal systems.

References

Akin, B. S. & Ugurlu, A. (2004). The effect of an anoxic zone on biological phosphorus removal by a sequential batch reactor. *Bioresource technology*, 94 (1): 1-7.

Attali, D., Bidshahri, R., Haynes, C. & Bryan, J. (2016). ddpcr: an R package and web application for analysis of droplet digital PCR data. *F1000Research*, 5.

Biorad. (2018). *What is Real-time PCR (qPCR)*. Available at: http://www.bio-rad.com/en-no/applications-technologies/what-real-time-pcr-qpcr?ID=LUSO4W8UU (accessed: 30.03.18).

Brankatschk, R., Bodenhausen, N., Zeyer, J. & Bürgmann, H. (2012). Simple absolute quantification method correcting for quantitative PCR efficiency variations for microbial community samples. *Applied and environmental microbiology*, 78 (12): 4481-4489.

Bråte, J., Logares, R., Berney, C., Ree, D. K., Klaveness, D., Jakobsen, K. S. & Shalchian-Tabrizi, K. (2010). Freshwater Perkinsea and marine-freshwater colonizations revealed by pyrosequencing and phylogeny of environmental rDNA. *The ISME journal*, 4 (9): 1144-1153.

Carvalheira, M., Oehmen, A., Carvalho, G. & Reis, M. A. (2014). The effect of substrate competition on the metabolism of polyphosphate accumulating organisms (PAOs). *water research*, 64: 149-159.

Cavalier-Smith, T., Lewis, R., Chao, E. E., Oates, B. & Bass, D. (2009). Helkesimastix marina n. sp.(Cercozoa: Sainouroidea superfam. n.) a gliding zooflagellate of novel ultrastructure and unusual ciliary behaviour. *Protist*, 160 (3): 452-479.

Chmielewski, R. & Frank, J. (2003). Biofilm formation and control in food processing facilities. *Comprehensive reviews in food science and food safety*, 2 (1): 22-32.

Comber, S., Gardner, M., Darmovzalova, J. & Ellor, B. (2015). Determination of the forms and stability of phosphorus in wastewater effluent from a variety of treatment processes. *Journal of Environmental Chemical Engineering*, 3 (4): 2924-2930.

Cordell, D., Drangert, J.-O. & White, S. (2009). The story of phosphorus: global food security and food for thought. *Global environmental change*, 19 (2): 292-305.

Cordell, D. & White, S. (2011). Peak phosphorus: clarifying the key issues of a vigorous debate about long-term phosphorus security. *Sustainability*, 3 (10): 2027-2049.

Correll, D. L. (1998). The role of phosphorus in the eutrophication of receiving waters: A review. *Journal of environmental quality*, 27 (2): 261-266.

De-Bashan, L. E. & Bashan, Y. (2004). Recent advances in removing phosphorus from wastewater and its future use as fertilizer (1997–2003). *Water research*, 38 (19): 4222-4246.

Desmidt, E., Ghyselbrecht, K., Zhang, Y., Pinoy, L., Van der Bruggen, B., Verstraete, W., Rabaey, K. & Meesschaert, B. (2015). Global phosphorus scarcity and full-scale P-recovery techniques: a review. *Critical Reviews in Environmental Science and Technology*, 45 (4): 336-384.

Donlan, R. M. (2002). Biofilms: microbial life on surfaces. *Emerging infectious diseases*, 8 (9): 881.

Eikås, S., Saltnes, T., Glestad, H. T. & Sørensen, G. (2017). Fosforgjenvinning.

Gernaey, K. V., van Loosdrecht, M. C., Henze, M., Lind, M. & Jørgensen, S. B. (2004). Activated sludge wastewater treatment plant modelling and simulation: state of the art. *Environmental Modelling & Software*, 19 (9): 763-783.

Gong, J. & Yang, C. (2012). Advances in the methods for studying gut microbiota and their relevance to the research of dietary fiber functions. *Food research international*, 48 (2): 916-929.

Gouveia, R. & Pinto, J. (2000). Optimal policies for activated sludge treatment systems with multi effluent stream generation. *Brazilian Journal of Chemical Engineering*, 17 (4-7): 979-990.

Illumina. (2017). *An introduction to Next-Generation Sequencing Technology*: Illumina. Available at: https://www.illumina.com/content/dam/illumina-marketing/documents/products/illumina_sequencing_introduction.pdf (accessed: 01.04.18).

Johnson, M., Zaretskaya, I., Raytselis, Y., Merezhuk, Y., McGinnis, S. & Madden, T. L. (2008). NCBI BLAST: a better web interface. *Nucleic acids research*, 36 (suppl_2): W5-W9.

Kofstad, P. K. & Pederson, B (2018). *Fosfor*. Store norske leksikon. Available at: https://snl.no/fosfor (accessed: 16.03.2018).

krugerkaldnes. (2018). *Standardprodeukter: Kaldnes® MBBR*. Available at: http://www.krugerkaldnes.no/_industri_/standardprodukter/ (accessed: 01.04.18).

Kuczynski, J., Stombaugh, J., Walters, W. A., González, A., Caporaso, J. G. & Knight, R. (2012). Using QIIME to analyze 16S rRNA gene sequences from microbial communities. *Current protocols in microbiology*: 1E. 5.1-1E. 5.20.

Lanham, A. B., Oehmen, A., Saunders, A. M., Carvalho, G., Nielsen, P. H. & Reis, M. A. (2014). Metabolic modelling of full-scale enhanced biological phosphorus removal sludge. *Water research*, 66: 283-295.

Lee, H. & Yun, Z. (2014). Comparison of biochemical characteristics between PAO and DPAO sludges. *Journal of Environmental Sciences*, 26 (6): 1340-1347.

Lenntech. (2018). *Phosphorus Removal from Wastewater*. Lenntech. Available at: https://www.lenntech.com/phosphorous-removal.htm (accessed: 05.03.18).

Mahami, T. & Adu-Gyamfi, A. (2011). Biofilm-associated infections: public health implications. *Inter. Res. J. Microbiol*, 2 (10): 375-381.

McIlroy, S. J. S., A.M. Albertsen, M. Nierychlo, M. McIlroy, B. Hansen, A.A. Karst, S.M. Nielsen, J.L. Nielsen, P.H. (2015). *MiDAS: the field guide to the microbes of activated sludge*. Database, Vol. 2015, Article ID bav062; doi:10.1093/database/bav062. MiDAS. Available at: http://www.midasfieldguide.org (accessed: 27.03.18).

Metzker, M. L. (2010). Sequencing technologies—the next generation. *Nature reviews genetics*, 11 (1): 31.

Meyer, R. L., Zeng, R. J., Giugliano, V. & Blackall, L. L. (2005). Challenges for simultaneous nitrification, denitrification, and phosphorus removal in microbial aggregates: mass transfer limitation and nitrous oxide production. *FEMS Microbiology Ecology*, 52 (3): 329-338.

Minnesota pollution control agency (2005). *Phosphorus Treatment and Removal Technologies* Minnesota Pollution Control Agency. Available at: https://www.pca.state.mn.us/sites/default/files/wq-wwtp9-02.pdf (accessed: 03.03.18).

Morse, G., Brett, S., Guy, J. & Lester, J. (1998). Phosphorus removal and recovery technologies. *Science of the total environment*, 212 (1): 69-81.

Nielsen, P. H., Mielczarek, A. T., Kragelund, C., Nielsen, J. L., Saunders, A. M., Kong, Y., Hansen, A. A. & Vollertsen, J. (2010). A conceptual ecosystem model of microbial communities in enhanced biological phosphorus removal plants. *Water research*, 44 (17): 5070-5088.

Oyserman, B. O., Noguera, D. R., del Rio, T. G., Tringe, S. G. & McMahon, K. D. (2016). Metatranscriptomic insights on gene expression and regulatory controls in Candidatus Accumulibacter phosphatis. *The ISME journal*, 10 (4): 810.

Pabinger, S., Rödiger, S., Kriegner, A., Vierlinger, K. & Weinhäusel, A. (2014). A survey of tools for the analysis of quantitative PCR (qPCR) data. *Biomolecular Detection and Quantification*, 1 (1): 23-33.

Patel, R. (2013). The long green revolution. *The Journal of Peasant Studies*, 40 (1): 1-63.

Pinheiro, L. B., Coleman, V. A., Hindson, C. M., Herrmann, J., Hindson, B. J., Bhat, S. & Emslie, K. R. (2011). Evaluation of a droplet digital polymerase chain reaction format for DNA copy number quantification. *Analytical chemistry*, 84 (2): 1003-1011.

Quast, C., Pruesse, E., Yilmaz, P., Gerken, J., Schweer, T., Yarza, P., Peplies, J. & Glöckner, F. O. (2012). The SILVA ribosomal RNA gene database project: improved data processing and web-based tools. *Nucleic acids research*, 41 (D1): D590-D596.

Reece, J. B. U., L.A. Cain, M.L. Wasserman, S.A. Minorsky, P.V. Jackson, R.B. (2011). *Amplifying DNA: The polymerase chain reaction (PCR) and its use in DNA cloning.* . (10th ed, pp. 414-416). San Francisco, CA: Pearson.

Rosselló-Mora, R. A., Wagner, M., Amann, R. & Schleifer, K.-H. (1995). The abundance of Zoogloea ramigera in sewage treatment plants. *Applied and environmental microbiology*, 61 (2): 702-707.

Rybicki, S. M. (1998). *New technologies of phosphorus removal from wastewater*. Proc. Of a Polish-Swedish Seminar, Joint Polish Swedish Reports, Report.

Saltnes, T., Sørensen, G. & Eikås, S. (2017). Biological nutrient removal in a continuous biofilm process. *Water Practice and Technology*, 12 (4): 797-805.

Saunders, A. M., Albertsen, M., Vollertsen, J. & Nielsen, P. H. (2016). The activated sludge ecosystem contains a core community of abundant organisms. *The ISME journal*, 10 (1): 11.

Seviour, R. J., Mino, T. & Onuki, M. (2003). The microbiology of biological phosphorus removal in activated sludge systems. *FEMS microbiology reviews*, 27 (1): 99-127.

Seviour, R. J. & Blackall, L. (2012). *The microbiology of activated sludge*: Springer Science & Business Media.

Sharpley, A. N., Daniel, T., Sims, T., Lemunyon, J., Stevens, R. & Parry, R. (2003). Agricultural phosphorus and eutrophication. *US Department of Agriculture, Agricultural Research Service, ARS–149*: 44.

Shen, N. & Zhou, Y. (2016). Enhanced biological phosphorus removal with different carbon sources. *Applied microbiology and biotechnology*, 100 (11): 4735-4745.

Shokralla, S., Spall, J. L., Gibson, J. F. & Hajibabaei, M. (2012). Next-generation sequencing technologies for environmental DNA research. *Molecular ecology*, 21 (8): 1794-1805.

Sigmaaldrich. (2018). *Polymerase Chain reaction: A Technical Guide to PCR Technologies*. Sigmaaldrich. Available at: https://www.sigmaaldrich.com/technical-documents/articles/biology/polymerase-chain-reaction.html (accessed: 20.03.18).

Sigmaaldrich. (2018). *Quantitative PCR: A Technical Guide to PCR Technologies*. Sigmaaldrich. Available at: https://www.sigmaaldrich.com/technical-documents/articles/biology/quantitative-pcr.html (accessed: 30.05.18).

Tarayre, C., Nguyen, H.-T., Brognaux, A., Delepierre, A., De Clercq, L., Charlier, R., Michels, E., Meers, E. & Delvigne, F. (2016). Characterisation of phosphate accumulating organisms and techniques for polyphosphate detection: a review. *Sensors*, 16 (6): 797.

Voelkerding, K. V., Dames, S. A. & Durtschi, J. D. (2009). Next-generation sequencing: from basic research to diagnostics. *Clinical chemistry*, 55 (4): 641-658.

Wang, L. K., Vaccari, D. A., Li, Y. & Shammas, N. K. (2005). Chemical precipitation. In *Physicochemical treatment processes*, pp. 141-197: Springer.

Withers, P. & Haygarth, P. (2007). Agriculture, phosphorus and eutrophication: a European perspective. *Soil Use and Management*, 23 (s1): 1-4.

Yang, R., Paparini, A., Monis, P. & Ryan, U. (2014). Comparison of next-generation droplet digital PCR (ddPCR) with quantitative PCR (qPCR) for enumeration of Cryptosporidium oocysts in faecal samples. *International journal for parasitology*, 44 (14): 1105-1113.

Yu, Y., Lee, C., Kim, J. & Hwang, S. (2005). Group-specific primer and probe sets to detect methanogenic communities using quantitative real-time polymerase chain reaction. *Biotechnology and bioengineering*, 89 (6): 670-679.

Zhu, Y., Zhang, Y., Ren, H.-q., Geng, J.-j., Xu, K., Huang, H. & Ding, L.-l. (2015). Physicochemical characteristics and microbial community evolution of biofilms during the start-up period in a moving bed biofilm reactor. *Bioresource technology*, 180: 345-351.

Appendix

Appendix A: PCR Reagents with Function

Table A1. The reagents used for first stage PCR and the function of them.

Reagents:	**Function:**
5 x HOT FIREPol® Blend Master Mix Ready to Load:	
5 x HOT FIREPol® DNA polymerase	A warm stable enzyme that synthesize the complementary DNA strand in the 5`→3`direction
Proofreading enzyme	Error correcting enzyme that has both the 5`→3`exonuclease activity in addition to 3`→5 proofreading activity
5 x Blend Master Mix Buffer	Optimize the conditions for "5 x HOT FIREPol® Blend Master Mix Ready to Load". Including it facilitates the primer binding
12,5 mM $MgCl_2$ 1 x PCR solution – 1,5 mM $MgCl_2$	Required for primer binding, T_m of template DNA and function as a cofactor for DNA polymerase
2 mM dNTPs of each 1 x PCR solution 200 µM dATP, 200 µM dCTP, 200 µM dGTP and 200 µM dTTP	Nucleotides which the DNA polymerase use as building blocks to synthesize the complementary DNA strand.
Bovine Serum Albumin (BSA)	BSA increases PCR yields from low purity templates. It also prevents adhesion of enzymes to the reaction tubes and tip surface.
Blue dye migration equivalent to 3,5-4,5 kb DNA fragment **Yellow dye** migration rat in excess of primers in 1% agarose gel: <35-45bp	Compounds that makes it possible to directly load the samples onto agarose gel and to track the dyes during the electrophoresis
Unknown compound	Compound that increases sample density for direct loading
Forward primer - 16S rRNA gene **Reverse primer - 16S rRNA gene**	The universal prokaryote primers PRK341F and PRK806R was used for amplification of the variable regions, V3 and V4, of the 16S gene. The 3`end of these primers are designed to bind to the 16S gene.
Forward primer – 18S rRNA gene **Reverse primer - 18S rRNA gene**	The PCR primers 3NDF[1] and V4_Euk_R2[2] target a 450bp region that encompass the variable V4 of the 18S rRNA gene. The 3`end of these primers are designed to bind to the 18S gene.
Nuclease-free water	Used to dilute the concentration of the other reagents to the proper final concentration. In addition it helps to avoid DNA degradation by

	nucleases as well as interference of the PCR reaction by ions which could be present in otherwise not nuclease free deionized water.
DNA template	DNA isolated from biofilms collected at wastewater treatment plants in Hamar

Table A2. The reagents used for index PCR and the function of them.

Reagents:	**Function:**
5 x FIREPol® Master Mix Ready to Load:	
FIREPol® DNA polymerase	A warm stable enzyme that synthesize the complementary DNA strand in the 5`→3`direction
5 x Reaction Buffer	Optimize the conditions for "5 x HOT FIREPol® Blend Master Mix Ready to Load". Including it facilitates the primer binding
12,5 mM $MgCl_2$ 1 x PCR solution – 1,5 mM $MgCl_2$	Required for primer binding, T_m of template DNA and function as a cofactor for DNA polymerase
1 mM dNTPs of each 1 x PCR solution 200 µM dATP, 200 µM dCTP, 200 µM dGTP and 200 µM dTTP	Nucleotides which the DNA polymerase use as building blocks to synthesize DNA strands
Blue dye migration equivalent to 3,5-4,5 kb DNA fragment **Yellow dye** migration rat in excess of primers in 1% agarose gel: <35-45bp	Compounds that makes it possible to directly load the samples onto agarose gel and to track the dyes during the electrophoresis
Unknown compound	Compound that increases sample density for direct loading
Forward index primer – rRNA 16S gene **Reverse index primer – rRNA 16S gene**	The universal prokaryote primers PRK341F and PRK806R was used for amplification of the variable regions, V3 and V4, of the 16S gene. The 3`end of these primers are designed to bind to the 16S gene. The 5`end of the primers are modified with an adaptor sequence which is complementary to oligonucleotide sequences on the flow cell surface of the Illumina sequence platform
Forward index primer – 18S rRNA gene **Reverse index primer – 18S rRNA gene**	– The PCR primers, 3NDF[1] and V4_Euk_R2[2], target a 450bp region that encompass the variable V4 of the 18S rDNA gene. The 3`end of these primers are designed to bind to the 18S gene. The 5`end of the primers are modified with an adaptor sequence which is complementary to oligonucleotide sequences on the flow cell surface of the Illumina sequence platform
Nuclease-free water	Used to dilute the concentration of the other reagents to the proper final concentration. In addition it helps to avoid DNA degradation by

	nucleases as well as interference of the PCR reaction by ions which could be present in otherwise not nuclease free deionized water.
DNA template	DNA isolated from biofilms collected at wastewater treatment plants in Hamar

Tabell A3. The reagents used for qPCR and the function of them

Reagents	**Purpose**
5x HOT FIREPol® EvaGreen® qPCR supermix:	
HOT FIREPol DNA Polymerase	A warm stable enzyme that synthesize the complementary DNA strand in the 5`→3`direction
5x EvaGreen qPCR buffer	Optimize the conditions for reagensene in the "5x HOT FIREPol® EvaGreen® qPCR supermix". Including it facilitates the primer binding
12,5 mM $MgCl_2$ 1x PCR solution – 2,5 mM	Required for primer binding, T_m of template DNA and function as a cofactor for DNA polymerase
dNTPs	Nucleotides which the DNA polymerase use as building blocks to synthesize DNA strands
EvaGreen dye	EvaGreen® dye is a green fluorescent nucleic acid dye. The dye is essentially nonfluorescent by itself but becomes highly fluorescent upon binding to dsDNA.
Internal reference based on ROX dye	ROX is an internal passive reference dye used to normalize the fluorescent reporter signal generated in qPCR
GC-rich Enhancer	The purpose of the GC-rich enhancer is to bring the melting temperature of GC rich regions closer into line with AT regions so that the primers anneal quickly and uniformly.
Blue visualization dye	Used for loading and visualize the PCR products on agarose gel
Forward primer - 16S rRNA gene **Reverse primer - 16S rRNA gene**	The universal prokaryote primers PRK341F and PRK806R was used for amplification of the variable regions, V3 and V4, of the 16S gene. The 3`end of these primers are designed to bind to the 16S gene.
Forward primer – 18S rRNA gene **Reverse primer - 18S rRNA gene**	The PCR primers 3NDF[1] and V4_Euk_R2[2] target a 450bp region that encompass the variable V4 of the 18S rRNA gene. The 3`end of these primers are designed to bind to the 18S gene.

Nuclease-free water	Used to dilute the concentration of the other reagents to the proper final concentration. In addition, it helps to avoid DNA degradation by nucleases as well as interference of the PCR reaction by ions which could be present in otherwise not nuclease free deionized water.
Template DNA	DNA isolated from biofilms collected at wastewater treatment plants in Hamar

Appendix B: PRK Illumina Primers

PRK Illumina forward primers (5' - 3'):

1. aatgatacggcgaccaccgagatct acactctttccctacacgacgctcttccgatctagtcaa CCTACGGGRBGCASCAG
2. aatgatacggcgaccaccgagatct acactctttccctacacgacgctcttccgatctagttcc CCTACGGGRBGCASCAG
3. aatgatacggcgaccaccgagatct acactctttccctacacgacgctcttccgatctatgtca CCTACGGGRBGCASCAG
4. aatgatacggcgaccaccgagatct acactctttccctacacgacgctcttccgatctccgtcc CCTACGGGRBGCASCAG
5. aatgatacggcgaccaccgagatct acactctttccctacacgacgctcttccgatctgtagag CCTACGGGRBGCASCAG
6. aatgatacggcgaccaccgagatct acactctttccctacacgacgctcttccgatctgtccgc CCTACGGGRBGCASCAG
7. aatgatacggcgaccaccgagatct acactctttccctacacgacgctcttccgatctgtgaaa CCTACGGGRBGCASCAG
8. aatgatacggcgaccaccgagatct acactctttccctacacgacgctcttccgatctgtggcc CCTACGGGRBGCASCAG
9. aatgatacggcgaccaccgagatct acactctttccctacacgacgctcttccgatctgtttcg CCTACGGGRBGCASCAG
10. aatgatacggcgaccaccgagatct acactctttccctacacgacgctcttccgatctcgtacg CCTACGGGRBGCASCAG
11. aatgatacggcgaccaccgagatct acactctttccctacacgacgctcttccgatctgagtgg CCTACGGGRBGCASCAG
12. aatgatacggcgaccaccgagatct acactctttccctacacgacgctcttccgatctggtagc CCTACGGGRBGCASCAG
13. aatgatacggcgaccaccgagatct acactctttccctacacgacgctcttccgatctactgat CCTACGGGRBGCASCAG
14. aatgatacggcgaccaccgagatct acactctttccctacacgacgctcttccgatctatgagc CCTACGGGRBGCASCAG
15. aatgatacggcgaccaccgagatct acactctttccctacacgacgctcttccgatctattcct CCTACGGGRBGCASCAG
16. aatgatacggcgaccaccgagatct acactctttccctacacgacgctcttccgatctcaaaag CCTACGGGRBGCASCAG

PRK Illumina reverse primers (5' - 3'):

1. caagcagaagacggcatacgagatcgtgat gtgactggagttcagacgtgtgctcttccgatctGGACTACYVGGGTATCTAAT
2. caagcagaagacggcatacgagatacatcg gtgactggagttcagacgtgtgctcttccgatctGGACTACYVGGGTATCTAAT
3. caagcagaagacggcatacgagatgcctaa gtgactggagttcagacgtgtgctcttccgatctGGACTACYVGGGTATCTAAT
4. caagcagaagacggcatacgagattggtca gtgactggagttcagacgtgtgctcttccgatctGGACTACYVGGGTATCTAAT
5. caagcagaagacggcatacgagatcactct gtgactggagttcagacgtgtgctcttccgatctGGACTACYVGGGTATCTAAT
6. caagcagaagacggcatacgagatattggc gtgactggagttcagacgtgtgctcttccgatctGGACTACYVGGGTATCTAAT
7. caagcagaagacggcatacgagatgatctg gtgactggagttcagacgtgtgctcttccgatctGGACTACYVGGGTATCTAAT

8. caagcagaagacggcatacgagattcaagt gtgactggagttcagacgtgtgctcttccgatctGGACTACYVGGGTATCTAAT
9. caagcagaagacggcatacgagatctgatc gtgactggagttcagacgtgtgctcttccgatctGGACTACYVGGGTATCTAAT
10. caagcagaagacggcatacgagataagcta gtgactggagttcagacgtgtgctcttccgatctGGACTACYVGGGTATCTAAT
11. caagcagaagacggcatacgagatgtagcc gtgactggagttcagacgtgtgctcttccgatctGGACTACYVGGGTATCTAAT
12. caagcagaagacggcatacgagattacaag gtgactggagttcagacgtgtgctcttccgatctGGACTACYVGGGTATCTAAT
13. caagcagaagacggcatacgagatttgact gtgactggagttcagacgtgtgctcttccgatctGGACTACYVGGGTATCTAAT
14. caagcagaagacggcatacgagatggaact gtgactggagttcagacgtgtgctcttccgatctGGACTACYVGGGTATCTAAT
15. caagcagaagacggcatacgagattgacat gtgactggagttcagacgtgtgctcttccgatctGGACTACYVGGGTATCTAAT
16. caagcagaagacggcatacgagatggacgg gtgactggagttcagacgtgtgctcttccgatctGGACTACYVGGGTATCTAAT
17. caagcagaagacggcatacgagatctctac gtgactggagttcagacgtgtgctcttccgatctGGACTACYVGGGTATCTAAT
18. caagcagaagacggcatacgagatgcggac gtgactggagttcagacgtgtgctcttccgatctGGACTACYVGGGTATCTAAT
19. caagcagaagacggcatacgagattttcac gtgactggagttcagacgtgtgctcttccgatctGGACTACYVGGGTATCTAAT
20. caagcagaagacggcatacgagatggccac gtgactggagttcagacgtgtgctcttccgatctGGACTACYVGGGTATCTAAT
21. caagcagaagacggcatacgagatcgaaac gtgactggagttcagacgtgtgctcttccgatctGGACTACYVGGGTATCTAAT
22. caagcagaagacggcatacgagatcgtacg gtgactggagttcagacgtgtgctcttccgatctGGACTACYVGGGTATCTAAT
23. caagcagaagacggcatacgagatccactc gtgactggagttcagacgtgtgctcttccgatctGGACTACYVGGGTATCTAAT
24. caagcagaagacggcatacgagatgctacc gtgactggagttcagacgtgtgctcttccgatctGGACTACYVGGGTATCTAAT
25. caagcagaagacggcatacgagatatcagt gtgactggagttcagacgtgtgctcttccgatctGGACTACYVGGGTATCTAAT
26. caagcagaagacggcatacgagatgctcat gtgactggagttcagacgtgtgctcttccgatctGGACTACYVGGGTATCTAAT
27. caagcagaagacggcatacgagataggaat gtgactggagttcagacgtgtgctcttccgatctGGACTACYVGGGTATCTAAT
28. caagcagaagacggcatacgagatcttttg gtgactggagttcagacgtgtgctcttccgatctGGACTACYVGGGTATCTAAT
29. caagcagaagacggcatacgagattagttg gtgactggagttcagacgtgtgctcttccgatctGGACTACYVGGGTATCTAAT
30. caagcagaagacggcatacgagatccggtg gtgactggagttcagacgtgtgctcttccgatctGGACTACYVGGGTATCTAAT
31. caagcagaagacggcatacgagatatcgtg gtgactggagttcagacgtgtgctcttccgatctGGACTACYVGGGTATCTAAT
32. caagcagaagacggcatacgagattgagtg gtgactggagttcagacgtgtgctcttccgatctGGACTACYVGGGTATCTAAT
33. caagcagaagacggcatacgagatcgcctg gtgactggagttcagacgtgtgctcttccgatctGGACTACYVGGGTATCTAAT
34. caagcagaagacggcatacgagatgccatg gtgactggagttcagacgtgtgctcttccgatctGGACTACYVGGGTATCTAAT
35. caagcagaagacggcatacgagataaaatg gtgactggagttcagacgtgtgctcttccgatctGGACTACYVGGGTATCTAAT
36. caagcagaagacggcatacgagattgttgg gtgactggagttcagacgtgtgctcttccgatctGGACTACYVGGGTATCTAAT

Appendix C: Eukaryotic α -and β-diversity

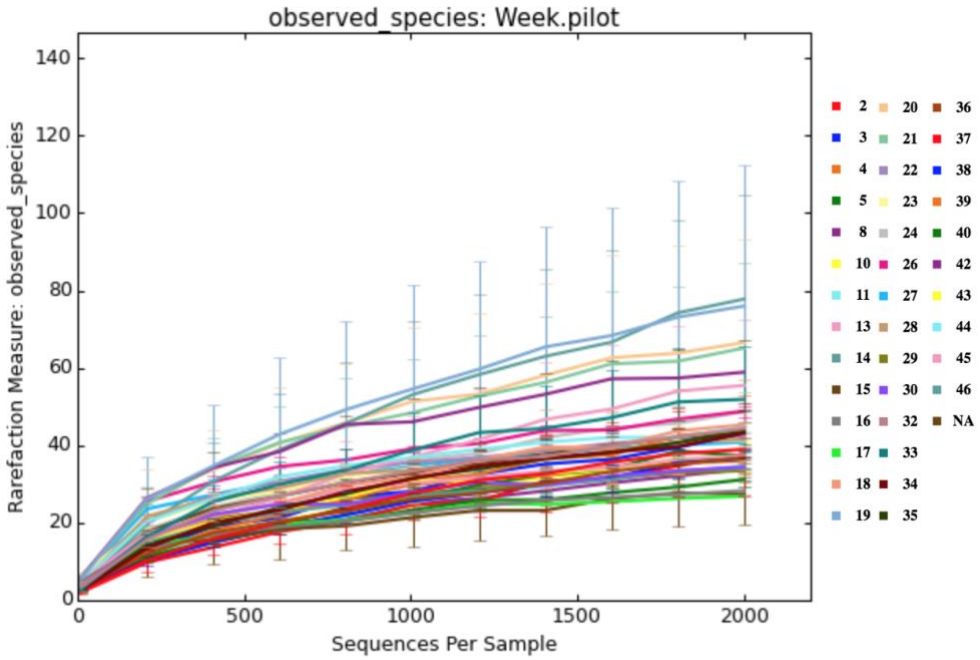

Figure C.1 Rarefaction curves of observed eukaryotic species in the number of sequences per sample from the established pilot plant. The Colours represent the weekly samples. The deviant represents the positive control (NA).

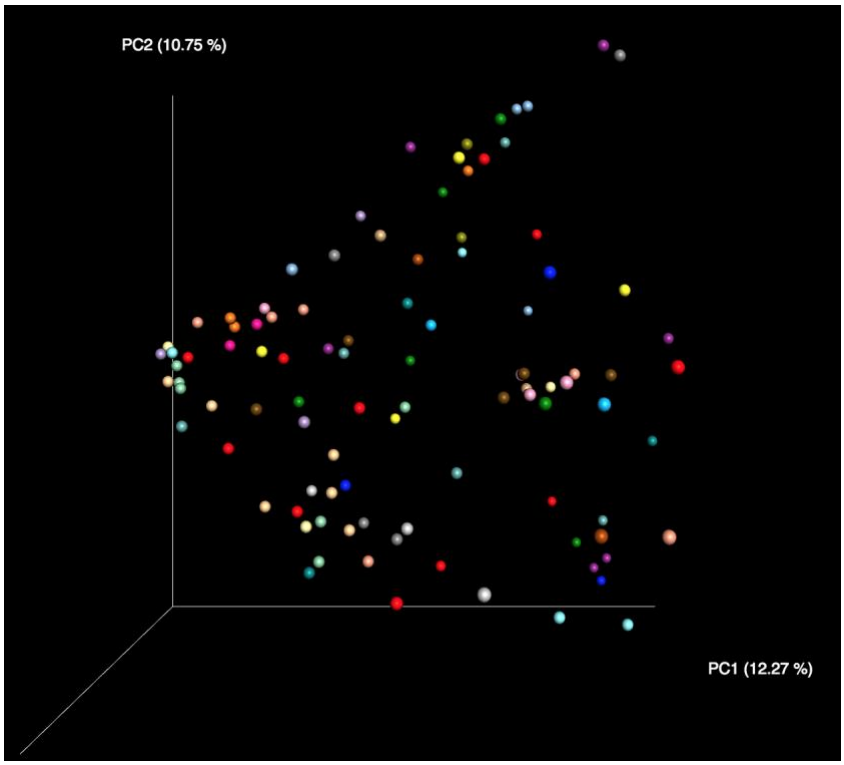

Figure C.2 Unweighted Unifrac PCoA plots. Variation between the weekly samples from the established Pilot plant.

Appendix D: Functional Bacteria Groups at Order/family/genus level

a)

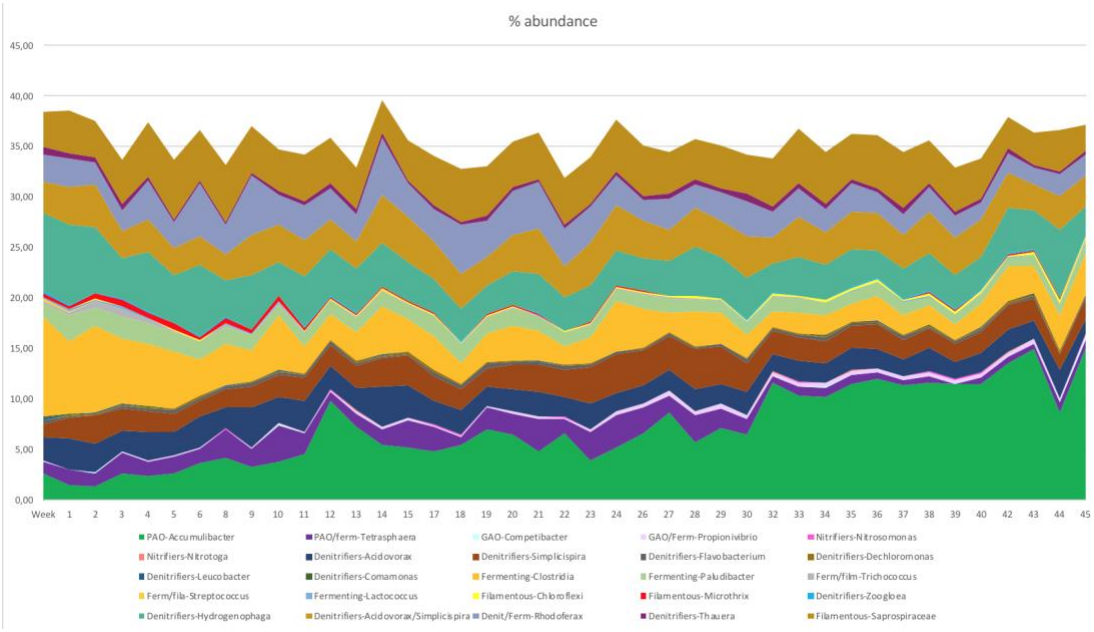

b)

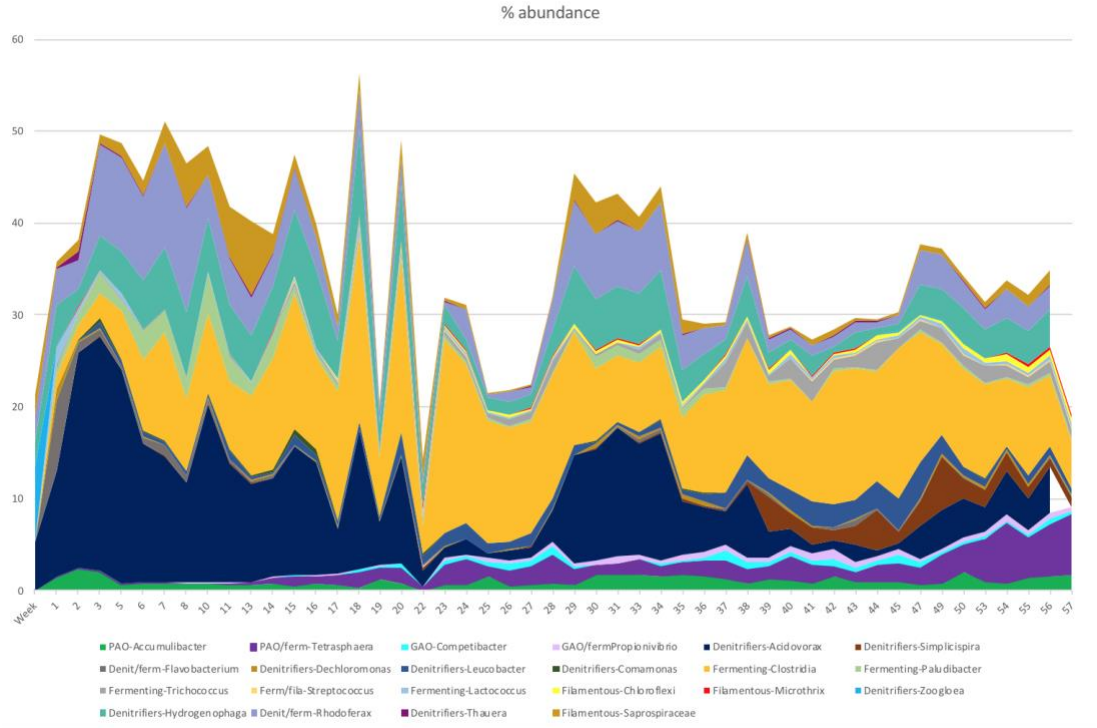

Figure D.1. Average % abundance of the functional bacterial (order/family/genus) found in the weekly samples form the established pilot -and the establishing full-scale plant. a) Average % abundance of the functional bacterial in the weekly pilot samples. Week 1 represent 27.10.16 and week 46 represent 06.09.17. b) Average % abundance of the functional bacterial in the weekly full-scale samples. Week 1 represent 03.06.16 and week 57 represent 29.06.17.

Appendix E: Wastewater Analyses in the Hias Continuous Biofilm Process Plants

Figure E.1 shows the average PO_4 load per day plotted against the material collection time from the established (a) -and the establishing plant (b). Both Figures show clear shifts from week to week. The average PO_4 load in the established plant was 0.046 g/m^2 per day, and ranged between 0.030-0.069 g/m^2 per day (Figure E.1.a). The average PO_4 load in the establishing plant was 0.059 g/m^2 per day, and ranged between 0.036-0.097 g/m^2 per day (Figure E.1.b) (Sondre Eikås, personal communication, 11 April, 2018).

a)

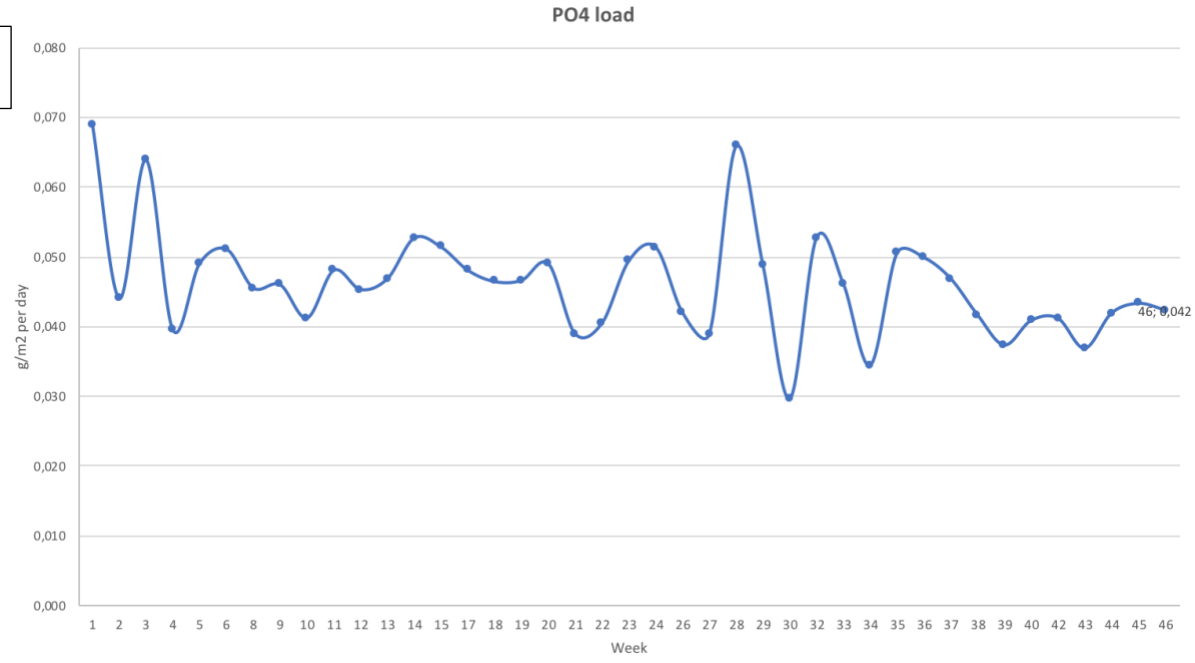

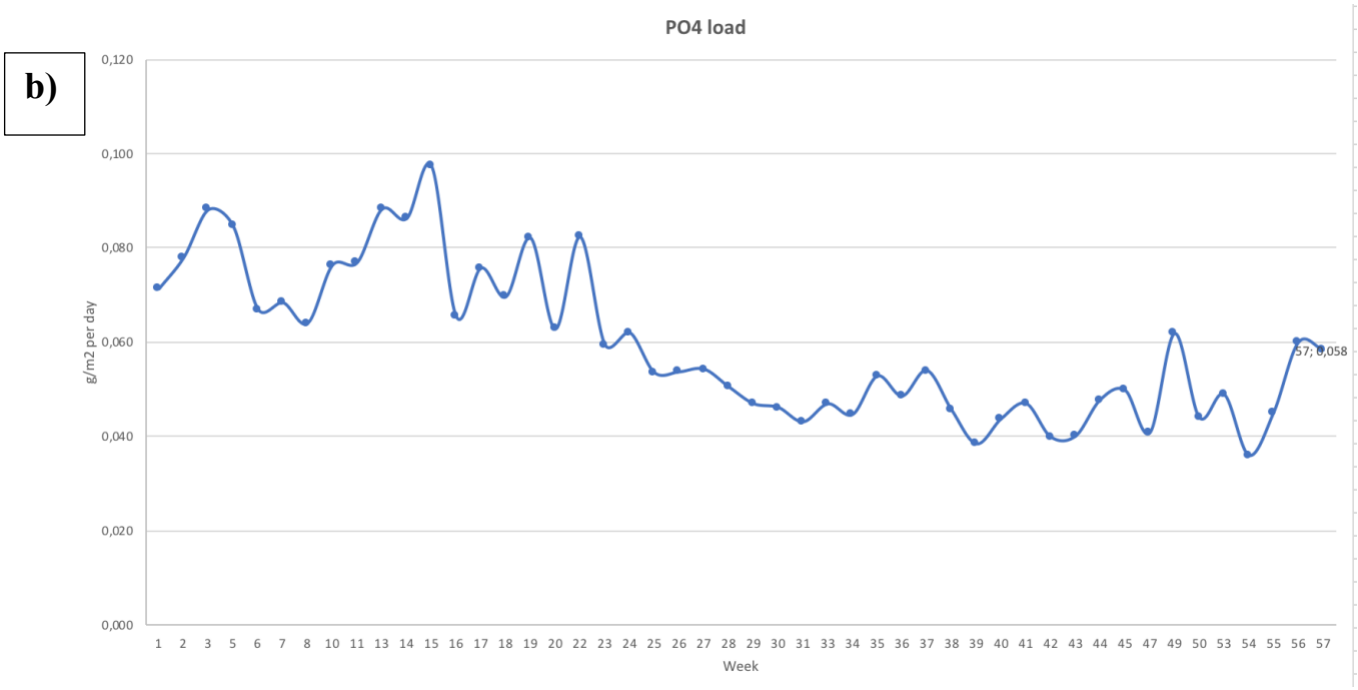

Figure E.1. Average PO_4 load per day measured during the weekly material collection from a) the established pilot plant and b) the establishing full-scale plant (Sondre Eikås, personal communication, 11 April, 2018).

Figure E.2 shows the average SCOD load per day plotted against the material collection time from the established (a) -and the establishing plant (b). The average SCOD load in the established plant was 3,11 g/m^2 per day, and ranged between 1.71-4.43 g/m^2 per day (Figure E.2.a). The average SCOD load in the establishing plant was 3,96 g/m^2 per day, and ranged between 2.51-6.06 g/m^2 per day (Figure E.2.b). (Sondre Eikås, personal communication, 11 April, 2018).

a)

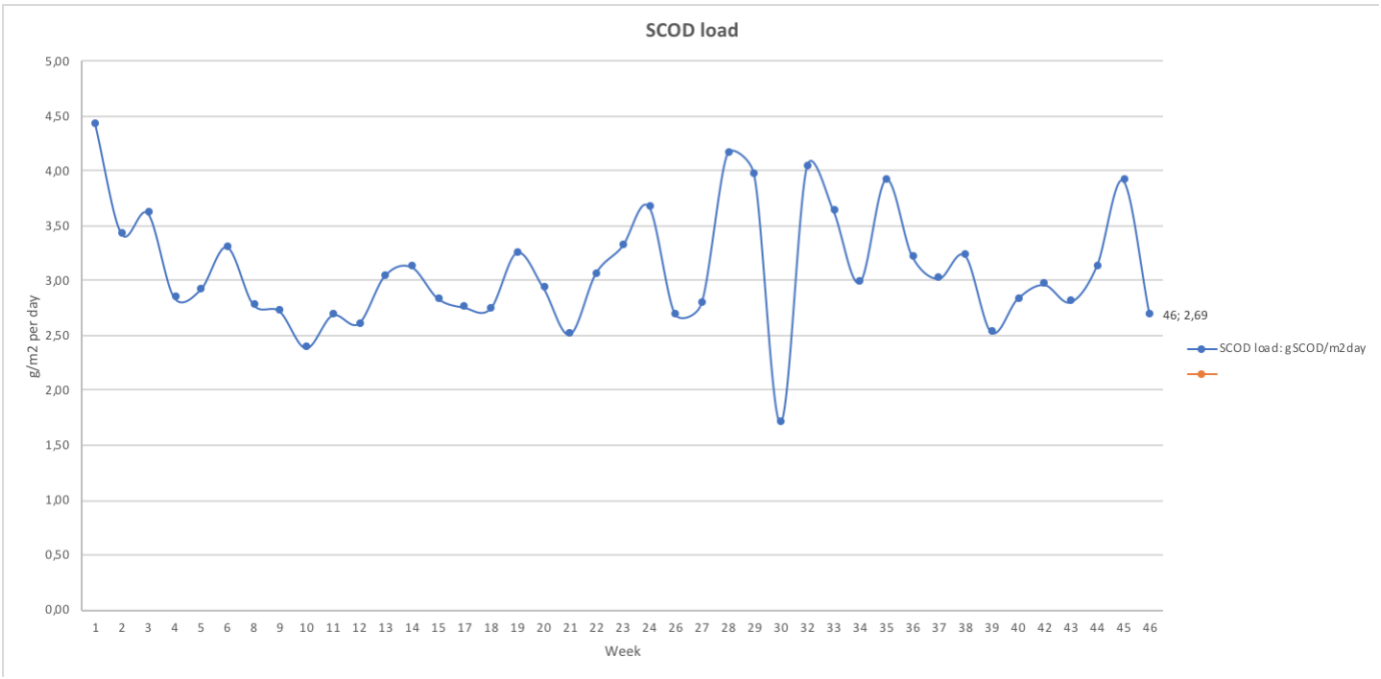

b)

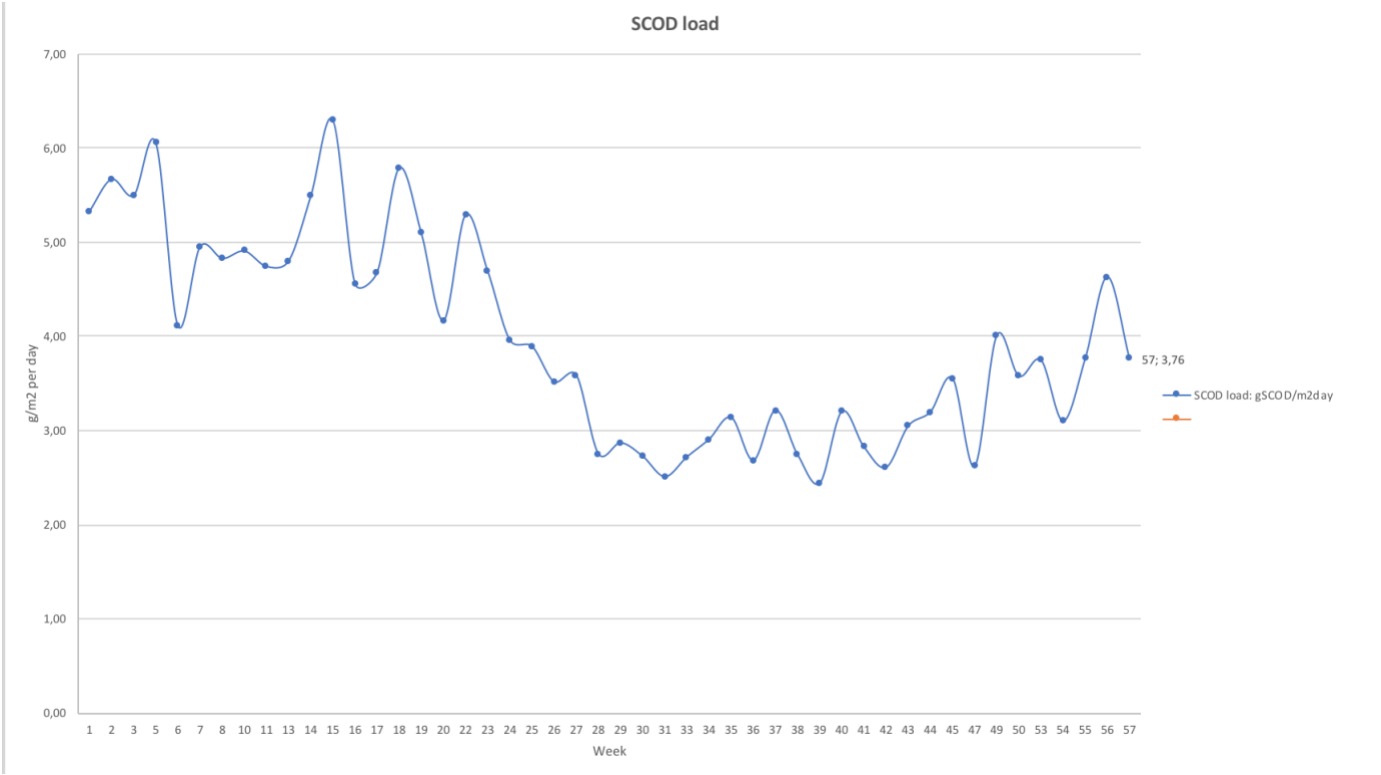

Figure E.2 Average SCOD load per day measured during the weekly material collection from a) the established pilot plant and b) the establishing full-scale plant (Sondre Eikås, personal communication, 11 April, 2018).

Figure E.3 show the wastewater temperature fluctuations during the material collection from the established (a) -and establishing plant. The temperature ranged between 6.80-13.90ºC in the established pilot plant (Figure E.3). A gradual decrease in temperature was detected from week 1-21, while a gradual increase in temperature was detected from week 22-46. The wastewater temperature in the establishing plant range between 6.80-14.80ºC (Figure E.3.b). From week 1-17 the temperature increased gradually, whereas from week 18-42 the temperature decreased gradually. From week 43-57 the temperature increased again (Sondre Eikås, personal communication, 11 April, 2018).

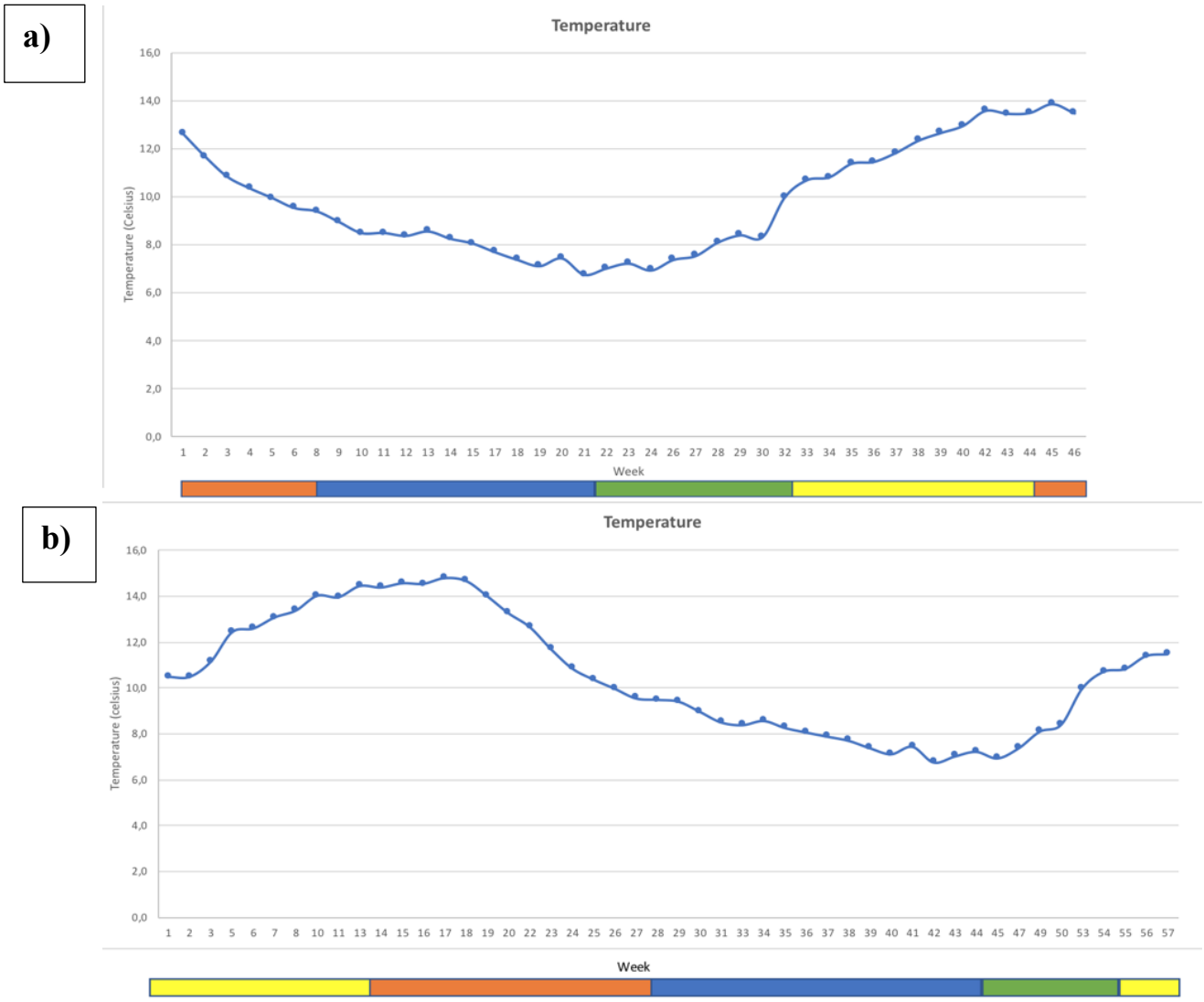

Figure E.3 The wastewater temperature measured during the weekly material collection in a) the established pilot plant and b) establishing full-scale plant (Sondre Eikås, personal communication, 11 April, 2018).

Figure E.4 shows the inlet wastewater volume per hour plotted against the weekly material collection from the established (a) -and establishing (b) plant. The average inlet wastewater volume in the established plant was 0.72 m^3/t, and ranged between 0.58-1.00 m^3/t (Figure E.4.a). Clear shifts were observed through the whole time-line. The average inlet wastewater volume in the establishing plant was 80 m^3/t, and ranged between 46-144 m^3/t (Figure E.4.b.). Clear shifts were detected through the time-line, with a gradual decrease from week 4-34, and gradual increase again from week 35 (Sondre Eikås, personal communication, 11 April, 2018).

a)

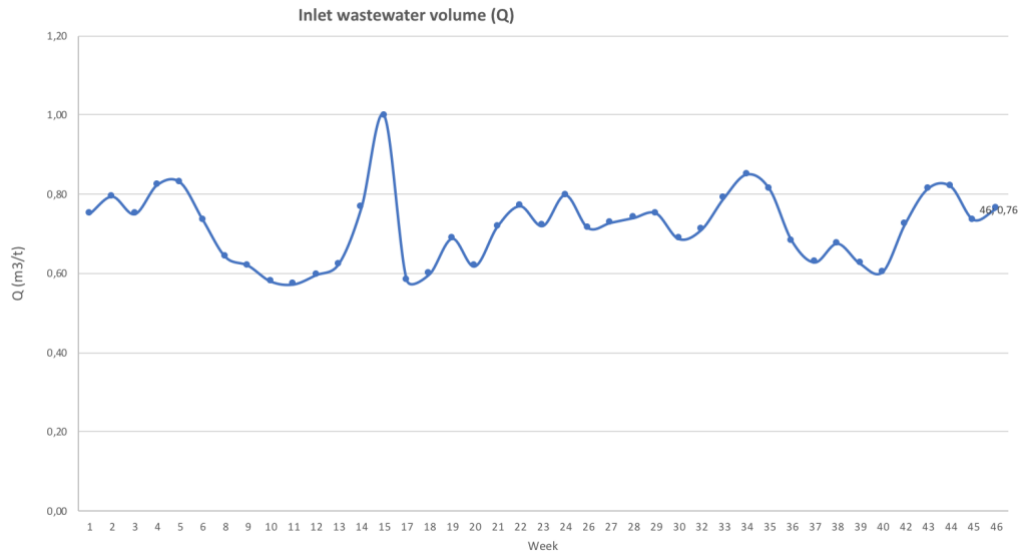

b)

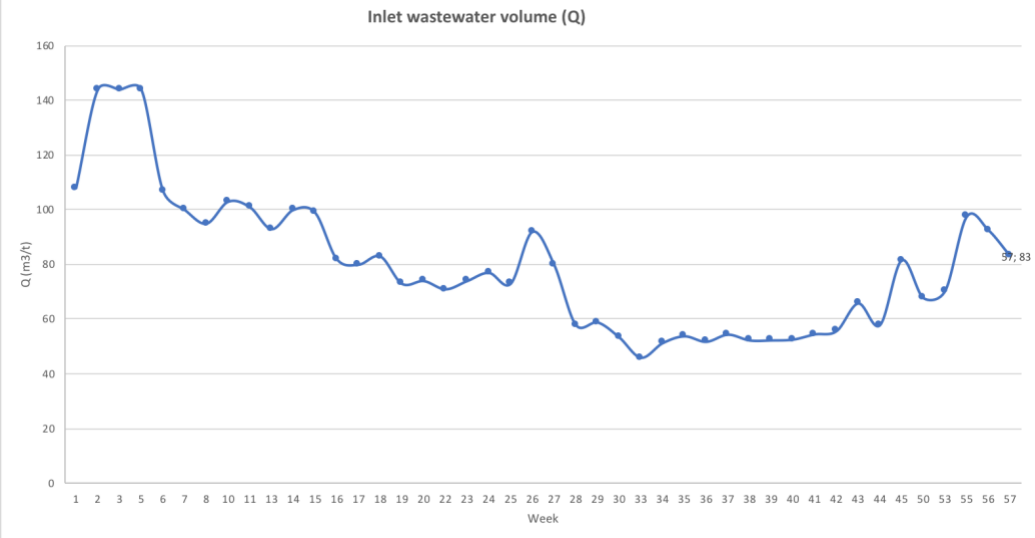

Figure E.4 Inlet wastewater volume per hour (m^3/t) measured at the same time as the weekly material collection in a) pilot plant and b) full-scale plant (Sondre Eikås, personal communication, 11 April, 2018).

Norges miljø- og biovitenskapelige universitet
Noregs miljø- og biovitskapelege universitet
Norwegian University of Life Sciences

Postboks 5003
NO-1432 Ås
Norway